EXPERIMENTAL RESEARCHES ON THE SURGING OF THE BLOWER

TADAYA ITŌ

Department of Mechanical Engineering

(Received October 31, 1960)

CONTENTS

Nomenclature

The following nomenclature is used in this paper:

p = pressure of air in the pipe-line
p_0 = mean pressure of air in the pipe-line
u = velocity of air in the pipe-line
u_0 = mean velocity of air in the pipe-line
Q = discharge volume of blower
K = bulk modulus of air
ρ = density of air
c = velocity of sound
κ = ratio of specific heat
t = time
t' = $t/(l/c)$
x = linear coordinates
x' = x/l
A = area of cross section of the pipe-line
l = length of pipe-line
V = volume of tank
P_t = effective total pressure of blower
u_p = peripheral valocity of vane-wheel
D = diameter of vane-wheel
b = outlet vane-height
n = number of revolutions of blower
S_0 = area of exit opening of the pipe-line
ζ = flow coefficient of exit opening
f = frequency
f_s = frequency of vibration of normal mode (index s)
ω = angular frequency
ω_s = angular frequency of vibration of normal mode (index s)
k = ω/c
k_s = ω_s/c

a = pressure amplitude of surging
ε = equivalent damping coefficient of free vibration of air column
ε_s = equivalent damping coefficient of vibration corresponding to normal mode (index s)
q = pressure variation of air in the pipe-line
v = velocity variation of air in the pipe-line
q_s = pressure variation in generalized coordinates
Q_s = generalized force

Introduction

In the running of such fluid machines of rotary type as the centrifugal pump and the blower, unstability of fluid flow or violent oscillation of fluid are experienced flequently. These phenomena are known as the surging of fluid machine.

In general, the surging is apt to occur when a machine is operated with small discharge or in cut-off condition, and for this reason, the range of discharge, in which the fluid flow is stable, is limited and this phenomenon causes much trouble in the running of machine.

When we use a blower as a supercharger for aircraft engine of reciprocal type or as a compressor for aircraft gas turbine, the violent surging can not be permited because there exists a serious danger of failure of the machine or interruption of the combustion process.

With increased use of blowers in the field mentioned above, the problem of surging has been taken up by various investigators recently. A general survey of the investigations up to the present day is as follows.

In 1947 Bullock, Wilcox and Moses[1] carried out a mainly experimental investigation and showed that the surging is a phenomenon of periodic variation of the pressure and the velocity which occurs in the range of discharge in which the machine has a rising characteristic, and its frequency is same throughout the pipe-line, and also that the frequency and the amplitude of pressure variation depend on the conditions of the pipe-line in a complex manner.

In 1948 Fujii[2] gave a theoretical treatment to the problem. In which he took up mainly the case of pipe-line of uniform cross section, and deduced some important conclusions about the nature of surging from the viewpoint that the surging phenomenon is a vibration of continuous body. In this theory, he confirmed that the surging phenomenon is nothing but a self-excited vibration of fluid column in the pipe-line caused by the rising characteristic of the blower.

In 1949 Shimoyama[3] also gave a theoretical treatment to the phenomenon based on the same standpoint as above but through a quite different mathematical method. In this paper, he derived an ordinary differential equation of second order which approximately describes the phenomenon and proposed a criterion for stability of air flow, and contrived a graphical method for estimating the amplitude of surging. The author's study is much indebted to his paper.

In 1953 Huppert and Benser[4] carried out a theoretical and experimental study. In which they considered a blower, the characteristic of which is discontinuous at the stall point, and indicated the possibility of a certain type of surging, in which cyclic shift between stalling and unstalling occurs in the compressor resulting from transient flow variations following an initial stall.

In 1955 Emmons, Pearson and Grant[5] proposed a theoretical model of surging from the standpoint that the system composed of a blower, ducts and volumes can be regarded as a Helmholtz resonator. In this theory, they derived a formula which gives the frequency of surging. The results of experimental study are also included in this report.

In 1956 Kusama, Tsuji and Oshida[6] proposed a theory from the viewpoint that the system has finite degrees of freedom, and deduced a stability criterion of the flow. They also carried out the experimental researches employing centrifugal blowers.

In 1960 Katto[7) 8) 9) 10)] carried out experimental and theoretical investigations for the surging of small fan duct systems. In these researches, he devised the equivalent lumped models for the vibrating air columns and utilizing these models he also gave the oscillation cycles of systems by phase plane integrations.

In addition to the studies mentioned above, fairly many reports have been presented by Pearson,[11) 12)] Bower,[13)] Stephenson,[14)] Finger,[15) 16)] Folley,[17)] Harada,[18)] Sherstyuk[19)] and so on,[37) 41) 42) 43) 44)] up to the present.

As stated above the nature of the surging phenomenon is becoming to be clarified gradually. However it can be said that the theoretical studies so far made, are based on the excessively simplified or idealized assumptions and, on the other hand, the experimental ones are rather fragmentary. This leaves the obvious duty for someone to carry out systematic experiments, and clarify the actual state in which the surging occurs, by considering the effects of the dimensions of the pipe-line, volume and accessories of the pipe-line on the surging and by clarifying the relation between the form of characteristic curve of the blower and the surging. In this paper the author deals with the surging phenomenon rather more experimentally but with some theoretical emphasis.

Chapter I. A Fundamental Consideration on the Surging Phenomenon

1. Preliminaries

As will be shown in the following chapters, careful study of the surging problem reveals the existence of several phenomena that can not be explained from the standpoint that the system has only finite degrees of freedom. So the author is of opinion that for complete understanding of the intrinsic nature of the phenomenon we must regard the system as having infinite degrees of freedom or as a continuous body, especially if the system has a long pipe-line.

Fujii[2)] investigated the problem from this standpoint and gave a fine theoretical model. In this theory, he derived the unstability condition of flow by determining the general solution of the equation of wave motion under the assumption of small oscillation and making it satisfy the boundary conditions of the system. He also showed the sustained wave form of surging by making use of his graphical method.

In his report, attention is mainly focussed on the pipe-line system having the blower at one end and the resistance (valve or nozzle) at the other end and the graphical solution for sustained wave form of surging is also given for this case.

However in the actual use of the blower, there are many systems in which the blower is placed at the midway of pipe-line. For these cases, it is easily presumed that both the stability condition of the flow and the sustained wave

form of the surging become multifarious. In order to obtain clear understanding for the surging phenomena which arise in actual pipe-lines of various construction, it is to be desired that the theoretical model is established for pipe-lines of the form mentiened above. So in advance of the experimental study of the surging, we deal with this problem from the viewpoint that the system is a continuous body.

2. Differential equations and boundary conditions

We consider the pipe-line as shown in Fig. 1.1, where the pipe length is denoted by l and the position of the blower by ξl. We here assume that the passage in the blower is negligiblly small compared with the pipe length and that there is no friction in the pipe-line. In Fig. 1.2, the characteristics of the blower and the valve are shown (indicated by $\bar{B}$ and $\bar{V}$ respectively), where the abscissa is discharge of the blower and the ordinate is the pressure, and the pressure in the suction pipe is taken as standard. The characteristics $\bar{B}$ expresses the effective static pressure and $\bar{V}$ the pressure drop at the valve, and the abscissa corresponding to the intersecting point E of the two curves indicates the discharge at the steady flow state.

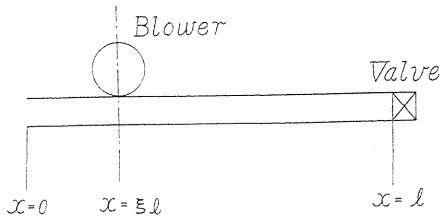

FIG. 1.1. Pipe-line.

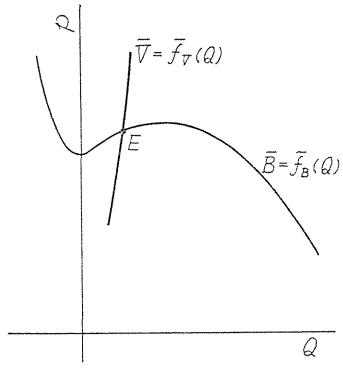

FIG. 1.2. Characteristics of blower and valve.

Because the surging occurs in the range of small discharge, it may be permitted in general to regard the value of the pressure corresponding to E as the difference between the pressure inside the valve and the atmosphere.

In the following we consider the differential equations which describe the phenomenon and the boundary conditions. Denoting the pressure, the density and the velocity of the fluid in the pipe-line by p, ρ and u respectively, the equation of motion of the fluid and the equation of continuity are written as follows:

$$\frac{\partial u}{\partial t}+u\frac{\partial u}{\partial x}+\frac{1}{\rho}\frac{\partial p}{\partial x}=0, \tag{1.1}$$

$$\frac{\partial \rho}{\partial t}+u\frac{\partial \rho}{\partial x}+\rho\frac{\partial u}{\partial x}=0. \tag{1.2}$$

When we confine our consideration to the case in which a variation of the

density is small, the second terms in Eqs. (1.1) and (1.2) can be omitted. And using the formula $dp/d\rho=c^2$, above equations reduce to

$$\frac{\partial u}{\partial t}+\frac{1}{\rho}\frac{\partial p}{\partial x}=0, \tag{1.3}$$

$$\frac{\partial u}{\partial x}+\frac{1}{\rho c^2}\frac{\partial p}{\partial t}=0, \tag{1.4}$$

where c is the velocity of sound. These two are the fundamental equations for succeeding discussion.

Eliminating p or u from these equations, we have well known equations of wave motion, namely;

$$\frac{\partial^2 u}{\partial t^2}=c^2\frac{\partial^2 u}{\partial x^2}, \tag{1.5}$$

$$\frac{\partial^2 p}{\partial t^2}=c^2\frac{\partial^2 p}{\partial x^2}. \tag{1.6}$$

But for ease of mathematical treatment, we adopt (1.3) and (1.4) rather than (1.5) and (1.6), and treat them with the characteristic method in the theory of partial differential equation. Namely we first define a set of curvilinear coordinates $\xi_0(x, t)=\alpha_0$(constant), $\eta_0(x, t)=\beta_0$(constant) in such a manner that ξ_0 and η_0 are mutually independent and the derivatives of p and u in the direction normal to the coordinate curves are indefinite, then by use of these ξ_0 and η_0 we transform the coordinates from x, t to α_0, β_0 and convert Eqs. (1.3) and (1.4) to a set of equivalent characteristic differential equations shown below

$$C_+ : \quad \frac{\partial t}{\partial \alpha_0}-\frac{1}{c}\frac{\partial x}{\partial \alpha_0}=0, \tag{1.7}$$

$$C_- : \quad \frac{\partial t}{\partial \beta_0}+\frac{1}{c}\frac{\partial x}{\partial \beta_0}=0, \tag{1.8}$$

$$\Gamma_+ : \quad \frac{\partial u}{\partial \alpha_0}+\frac{1}{\rho c}\frac{\partial p}{\partial \alpha_0}=0, \tag{1.9}$$

$$\Gamma_- : \quad \frac{\partial u}{\partial \beta_0}-\frac{1}{\rho c}\frac{\partial p}{\partial \beta_0}=0. \tag{1.10}$$

Writing in the non-dimentional form, we have

$$C_+ : \quad \frac{\partial\left(\frac{t}{l/c}\right)}{\partial \alpha_0}-\frac{\partial\left(\frac{x}{l}\right)}{\partial \alpha_0}=0, \tag{1.11}$$

$$C_- : \quad \frac{\partial\left(\frac{t}{l/c}\right)}{\partial \beta_0}+\frac{\partial\left(\frac{t}{l}\right)}{\partial \beta_0}=0, \tag{1.12}$$

$$\Gamma_+ : \quad \frac{\partial\left(\frac{u}{c}\right)}{\partial \alpha_0}+\frac{1}{2}\frac{\partial\left(\frac{p}{(1/2)\rho c^2}\right)}{\partial \alpha_0}=0, \tag{1.13}$$

$$\Gamma_- : \quad \frac{\partial\left(\frac{u}{c}\right)}{\partial \beta_0}-\frac{1}{2}\frac{\partial\left(\frac{p}{(1/2)\rho c^2}\right)}{\partial \beta_0}=0. \tag{1.14}$$

Integrating above differential equations under the condition that α_0 or β_0 is constant, we have

$$C_+ : \frac{t}{(l/c)} - \frac{x}{l} = R(\beta_0), \tag{1.15}$$

$$C_- : \frac{t}{(l/c)} + \frac{x}{l} = S(\alpha_0), \tag{1.16}$$

$$\Gamma_+ : \frac{u}{c} + \frac{1}{2}\frac{p}{(1/2 \cdot \rho c^2)} = r(\beta_0), \tag{1.17}$$

$$\Gamma_- : \frac{u}{c} - \frac{1}{2}\frac{p}{(1/2 \cdot \rho c^2)} = s(\alpha_0), \tag{1.18}$$

where $R(\beta_0)$, $r(\beta_0)$, $S(\alpha_0)$ and $s(\alpha_0)$ are arbitrary functions of β_0 or α_0.

By above equations, namely by the curvilinear coordinates containing α_0 and β_0 as parameters, a corespondence between a point $(x/l,\ t/(l/c))$ on the $x/l,\ t/(l/c)$ plane and a point $(u/c,\ p/(1/2)\rho c^2)$ on the $u/c,\ p(1/2)\rho c^2$ plane is established. In our case the curvilinear coodinates, or the so-called characteristic C_+, C_-, Γ_+ and Γ_- are straight lines having the inclinations $+1$, -1, -2 and $+2$ respectively. This state is shown in Fig. 1.3. C_+ and C_- represent the loci of wave motions which propagate in the positive and negative direction respectively, and the small domains 1, 2, 3 and 4 in the left figure correspond to the points 1, 2, 3 and 4 in the right respectively; these points indicates the state of liquid.

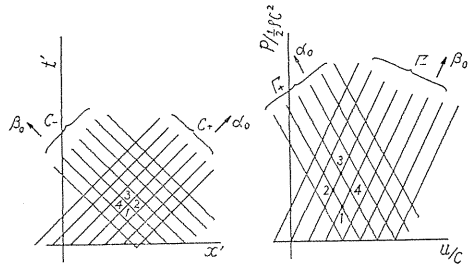

FIG. 1.3. Curvilinear coordinates.

A graphical solution method where the solution is obtained by accomplishing the correspondence between the $(x,\ t)$ and $(u,\ p)$, satisfying the boundary conditions on the two planes, has been applied to such problems as the water hammer and the gas flow in the exaust turbine,[21] but not to the surging problem yet. It is however not adequate to use this graphical method for the deduction of the universal characters of the surging, for examples, the stability criterion of the flow (or the condition for the occurence of surging) or the role of the blower in the surging phenomena, because this method gives the individual solution corresponding to the particular initial or boundary conditions.

In order to deduce the universal characters of the surging, we treat the problem analytically by the aid of Eqs. (1.15)~(1.18) and the boundary conditions.

In the following we consider the boundary conditions.

Refering to Fig. 1.1 and Fig. 1.2, we take the following equations as the

conditions at the suction end of the pipe-line,

$$\left.\begin{aligned} p_{x=0} &= P_a - \zeta_1 \frac{\rho u_{x=0}^2}{2} \qquad \text{(for positive flow)}, \\ p_{x=0} &= P_a \qquad\qquad\qquad\quad \text{(for negative flow)}, \end{aligned}\right\} \tag{1.19}$$

where P_a is the atmospheric pressure and $\zeta_1 \frac{\rho u_{x=0}^2}{2}$ is the sum of the pressure drop due to the suction and the pressure loss of inflow. The condition at valve is as follows:

$$p_{x=l} = \bar{f}_V(Q_{x=l}), \tag{1.20}$$

where $Q=uA$ holds if the area of the cross section of the pipe-line is denoted by A.

Next, concerning the blower, we have two conditions: one is that the continuity of the flow is fulfilled and the other is that the pressure difference between the delivery and the suction pipe is equal to the static pressure afforded by the blower.

Indicating the values corresponding to the suction and the delivery pipe by suffixes L and H respectively, we have at $x=\xi l$

$$Q = Q_L = Q_H, \tag{1.21}$$

$$p_H = p_L + \bar{f}_B(Q). \tag{1.22}$$

Shifting the ordinate in Fig. 1.2 to the position of E, and adopting the nondimentional values $p/(1/2)\rho c^2$ and u/c instead of p and Q, we obtain Fig. 1.4.

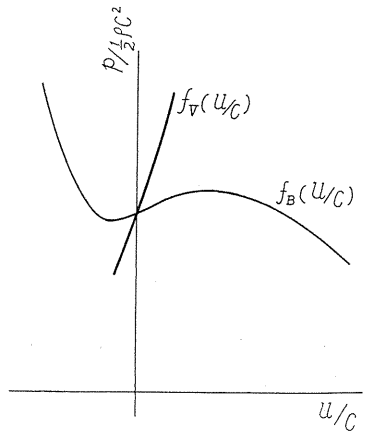

FIG. 1.4. Characteristics of blower and valve on $p/(1/2)\rho c^2$, u/c plane.

Next, neglecting the pressure drop due to suction and pressure loss of inflow, and taking the atmospheric pressure as standard, Eqs. (1.19)~(1.22) reduce to

$$\left(\frac{p_L}{(1/2)\rho c^2}\right)_{x=0} = 0, \tag{1.23}$$

$$\left(\frac{p_H}{(1/2)\rho c^2}\right)_{x=l} = f_V\{(u_H/c)_{x=l}\}, \tag{1.24}$$

$$(u_L/c)_{x=\xi l} = (u_H/c)_{x=\xi l}, \tag{1.25}$$

$$\left(\frac{p_H}{(1/2)\rho c^2}\right)_{x=\xi l} = \left(\frac{p_L}{(1/2)\rho c^2}\right)_{x=\xi l} + f_B\{(u_L/c)_{x=\xi l}\}. \tag{1.26}$$

In the succeeding discussion we use above equations as the boundary conditions.

Our aim is to examine the characters of solution of (1.15)~(1.18) which satisfies above boundary conditions. Here, for brevity, we use the notations t', x' instead of $t/(l/c)$, x/l and write newly p, u instead of $p/(1/2)\rho c^2$, u/c. Then Eqs. (1.15)~(1.18) and the boundary conditions (1.23)~(1.26) can be written in the following forms:

$$C_+ : \ t' - x' = R(\beta_0), \tag{1.27}$$

$$C_- : \ t' + x' = S(\alpha_0), \tag{1.28}$$

$$\Gamma_+ : \ (2u + p)/2 = r(\beta_0), \tag{1.29}$$

$$\Gamma_- : \ (2u - p)/2 = s(\alpha_0), \tag{1.30}$$

$$(p_L)_{x=0} = 0, \tag{1.31}$$

$$(p_H)_{x=1} = f_V\{(u_H)_{x=1}\}, \tag{1.32}$$

$$(u_L)_{x=\xi} = (u_H)_{x=\xi}, \tag{1.33}$$

$$(p_H)_{x=\xi} = (p_L)_{x=\xi} + f_B\{(u_L)_{x=\xi}\}. \tag{1.34}$$

3. Propagation of disturbance

Investigation of the instability condition of the flow, or the influence of the blower on the vibration of the fluid column by the aid of above equations is equivalent to that of the change of amplitude of a disturbance with the lapse of time.

For this purpose it is required to study the feature of propagation of a disturbance (or wave), and this section is devoted to this subject.

We consider the x', t' plane (*i.e.*, $t/(l/c)$, x/l plane) as shown in Fig. 1.5.

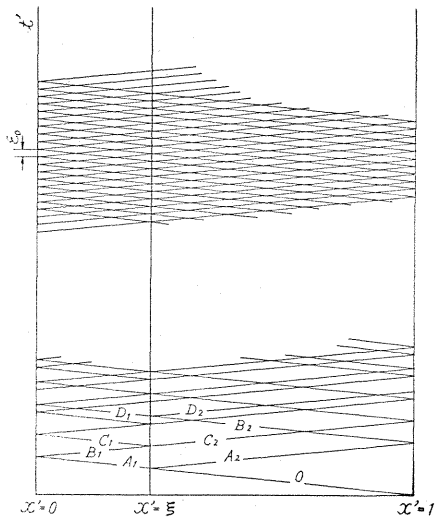

FIG. 1.5. Loci of propagating disturbance.

Assuming that the disturbance O starts from the valve position $x'=1$ and propagates toward upstream, when it reaches the blower position $x'=\xi$, it is

affected by the blower in a manner governed by the conditions (1.33) and (1.34), and resultant states, which are denoted by A_1 and A_2, propagate again toward upstream and downstream respectively. The disturbance A_1 is transformed into B_1 by the reflection at the suction end $x'=0$, and this reflection depends on the condition (1.31). The disturbance A_2, which propagates toward downstream, is also transformed into B_2 at the valve $x'=1$ by the reflection which is governed by the condition (1.32), and such processes are continued. Obviously these loci of propagaiton of disturbances correspond to C_+ and C_- mentioned in the preceding section.

It can be proved that, if the ratio of the suction pipe length to the delivery pipe length ($m' : n'$) is rational, the x', t' plane becomes to be covered after a certain period of time by numerous equally spaced (the distance is denoted by ε_0 in Figure) loci of disturbance. It can be also proved that m' bands of width ($\varepsilon_0 = A_0'/m'$) are contained in a period of time A_0' in which a disturbance goes and returns through the suction pipe, and n' bands in a period of time B_0' in which the disturbance does the same in the delivery pipe. The proofs are omitted here.

If ξ (or $m' : n'$) is irrational, the value of ε_0 can not be defined. But even in this case, since we can select an approximate rational number with desired accuracy, it may be permitted to use the results of the succeeding treatment, where the value of ξ is assumed to be a rational number, for the case where ξ is an irrational number.

In addition, for the case where $\xi=0$, or the blower is at the suction end of the pipe-line, we take $A'=0$, $B'=\varepsilon_0$, $m'=0$ and $n'=1$, as is seen from Fig. 1.5.

4. Condition of stability

Suppose the blower is in a steady running at point E in Fig. 1.2. If an infinitesimal disturbance in a pipe-line grows up with time until it becomes impossible for the system to maintain the equilibrium state corresponding to point E, then this equilibrium is said to be unstable. On the contrary if a disturbance dies down with time and the equilibrium state E is recovered, the state E is stable. Our aim in this section is to deduce the condition under which an equilibrium state is stable (or unstable), refering to the discussion of preceding section, and to examine the role of the blower in surging phenomenon.

Taking the zero point of the abscissa at the point corresponding to the working discharge of the blower as is shown in Fig. 1.4, we discuss the problem on the assumption that only small oscillation can occur. On this standpoint, we can write the blower characteristic $f_B(u)$ in Eq. (1.34) and the valve characteristic $f_V(u)$ in Eq. (1.32) in linear forms, namely:

$$f_B(u) = \bar{a} + \bar{b}\,u, \tag{1.35}$$

$$f_V(u) = \bar{a} + \bar{g}u, \tag{1.36}$$

where $\bar{b}$ is the inclination of the characteristic curve of the blower.

Hereafter we preceed our discussion making use of Eqs. (1.27)~(1.34) of Section 2. Solving Eqs. (1.29) and (1.30), we have

$$u = (r+s)/2, \tag{1.37}$$

$$p = r - s. \tag{1.38}$$

In these equations, and also throughout this section we use for brevity the notations r and s instead of $r(\beta)$ and $s(\alpha)$ respectively.

Next, rewriting the boundary conditions (1.31)~(1.34) by use of Eqs. (1.35)~(1.38), we have

$$\text{at } x'=0, \qquad r_L = s_L, \tag{1.39}$$

$$\text{at } x'=1, \qquad r_H - s_H = \bar{a} + \bar{g}\frac{r_H + s_H}{2}, \tag{1.40}$$

$$\text{at } x'=\xi=\frac{m'}{m'+n'}, \qquad r_L + s_L = r_H + s_H, \tag{1.41}$$

$$\text{and } r_H - s_H = r_L + s_L + \bar{a} + \bar{b}\frac{r_L + s_L}{2}. \tag{1.42}$$

Further, we can write Eqs. (1.41) and (1.42) in different forms, namely:

$$\text{at } x'=\xi=\frac{m'}{m'+n'}, \qquad r_H = \frac{(\bar{b}+4)}{4}r_L + \frac{\bar{b}}{4}s_L + \frac{\bar{a}}{2}, \tag{1.41'}$$

$$-s_H = \frac{\bar{b}}{4}r_L + \frac{(\bar{b}-4)}{4}s_L + \frac{\bar{a}}{2}, \tag{1.42'}$$

$$\text{or} \qquad -r_L = \frac{(\bar{b}-4)}{4}r_H + \frac{\bar{b}}{4}s_H + \frac{\bar{a}}{2}, \tag{1.41''}$$

$$s_L = \frac{\bar{b}}{4}r_H + \frac{(\bar{b}+4)}{4}s_H + \frac{\bar{a}}{2}. \tag{1.42''}$$

Next, with above equations, we deduce an equation which represents the vicissitude of a small disturbance with time, by establishing the correspondence between the loci of the disturbance on x', t' plane (in other words, the characteristics C_+ and C_-) and the points on p, u plane which represent the states of the fluid.

From (1.37) and (1.39), we obtain $r_L = u_{x=0}$, that is, r_L is the velocity variation at the suction end of the pipe-line. By examining the variation of r_L with time we can see the vicissitude of small disturbance (or propagating wave of small amplitude). Since this vicissitude can be well examined without loss of generality in the situation where x', t' plane is covered already with the bands of loci of disturbances of width ε_0, and where the disturbances arrive at suction end $x'=0$ one after another at constant time interval, so we treat the problem under this condition.

Now, considering the process in which a small disturbance, which corresponds to a band of width ε_0, starts from $x'=0$ and passes through the blower position $x'=\xi l$, reflects at the valve $x'=1$, passes again through the blower position and returns to the suction end $x'=0$, we persue the corresponding variation of r_L on the p, u plane.

Drawing this process as is shown in Fig. 1.6, and mapping this on the x', t' plane and the p, u plane we have Fig. 1.7 (a) and (b). In Fig. 1.7 (a) a band of width ε_0 on the x', t' plane is shown by a straight line and in Fig. 1.7 (b), corresponding feature on the p, u plane is shown. And in both figures the corresponding points are indicated by the suffixes of the same numerals and on the p, u plane the quantities corresponding to suction pipe are indicated by adding a

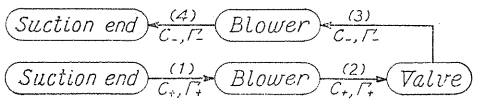

FIG. 1.6

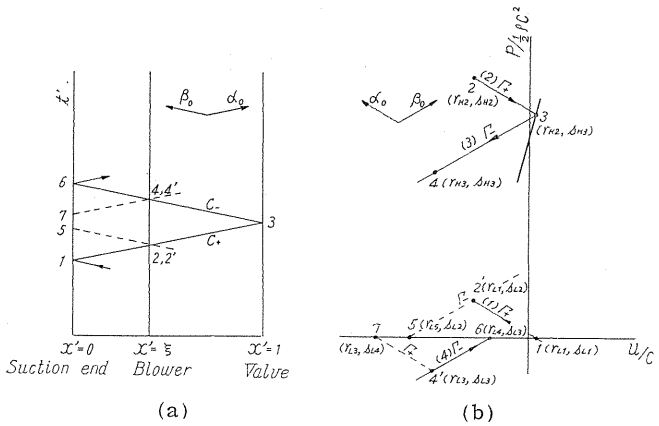

FIG. 1.7. Correspondence between the points on x', t' plane and those on $p/(1/2)\rho c^2$, u/c plane.

prime. Besides, a state of the fluid corresponding to a point on p, u plane are represented by a set of (r, s), as is seen in Eqs. (1.37) and (1.38). The correspondence between both figures are obtained with help of Eqs. (1.27)$\sim$(1.30) in the following manner.

Namely the process (1) in Fig. 1.6 is characterized by a constant value of β_0 (for example β_0') on the x', t' plane as is seen from Eq. (1.27), and a Γ_+ of Eq. (1.29) corresponds to the same value β_0' on the p, u plane, so the state of fluid at the suction side of the blower and at the moment when this process is finished, or, in other words, when the disturbance (r_{L1}, s_{L1})* just arrives at the blower position, is represented by a point (r_{L1}, s_{L2}) on the same Γ_+ (denoted by numeral 2′). This is seen from the fact that β_0' *i.e.* r_{L1} is held constant and only α_0 varies. The state of the fluid in the delivery pipe at the blower position is represented by a point (r_{H2}, s_{H2}) (denoted by numeral 2) which is related to point (r_{L1}, s_{L2}) by Eqs (1.41′) and (1.42′). The similar discussion applies correspondingly to the process (2), (3) and (4).

As shown above, using the notations in Fig. 1.7 (b), and pursuing the each process of Fig. 1.6, we can obtain the relation between two values of r_L corresponding to the point 1 (r_{L1}, s_{L1}) and 6 (r_{L4}, s_{L3}) respectively. In other words we can know the change of magnitude of the velocity variation at suction end between before and after the period which is required for a disturbance to make a round trip through the pipe-line, in the following manner.

Using Eqs. (1.41′) and noting that the starting point is (r_{L1}, s_{L1}), we have Eq. (1.43) for the moment when the process (1) is just completed,

* This is denoted by numeral 1 in Fig. 1.7 (b) and because this point corresponds to the suction end of the pipe-line, it is clear that this point exists on the u axis.

$$r_{H2}=\frac{(\bar{b}+4)}{4}r_{L1}+\frac{\bar{b}}{4}s_{L2}+\frac{\bar{a}}{2}, \tag{1.43}$$

and for the monent the process (2) is completed, by Eq. (1.40) we have

$$s_{H3}=\frac{2-\bar{g}}{\bar{g}+2}r_{H2}-\frac{2\bar{a}}{\bar{g}+2}, \tag{1.44}$$

after the process (3) is completed, by Eq. (1.42″) we have

$$s_{L3}=\frac{\bar{b}}{4}r_{H3}+\frac{(\bar{b}+4)}{4}s_{H3}+\frac{\bar{a}}{2}, \tag{1.45}$$

finally after the process (4) is completed, by Eq. (1.39)

$$r_{L4}=s_{L3}, \tag{1.46}$$

and consequently from (1.45) and (1.46) we have

$$r_{L4}=\frac{\bar{b}}{4}r_{H3}+\frac{(\bar{b}+4)}{4}s_{H3}+\frac{\bar{a}}{2}. \tag{1.47}$$

In this equation, as the values with suffix H correspond to the state of the fluid in the delivery pipe, we replace these by the values with suffix L which correspond to the suction pipe and introducing Eqs. (1.44), (1.43), (1.41′) and (1.46), we obtain

$$(\bar{b}-4)r_{L4}+\bar{b}r_{L3}-\frac{(\bar{g}-2)}{(\bar{g}+2)}\bar{b}s_{L2}-\frac{(\bar{g}-2)(\bar{b}+4)}{(\bar{g}+2)}r_{L1}=0. \tag{1.48}$$

However, as is seen from Fig. 1.7 (b), the point 2′ (r_{L1}, s_{L2}) and the point 5 (r_{L5}, s_{L2}) lie on the same Γ_-, furthermore on the u axis, which corresponds to $x'=0$, $s_{L2}=r_{L5}$ is satisfied because of Eq. (1.39). Consequently Eq. (1.48) reduces to the following form:

$$(\bar{b}-4)r_{L4}+\bar{b}r_{L3}-\frac{(\bar{g}-2)}{(\bar{g}+2)}\bar{b}r_{L5}-\frac{(\bar{g}-2)(\bar{b}+4)}{(\bar{g}+2)}r_{L1}=0. \tag{1.49}$$

In this equation, r_{L1}, r_{L5}, r_{L3} and r_{L4} are the magnitudes of the velocity variation at the points 1, 5, 7 and 6 respectively. Consequently this equation describes the vicissitude of a small disturbance.

Because the relation among the four values of r_L expressed in this equation is true for any band of width ε_0, we may select a band as standard and write r_{L1} as r_z, where we consider r_{L1} corresponds to zth band from the standard band.

Considering that m', n' and $N(N=m'+n')$ bands are contained between r_{L5} and r_{L1}, r_{L3} and r_{L1}, and r_{L4} and r_{L1} respectively as stated before, we may write as $r_{L5}=r_{z+m}$, $r_{L3}=r_{z+N-m'}$ and $r_{L4}=r_{z+N}$, and with these notations Eq. (1.49) reduces to

$$(\bar{b}-4)r_{z+N}+\bar{b}r_{z+N-m'}-\frac{(\bar{g}-2)}{(\bar{g}+2)}br_{z+m'}-\frac{(\bar{g}-2)(\bar{b}+4)}{(\bar{g}+2)}r_z=0. \tag{1.50}$$

This is the fundamintal equation which determine the stability or unstability of

phenomenon. We deduce the condition of stability with this equation in the following.

As Eq. (1.50) is a difference equation which expresses the linear relation among the four values of r, we may put $r=CX^z$ and we have

$$(\bar{b}-4)X^N+\bar{b}X^{N-m'}-G\bar{b}X^{m'}-G(\bar{b}+4)=0, \tag{1.51}$$

where

$$G=\frac{\bar{g}-2}{\bar{g}+2}.$$

When Eq. (1.51) has no multiple root, using the N roots of Eq. (1.51) we may write r_z as follows:

$$r_z=\sum_{i=1}^{N}c_iX_i^z. \tag{1.52}$$

Consequently for the decrease of r_z with increasing z, or with the lapse of time, the condition $|X_i|<1$ must be satisfied. Accordingly it is clarified that the condition of stability is equivalent to the condition that all roots of Eq. (1.51) exist within the unit circle on the complex plane. This statement is also true when Eq. (1.51) has some multiple roots.

Now, the necessary and sufficient condition under which all roots of an algebraic equation of N degrees exist within the unit circle was given by Schur in a form shown below.[22] Namely, in the equation of the form

$$f(z)=a_0z^N+a_1z^{N-1}+\cdots+a_N=0,$$

we define D_N as

$$D_N=\begin{vmatrix} a_0 & a_1 & \cdots & a_{N-1} & a_N & & & 0 \\ & a_0 & \cdots & & a_{N-1} & a_N & & \\ & & \ddots & & \vdots & & \ddots & \\ & & & \ddots & & \ddots & & \\ 0 & & & & \ddots & & & \\ & & & a_0 & a_1 & \cdots & \cdots & a_N \\ \hline \bar{a}_N & \bar{a}_{N-1} & \cdots & \bar{a}_1 & \bar{a}_0 & & & 0 \\ & \bar{a}_N & \cdots & & \bar{a}_1 & \bar{a}_0 & & \\ & & \ddots & & \vdots & & \ddots & \\ & & & \ddots & & \ddots & & \\ 0 & & & & \ddots & & & \\ & & & \bar{a}_N & \bar{a}_{N-1} & \cdots & \cdots & \bar{a}_0 \end{vmatrix} \tag{T.1}$$

then defining D_{N-1} as the determinant which results from removing two rows and two columns corresponding to Nth and $2N$th from D_N, and defining other determinants D_i's successively in the same manner until $D_1=\begin{vmatrix} a_0 & a_N \\ a_N & a_0 \end{vmatrix}$ is reached, the above mentioned Schur's condition is that all determinants D_i's are positive.

Finally, in our case, the condition under which the phenomenon is stable is stated as follows:

"The stability criteria for the phenomenon is that the all Schur's determinants of Eq. (1.51) are positive".

Thus we have obtained the mathematical representation of the condition of stability. However it is not so easy to decide the stability by the calculation of all D_i's, except the cases where $\xi = m'/(m'+n') = m'/N$ is a convenient number.

To cope with this, we must adopt adequate methods, for example, the numerical calculation of the roots of Eq. (1.51) for given $\bar{b}$ and G. However we show some simple examples in the following;

(i) The case in which the blower is connected to the suction end of the pipe-line ($\xi=0$). From the preceding discussion, we have $N=1$ and $m'=0$. Then Eq. (1.51) becomes an equation of one degree, and the condition of stability is easily obtained as follows;

$$\left| \frac{\frac{\bar{g}}{2}-1}{\frac{\bar{g}}{2}+1} \cdot \frac{\frac{\bar{b}}{2}+1}{\frac{\bar{b}}{2}-1} \right| < 1, \tag{T.2}$$

and this coincides with the stability criterion deduced by S. Fujii[2] by another method.

(ii) The case in which the blower is placed at the middle of the pipe-line ($\xi=0.5$). In this case $N=2$ and $m'=1$, then from $D_1>0$ and $D_2>0$, we have

$$\text{from } D_1>0, \qquad \left|1-\frac{2\bar{g}}{\bar{b}}\right| > 1, \tag{T.3}$$

$$\text{from } D_2>0, \qquad \left| \frac{\frac{\bar{g}}{2}-1}{\frac{\bar{g}}{2}+1} \cdot \frac{\frac{\bar{b}}{4}+1}{\frac{\bar{b}}{4}-1} \right| < 1, \tag{T.4}$$

in addition, when both $\bar{b}$ and $\bar{g}$ are positive, the former condition reduces to $\bar{g}>\bar{b}$.

In the following we examine the role of the blower for the vicissitude of disturbance, with the aid of Eq. (1.51). For this purpose we consider a case in which the disturbance reflects at the valve without any loss of energy and the vicissitude of the disturbance depends on the blower alone. That is, we assume that the valve is closed entirely. For this case, from Eq. (1.36) we have $\bar{g}=\infty$, and Eq. (1.51) reduces to the next form;

$$(\bar{b}-4)\,X^N+\bar{b}X^{N-m'}-(\bar{b}+4)=0. \tag{1.53}$$

Considering the relation between the roots and coefficients, we have

$$\prod_{i=1}^{N}|X_i| = \left|\frac{\bar{b}+4}{\bar{b}-4}\right|,$$

consequently if $\bar{b}>0$, $\left|\frac{\bar{b}+4}{\bar{b}-4}\right| > 1$ holds,

that is, it is clarified that if $\bar{b}>0$ is satisfied, at least one root exists outside of the unit circle and the phenomenon is unstable; in other words if the blower has a rising characteristic at the working discharge, it amplifies the disturbance regardless of its position in the pipe-line. Next, if $\bar{b}=0$ is satisfied we have easily $X^N=-1$ from Eq. (1.53), and this shows that all roots of Eq. (1.53) distribute on

the unit circle, and then the disturbance is neither amplified nor depressed by the blower (hereafter denote this as neutral). Next we examine if $\bar{b}<0$ is the condition of stability. Calculating Schur's D_1, we have

$$D_1 = \begin{vmatrix} (\bar{b}-4) & -(\bar{b}+4) \\ -(\bar{b}+4) & (\bar{b}-4) \end{vmatrix} = -8\bar{b}.$$

Consequently it is easily seen that $\bar{b}<0$ is a necessary condition for stability. To examine whether $\bar{b}<0$ is a sufficient condition or not, we must calculate all Schur's determinants D_i's, howsver it is very troublesome. We can instead discuss this problem rather more easily by the aid of Rouché's theorem,[23] but the process of discussion is omitted here.

The results obtained so far can be summarized as follows;

$\bar{b}<0$ is a sufficient condition for stability except for the cases in which the blower position coincides with a node of any normal mode of vibration of air column, where the state is neutral.

From above discussion we can conclude that if the inclination of the characteristic curve of the blower at the working discharge is negative ($\bar{b}<0$), the blower depresses the small disturbance except for the cases in which the blower position coincides with a node of any normal mode of vibration, if the inclination is horizontal ($\bar{b}=0$), the blower neither amplifies nor depresses and if the inclination is positive ($\bar{b}>0$, or the blower has rising characteristic), the blower always amplifies the small disturbance. In addition, when we examine the role of the blower under the condition that the valve is full open, where the disturbance reflects completely like the preceding case, the same conclusion can be obtained.

In the next place we examine the influence of valve on the propagation of disturbance. For this, we take up the case of $\bar{b}=0$ in which the blower has no influence on the vicissitude of disturbance. In this case Eq. (1.51) reduces to

$$X^N = -\frac{\bar{g}-2}{\bar{g}+2}, \tag{1.54}$$

and the condition of stability is written as

$$\left|\frac{\bar{g}-2}{\bar{g}+2}\right| < 1. \tag{1.55}$$

Because ordinary valves have such characteristic that the rate of outflow increases with the pressure at the valve end of the pipe-line, or $\bar{g}>0$, it is clear from Eq. (1.55) that valves depress the disturbunce excepting the cases of $\bar{g}=\infty$ and $\bar{g}=0$.

Further for $\bar{g}=\infty$ and $\bar{g}=0$, $X^N=-1$ and $X^N=1$ are fulfilled, and these correspond to the closed and full open states of the valve respectively, and as the reflection of disturbance is complete for both cases, it is clear that a valve does not affect the vicissitude of disturbance.

Finally, when we take the effect of valve into consideration, it can be concluded that the disturbance is always depressed if $\bar{b}\leqq 0$, and possibly amplified only in the case of $\bar{b}>0$. Fujii[2] deduced the similar conclusion for the case in which the blower is connected to the suction end of the pipe-line, however it is

interesting that the conclusion is also true for more general cases.

In this section we deduced the mathematical representation of the condition of stability and discussed the relation between the vicissitude of disturbance and the characteristics of the blower and the valve.

5. Graphical solutions of surging

In the preceding discussion, it is clarified that there is a posibility of amplification of a small disturbance near the working point of the blower only when the blower has a rising characteristic ($\bar{b}>0$) at the working point.

However even in such a case as above, where the vibration diverges, the reflection of disturbance becomes to obey the rule for the decending characteristic ($\bar{b}<0$) with the increasing amplitude, as seen from the form of the characteristic curve in Fig. 1.2, so it can be easily presumed that the amplification of the disturbance is restricted within a certain limit.

In this section we examine the behavior of disturbance with large amplitude by a graphical method. Here as a graphical method, we adopt the method of characteristic. In this method, the boundary conditions (Eqs. (1.31) ~ (1.34)) must be fulfilled graphically and this is done in this particular problem in the following manner.

In Fig. 1.8 (a) and (b), an example is shown.

This shows the process of solution for the case where the valve is closed abruptly from the state T_1 or T_1' (the prime indicates the state in the suction pipe) to the state T_2, and in this case the blower is at the midpoint of the pipe-

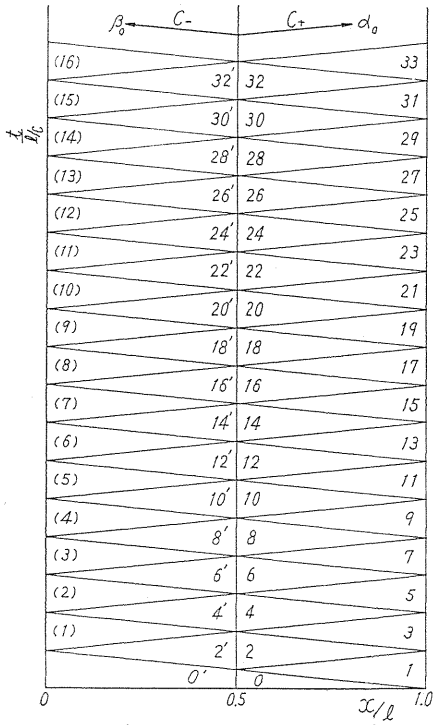

FIG. 1.8 (a). An example of procedure of graphical solution.

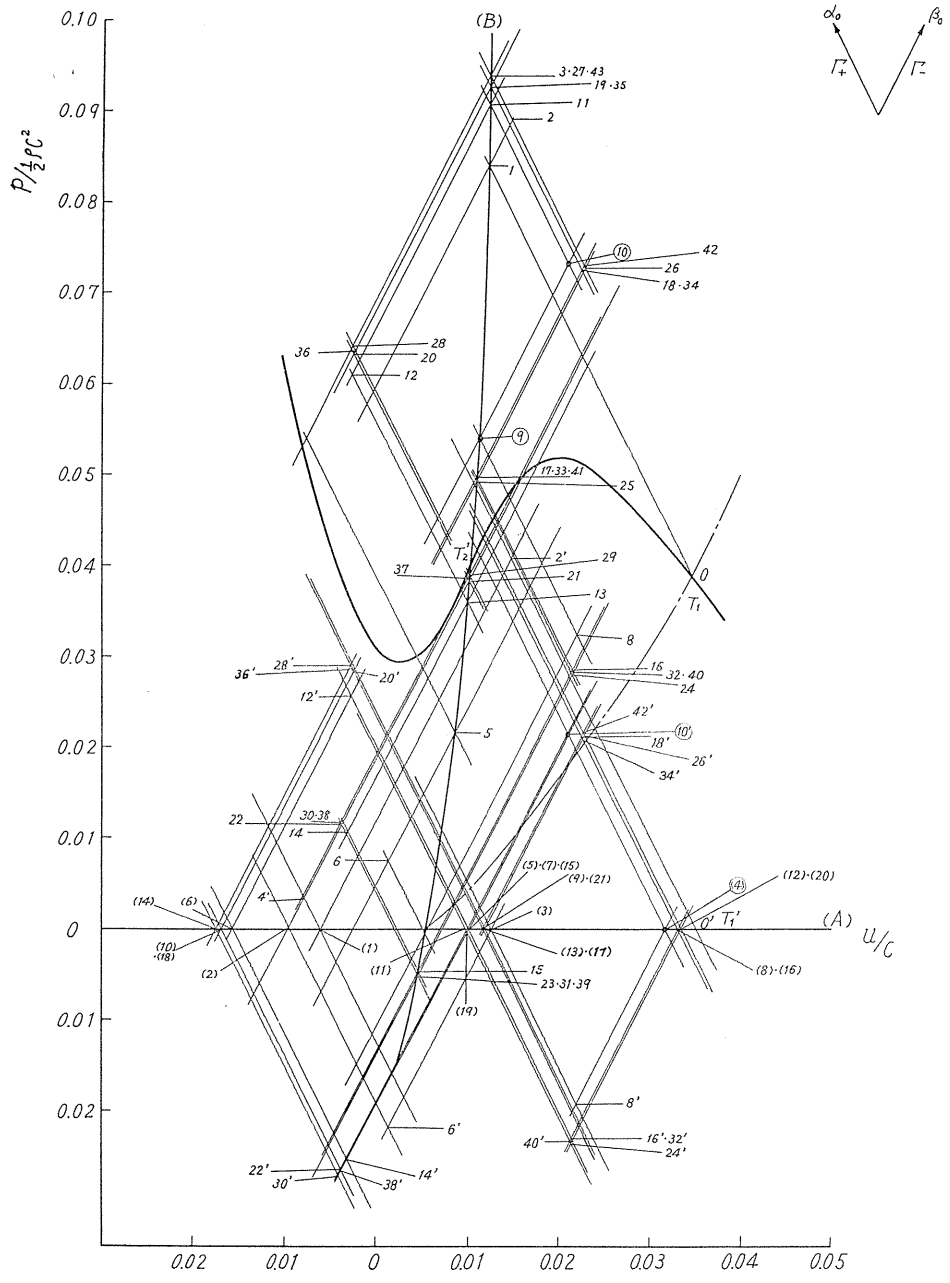

FIG. 1.8 (b). An example of procedure of graphical solution.

line. However, the following statement about the manner of fulfilling the boundary condition is quite general. Fig. 1.8 (a) and (b) show t', x' plane (*i.e.* $t/(l/c)$, x/l plane) and p, u plane (*i.e.* $p/(1/2)\rho c^2$, u/c plane) respectively, and a point on the p, u plane indicated by the same numeral with that written in a

small domain on t', x' plane, represents the state of fluid corresponding to that small domain. The boundary condition (1.31) corresponding to the suction end and (1.32) corresponding to the valve end can be represented on the p, u plane by two lines (A) and (B) respectively, as is generally known. The conditions at the blower position, (1.33) and (1.34), can be fulfilled in the following manner.

We locate two points which represent the states of the fluid in the suction and the delivery pipe at the blower position, for example 10 and 10′, which are enclosed by small circles in Fig. (b). This can be done considering the following requirements. First they must lie on the Γ_- and Γ_+ line respectively which pass through points 9 and (4), the points determined by the preceding step. Secondly they must have the same abscissa in order to satisfy the condition (1.33). Finally the difference of the values of ordinate between these two points must be equal to the ordinate of the characteristic curve corresponding to the common abscissa in order to satisfy the condition (1.34).

The results mentioned below are obtained in this manner. In this case because the surging commences in general in the running state where the valve is fairly closed, we treat the problem under such condition. We also assume that the initial disturbance is caused by an abrupt change of the valve opening.

Fig. 1.9 shows a special case in which the blower is connected to suction end of pipe-line. For this case Fujii[2] gave the solution by another graphical method, but for the sake of comparison with other cases we show the results here. In Fig. 1.9 the abscissa is non-dimensional time $t/(l/c)$, and the ordinate

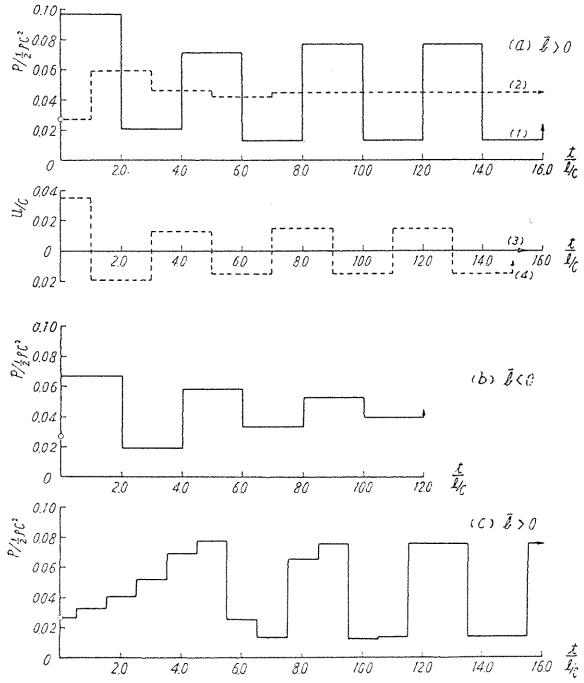

FIG. 1.9. Graphical solutions of surging ($\xi=0$ and valve is closed).

is non-dimentional pressure $p/(1/2)\rho c^2$ or non-dimensional velocity u/c.

(a) and (b) show the solutions corresponding to the cases in which the valve is closed abruptly from the stable running state of the blower. In (a) the blower

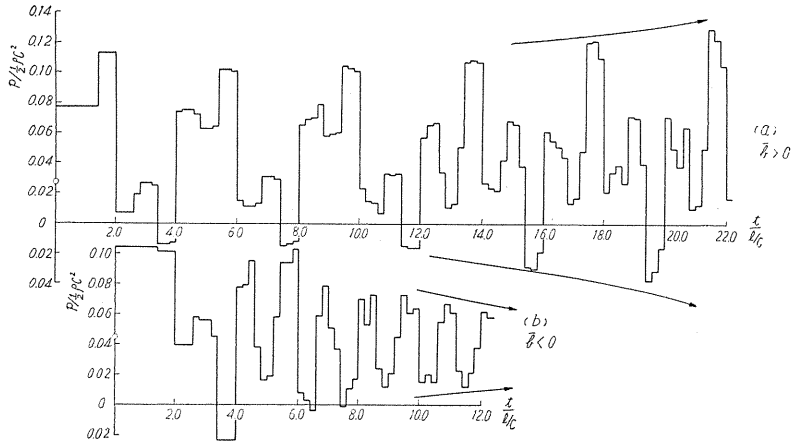

FIG. 1.10. Graphical solutions of transient pressure waves ($\xi=0.3$ and valve is closed)

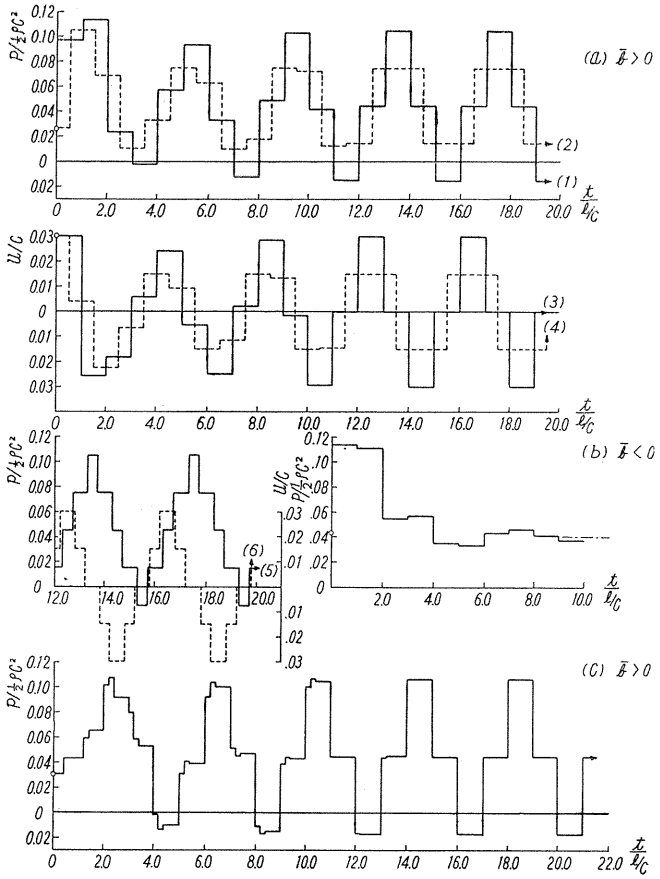

FIG. 1.11. Graphical solutions of surging ($\xi=0.5$ and valve is closed).

has a rising characteristic at cut-off ($\bar{b}>0$) and the lines (1), (2) show the pressure variations after the closing of the valve at the valve end and the blower end respectively, and (3), (4) show the velocity variations. In (*b*), the blower has a decending characteristic at cut-off ($\bar{b}<0$), and the pressure variation at valve end is described. Curve (*c*) shows the pressure variation at valve end which takes place after a stepwise closing of the valve, where $\bar{b}>0$ at cut-off. Comparing (*a*) with (*c*), it is clear that the pressure and the velocity variations converge to fixed rectangular waves irrespective of the nature of initial disturbance when $\bar{b}>0$, and from (*b*) it is also clear that when $\bar{b}<0$, an initial disturbance damps and a new equilibrium state is reached.

Fig. 1.10 shows a transient state of the pressure variation at valve end in the case where the blower position $\xi=0.3$ (m': $N=3$: 10) and the valve is closed abruptly. In this figure the blower characteristic at cut-off is $\bar{b}>0$ in (*a*) and $\bar{b}<0$ in (*b*) and for respective cases the vibration diverges or converges. The final wave form is not shown here.

Fig. 1.11 shows the results for the case of $\xi=0.5$ (m': $N=1$: 2) and the sign of $\bar{b}$ after the closing of the valve is shown in the figure.

Fig. (*a*) shows the case of abrupt closing of the valve and line (1) is the pressure variation at valve end, (3) is the velocity variation at suction end, (2) is the pressure variation at delivery side of the blower, (4) is the velocity variation at the same point (velocity variation is same as the suction side), (5) is the final form of the pressure variation at a point, the distance of which from the suction end is equal to 70% of the length of the pipe-line, (6) is that of the velocity variation at a point corresponding to 20% of the pipe length.

Further, (*b*) shows the pressure variation at valve end in the case of $\bar{b}<0$. and (*c*) shows the case of stepwise closing of the valve.

Fig. 1.12 shows the results for the case of the blower position $\xi=0.4$ (m': $N=2$: 5) and abrupt closing of the valve ($\bar{b}>0$). Line (1) shows the pressure variation at valve end, and (2), at the blower position, (3) is the static pressure of the blower, (4) is the velocity variation at suction end and (5), at the blower position (final wave form).

Next, Fig. 1.13 shows the results for the cases in which the valve is open to a certain degree, and the blower position is $\xi=0.5$ (m': $N=1$: 2). In this figure, (*a*) and (*b*) correspond to unstable $\left(\left|\frac{\frac{\bar{g}}{2}-1}{\frac{\bar{g}}{2}+1}\cdot\frac{\frac{\bar{b}}{4}+1}{\frac{\bar{b}}{4}-1}\right|>1\right)$ and stable $\left(\left|\frac{\frac{\bar{g}}{2}-1}{\frac{\bar{g}}{2}+1}\cdot\frac{\frac{\bar{b}}{4}+1}{\frac{\bar{b}}{4}-1}\right|<1\right)$ state respectively (cf. (T.4)), and the line (1) is the pressure variation at valve end, and (2), at the blower position (delivery side), (3) is the velocity variation at suction end, and (4), at the blower position and (5) is the velocity variation at valve end.

From Fig. (*a*) it is seen that when the condition of stability is not satisfied at the working point of the blower, the final wave form of disturbance is asymmetrical.

The characters of surging obtained from above treatment are summarized as

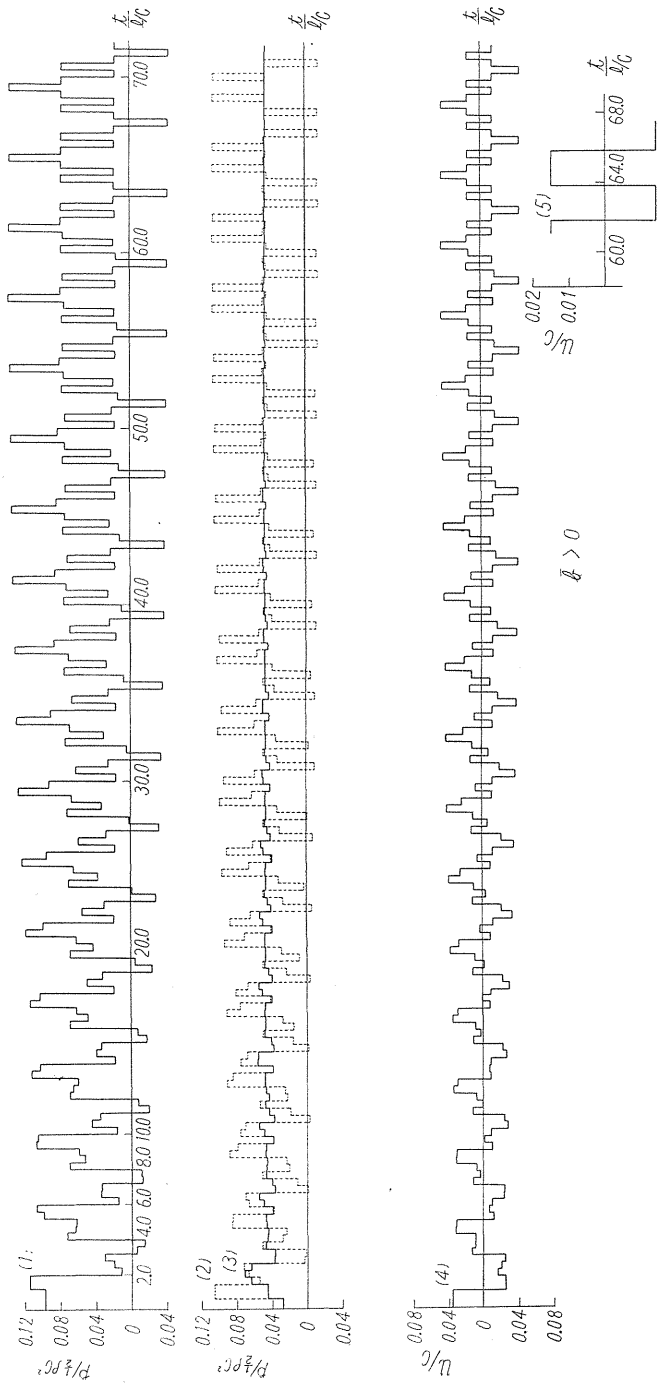

FIG. 1.12. Graphical solutions of surging ($\bar{\xi}$=0.4 and valve is closed).

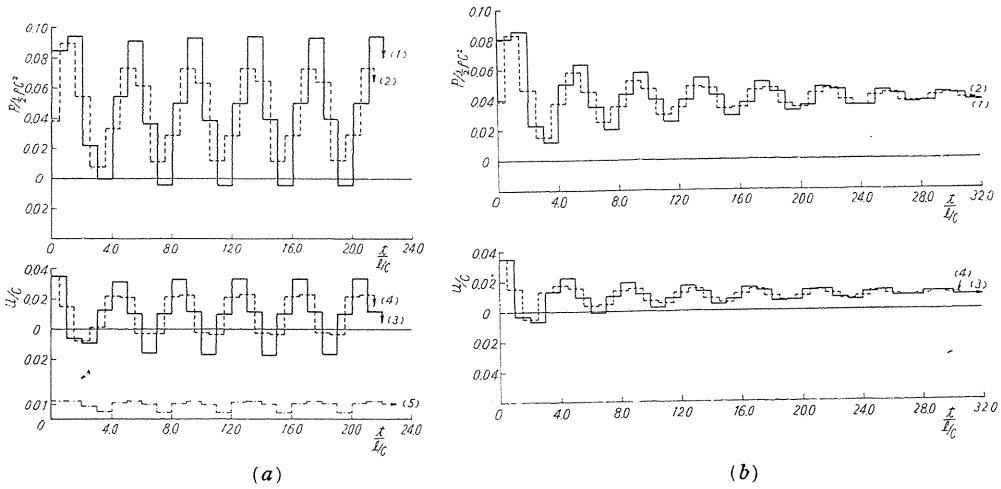

(a) (b)

FIG. 1.13. Graphical solutions of surging ($\xi=0.5$ and valve is slightly open). Working point of blower is unstable in (a) and stable in (b).

follows:

(i) When the condition of stability is not satisfied (especially if the valve is closed entirely, this corresponds to $\bar{b}>0$) at the working point of the blower, a disturbance build up into a fixed sustained vibration irrespective of its initial form, however the wave form changes along the pipe-iine. The final wave form depends on the blower position.

(ii) When the condition of stability is satisfied (especially if the valve is closed entirely, this correspond to $\bar{b}<0$), an initial disturbance damps and a new equilibrium state is reached.

(iii) When the valve is entirely closed or fairly closed, the fundamental period of sustained vibration is $4l/c$ and this is equal to that of free vibration of air column in the pipe-line.

(iv) When the valve is entirely ciosed, the final form of velocity variation at the blower position is rectangular (cf. the line (4) of Fig. 11 (a) and the line (5) in Fig. 1.12), however when the valve is open to a certain degree, above statement does not hold (cf. the line (4) in Fig. 13 (a)).

In the above we have studied the characters of surging which occurs in the pipe-line with uniform cross section. Next, we show an example of the case in which the pipe-line has a discontinuous change of the cross section in Fig. 1.14. In this pipe-line, the blower position is $\xi=0.5$ (m': $N=1:2$), the areal ratio is 1 : 2 (suction pipe versus deiivery pipe), the position of the discontinuity of the cross section coincides with the blower position and the valve is closed entirely (where, $\bar{b}>0$). In this case as the boundary condition at the blower position, we must take the following equation instead of Eq. (1.33),

$$A_L(u_L)_{x=\frac{1}{2}l}=A_H(u_H)_{x=\frac{1}{2}l}$$

where A_L and A_H denote the areas of suction and delivery pipe respectively.

In Fig. 1.14, line (1), (2) and (3) in (a) show the pressure variation at valve end, the velocity variation at suction end and the pressure variation at the blower

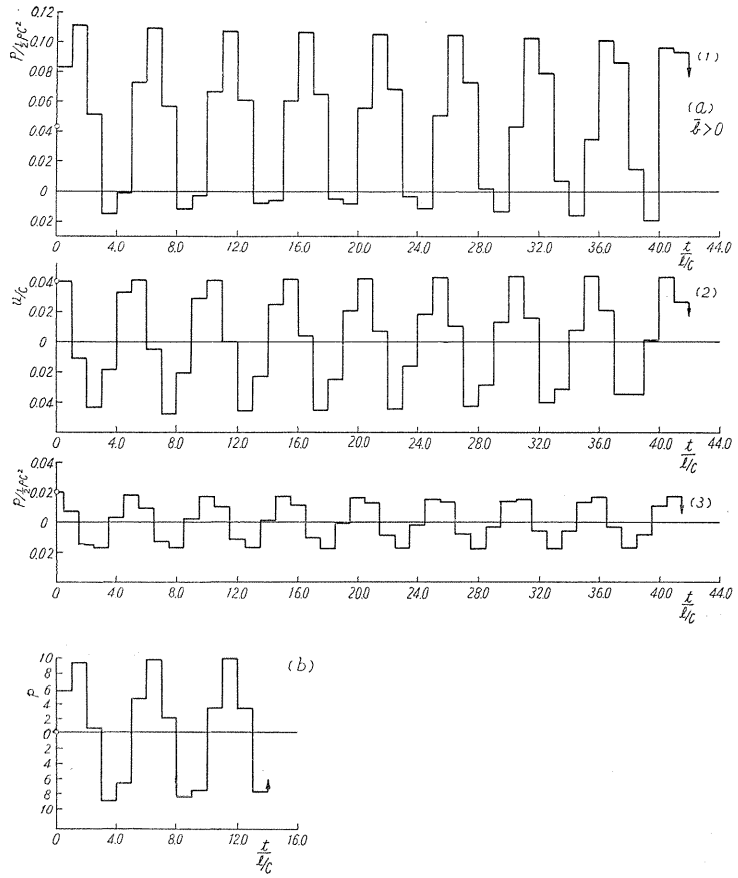

FIG. 1.14. Wave forms of surging in a pipe-line with a discontinuous cross section ($\xi=0.5$, areal ratio $=1:2$ and valve is closed).

position (suction side) respectively, and (b), which is shown for the sake of comparison, is an example of free vibration in the same pipe-line and shows the pressure variation at valve end, where the scale of ordinate is adequately chosen. As is seen in Fig. (b), the free vibration in such a pipe-line has no periodicity in a strict sense, namely the frequencies corresponding to normal modes of vibration of air column are expressed in the form $f=\gamma c/4l$, where γ's are the roots of the following equation,[24]

$$\frac{u_L}{u_H}=\frac{A_H}{A_L}=\tan\gamma\frac{\pi\bar{\xi}}{2}\cdot\tan\gamma\frac{\pi(1-\bar{\xi})}{2}, \tag{1.56}$$

and the values of γ are generally incommensurable each other. The surging which commences in the pipe-line of this type also has no periodicity, but its amplitude is nearly constant.

By compareing (a) with (b), it is seen that the existence of the blower has no influence on the mode of vibration as was case with the pipe-line with uniform

cross section. Nevertheless, it may be expected that the surging in such a pipe-line as this is observed in many cases as a periodic vibration having the frequency corresponding to the lowest value of γ of Eq. (1.56), because the components of higher frequencies are apt to die down.

6. On frequency of surging

As was seen in the preceding treatment, when we assume that the change of density of the air is small, the fundamental frequency of surging which occurs in a pipe-line with uniform cross section is equal to that of the free vibration and the magnitude of which is $c/4l$ with c being a constant, if the valve at pipe end is entirely or nearly closed.

On the other hand, when the blower of high pressure type is used, the change of density may not be neglected, and the frequency of surging would be different from $c/4l$.

When we treat the problem taking the change of density into account, we must adopt Eqs. (1.1) and (1.2) instead of Eqs. (1.3) and (1.4), but here we rather give an approximate treatment to the problem of the frequency of surging which occurs in a pipe-line with a blower of high compression ratio. That is, we assume that the sound velocities in the suction and the delivery pipe are different each other due to the change of state of the air, but the propagation of disturbance obeys Eqs. (1.3) and (1.4) as was the case in the preceding sections.

Under above assumption it can be considered that the effect of the change of state of the air on the frequency of surging is composed of the following two factors. The first is that the sound velocity in the delivery pipe differs from that in the suction pipe, and the second is that the mode of vibration changes caused by the discontinuity of density at the blower position. The extents of influence of the two factors on the frequency depend on both the compression ratio of the blower and the blower position.

The above statement about the second factor means that the abrupt change of density at the blower position causes discontinuity of volumetric flow and the change of mode results alike the case of the pipe-line with discontinuous cross section (cf. Eq. (1.56)), even if the system has the uniform cross section.

Next we compare the frequency of surging with that of free vibration under the atmospheric pressure for a pipe-line of uniform cross section with a closed valve end. Assuming that the compression is adiabatic, we have

$$\frac{c_H}{c_L} = \left(\frac{p_H}{p_L}\right)^{\kappa-1/2\kappa}, \tag{1.57}$$

where c is the sound velocity, κ is the ratio of specific heat and suffixes H and L indicate the values corresponding to delivery and suction pipe respectively. The ratio of velocities in the suction and the delivery pipe is

$$\frac{u_L}{u_H} = \frac{\rho_H}{\rho_L} = \left(\frac{c_H}{c_L}\right)^{2/\kappa-1}. \tag{1.58}$$

Accordingly if the compression ratio of the blrower (p_H/p_L) is given, c_H/c_L and u_L/u_H are known, and when the suction pipe open to the atmosphere we can put

$c_L \fallingdotseq c_a$ (c_a is the sound velocity in the atmosphere).

The influence of the first factor mentioned above on the frequency of surging is estimated by Eqs. (1.57), under the consideration that because the sound velocity is high in the delivery pipe ($c_H > c_L \fallingdotseq c_a$), in proportion to this the frequency of surging becomes high.

Then the influence of the second factor is estimated by Eq. (1.56), considering that the air column vibrates with the same frequency as the fundamental frequency of a pipe-line with discontinuous cross section which would give the same discontinuity of the flow velocity as the value of u_L/u_H obtained by Eq. (1.58). The results of calculation are shown in Fig. 1.15. In this figure the abscissa is the compression ratio of the blower, the ordinate is the ratio of the frequency of surging (denoted by f_s), which is calculated in the foregoing manner, to that of free vibration under the standard state $f_a = c_a/4l$, and the parameter is the blower position ξ.

The dotted lines in the figure are the calculated values obtained taking the change of the sound velocity alone (*i.e.* the first factor) into account, the chain lines are the calculated values which descibe the effect due to discontinuity of the flow velocity (*i.e.* the second factor), and the full lines show the combination of above two effects, where the combination is obtained by multiplication.

As is seen from the dotted lines, the value of f_s/f_a increases with the compression ratio because the sound velocity also increases with this, and the degree of influence of this first factor becomes larger with the ratio of the length of delivery pipe to the total length of the pipe-line (or with decreasing ξ).

Next, the influence due to the change of mode of vibration reaches its maximum when the blower is located at the middle of the pipe-line ($\xi = 0.5$) and $f_s/f_a < 1$ is always fulfilled.

Accordingly when we take both influences into account, f_s/f_a becomes larger or smaller than unity as the case may be, as seen from the full lines (the full line corresponding to $\xi = 0$ coincides with the dotted line), in other words the frequency of surging becomes larger or smaller than that of the free vibration of air column under the standard state.

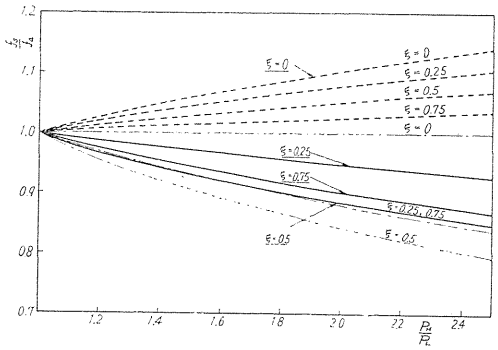

FIG. 1.15. Effect of compression ratio of blower on frequency of surging.

7. Conclusions

The results obtained from the study in this chapter may be summarized as

follows:

1. The condition of stability of a small disturbance in a pipe-line with a blower is equivalent to the condition under which all roots of Eq. (1.51) exist within the unit circle on the complex plane; namely the condition is that all Schur's determinants of Eq. (1.51) have positive values.

2. There is a possibility of amplification of a small disturbance near the working point of the blower only if the blower has a rising characteristic ($\bar{b}>0$) at the working point. And if the valve at pipe end is full open or entirely closed, $\bar{b}<0$ is the necessary and sufficient condition for stadility, however if the blower position coincides with a node of any normal mode of vibration of air column, the small disturbance is not depressed even if the condition $\bar{b}<0$ is satisfied.

3. When the cross section of pipe-line is uniform, and if the condition of stability is not satisfied, a disturbance builds up into a fixed sustained vibration independent of its initial form, however the wave form changes along the pipe-line. The final wave form depends on the blower position.

4. When the cross section of the pipe-line is uniform, the wave form of surging is periodic in a strict sense. On the other hand, when the pipe-line has a discontinuous change of cross section, above statement does not hold, but it may be likely that the surging in such a pipe-line is also observed as a periodic vibration if the component corresponding to a normal mode is dominant.

5. When the valve at pipe end is entirely closed, the final form of velocity variation at blower position is rectangular. However, when the valve is open to a certain degree above statement does not hold.

6. In the pipe-line with a blower of high compression ratio, the frequency of surging may be higher or lower than that of the free vibration of air column under the standard state, due to the fact that the state of air in the suction and the delivery pipe are appreciably different between each other.

Chapter II. Preparative Experiments[25]

1. Preliminaries

In the preceding chapter we have treated the surging phenomenon from the theoretical viewpoint. And when we deduce and solve the differential equtions, some idealized conditions were used; for instance, passage in the blower was represented by a point, and pipe friction was neglected.

So to obtain the detailed knowledge of the surging phenomenon we must do the experimental research. The theory suggests that the condition of stability of air column is influenced by the shape of the characteristic curve and that there is a close connection between the free vibration and the surging phenomenon.

So in this chapter, we deal with the problems of the free vibration and measurement of the characterlstic curves of blowers.

As to the problem of frequency of free vibrating air column, many studies have been done up to now, but only few experimental data[26][27] for the air column of large scale, such as that of the actual pipe system of the blower, have been presented.

And as to the problem of damping, Rayleigh and Lamb[28] treated it theoretically on the standpoint of acaustics, and recently P. Hadlatsch[29][30] studied the damping effects of the valve or opening, that is inserted in the pipe-line system,

on the propagating pressure wave from the thermodynamical viewpoint. But in the former theory, the problem is treated under excessively idealized coditions and the latter theory is too intricate, and experimental data are very few.

In this chapter the probrem of free vibration of air column in the pipe-line systems are treated experimentally, and especially, the effects of valve or opening in the pipe systems on the vibration are discussed.

2. Measurement of characteristic curves of blowers

We use two single-stage centrifugal blowers with no guide vane (blower B_1 and B_2). The types of blowers and dimensions of vane-wheels are summarized in Table 2.1.

TABLE 2.1. Dimensions of Vane-wheel

Blower	Related number of revolutions (r.p.m.)	Discharge (m^3/mn)	Effective total pressure (kg/m^2)	No. of vane-wheel	Diameter of vane-wheel (mm)	Outlet vane-height (mm)	Outlet vane angle	Inlet vane angle	Number of vane	Type of vane
B_1	3300	1.5	200	No. 1 No. 2	320 320	23.5 23.9	41°.58′ 25°	30° 30°	12 8	Backward curved Backward curved
B_2	2400	9.5	300	No. 3	514	23.0	68°.51′	24°	16	Straight

Two parts of the characteristic curve of each blower, namely the positive and negative discharge region, are measured separately. Fig. 2.1 (*a*) and (*b*) show the respective pipe-line systems for the measurement. When we measure the negative discharge region, a supplemental blower is used to obtain the negative flow in the blower test. And the rate of negative discharge is controlled by changing the number of revolutions of the supplemental blower.

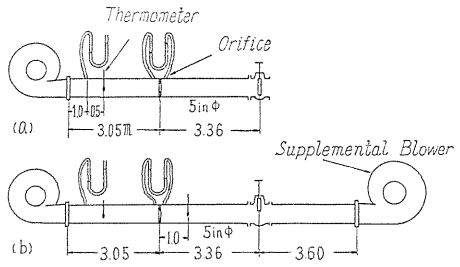

FIG. 2.1. Pipe-line systems for measurement of characteristic curve of blower.

Characteristic curves of the two blowers are shown in Fig. 2.2, in terms of φ and ψ (ψ is non-dimensional coefficient of total pressure and φ is that of discharge). These values are calculated by the following formulae,

$$\varphi = Q/\pi D b u_p, \quad \psi = P_t/(\rho u_p^2/2) \tag{2.1}$$

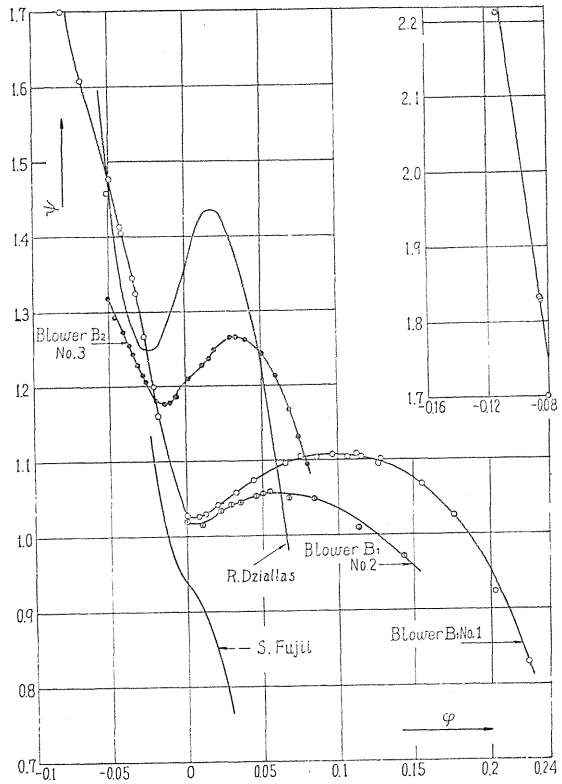

FIG. 2.2. Characteristic curves of blowers.

where

Q: discharge m^3/s,
D: diameter of vane-wheel m,
b: outlet vane height m,
u_b: peripheral velocity of vane-wheel m/s,
P_t: effective total pressure kg/m^2,
ρ: density of air $kg.s^2/m^4$.

For comparison, characteristic curves of pumps, given by S. Fujii[31] and R. Dziallas[32] respectively, are included in the same figure.

3. Experiments on free vibration of air columns

(3-1) Experimental apparatus and methods of experiments

Two types of pipe-lines with an open end are tested, one has a volume at another end of the pipe-line (Fig. (*a*)) and the other is without a volume (Fig. (*b*)). These are shown in Fig. 2.3. Dimensions of tested pipe-lines are summarized in Table 2.2. The pipe-lines are constructed by steel pipes (5 in. in diamerer, 0.01335 m^2 in mean cross sectional area).

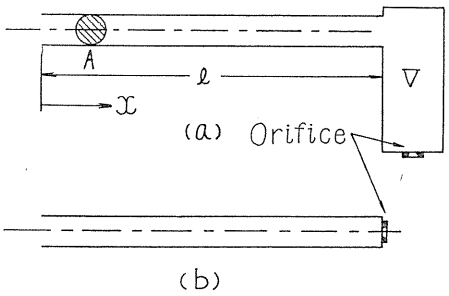

FIG. 2.3. Pipe-lines for measurement of free vibration of air column.

TABLE 2.2. Dimensions of Pipe-lines

Volume of tank $V=390.3\,l$		$V=127.8\,l$		$V=0\,l$	
No. of pipe-line	Length of pipe-line (lm)	No. of pipe-line	Length of pipe-line (lm)	No. of pipe-line	Length of pipe-line (lm)
I-1	1.541	II-1	1.698	III-1	7.938
I-2	3.091	II-2	3.252	III-2	3.060
I-3	4.601	II-3	4.758	III-3	4.575

For each pipe-line, many wall-orifices with various diameter are attached to the tank wall or clossed end and their effects on the vibrating air columns are examined. Moreover, using the pipe-lines of No. I-3 and III-3, the effects of valve, which is inserted into the pipe-line, on the vibration are studied. That is, various thin circular plates with concentric opening (these are regarded as the models of valves) are attached at various positions of pipe-lines, and effects of these are studied. The pipe-lines used later for the experiments of surging are also tested. The types of these pipe-lines are similar to those shown in Fig. 2.3, except that the blower B_1 is connected to their open ends, but the blower is not driven in the experiments of free vibrations. And the lengthes of these pipe-lines are in the range of 1.5~31.5 m.

To excite the free vibration of air column in the pipe-lines, we use a piston. That is, the piston is inserted into the pipe from the open end and drawn out abruptly. For the pipe-lines with the blower, the piston cannot be inserted, so for such pipe-lines we use the compressor of reciprocal type. Namely, at first the suction opening of the blower and exit opening of the pipe-line are coverd up by the rubber plates, and then air is sent into the pipe by the compressor through the small tap attached to the pipe-wall, and after the pressure rise of the air-column is attained, the rubber plates are removed abruptly, then the air column vibrates. The magnitude of pressure amplitude are about 150 kg/m^2.

To measure the pressure vibration, a pressure indicator has been made as in Fig. 2.4. This is connected to a pressure tap on the wall of the pipe-line or the tank through a short rubber tubing (about 40 mm in length and 10 mm in diameter), and the pressure variation is recorded on bromide paper by an optical method.

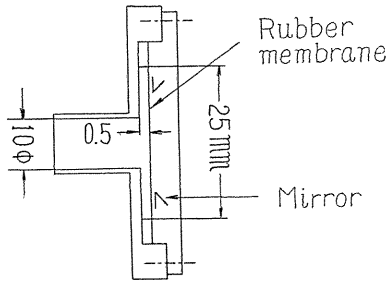

FIG. 2.4. Pressure indicator for measurement of free vibration.

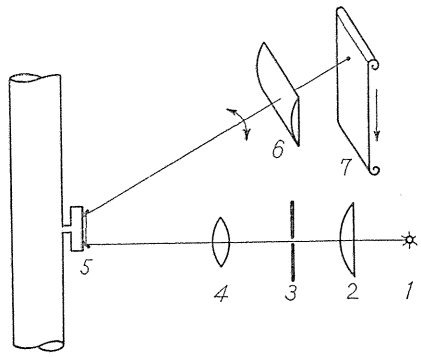

FIG. 2.5. Optical system.

Fig. 2.5 shows the optical system. In this figure, light source 1 is a lamp with a linear filament and the image of the filament is focused on the slit 3 by a condensing lens 2. And by a lens 4 and a cylindrical lens 6 the light beams through the slit 3 are converged on bromide paper 7 as a point.

A rubber diaphragm with two small mirrors (cf. Fig. 2.4.) vibrates according to the pressure variation in the pipe-line and the record is taken. Further, the standard tuning-forks, their period are 1/50 sec. and 1/100 sec. respectively, are used for the time index in the record.

(3-2) Results of experiments for pipe-lines without blower

At first we show the experimental results as to the frequency. The measured values of frequency of fundamental mode of vibration of air columns in the pipe-lines shown in Table 2.2, are summarized in Table 2.3. However these values correspond to the cases in which the exit openings (or orifices) of pipe-lines are closed.

TABLE 2.3. Frequency (fundamental mode $s=1$)

$V=390.3\,l$			$V=127.8\,l$			$V=0\,l$		
Length of pipe-line (m)	Measured value (c/s)	Calculated value (c/s)	Length of pipe-line (m)	Measured value (c/s)	Calculated value (c/s)	Length of pipe-line (m)	Measured value (c/s)	Calculated value (c/s)
1.541	7.58	8.01	1.698	12.47	13.07	3.060	27.30	27.80
3.091	5.44	5.60	3.252	8.97	9.20	4.575	18.25	18.60
4.601	4.43	4.56	4.758	7.26	7.43	7.938	10.55	10.73

In the above table, the calculated values are obtained by the following formulae originated from acoustics,[3]

$$k_s l \cdot \tan k_s l = Al/V, \quad f_s = k_s c/2\pi \tag{2.2}$$

where f_s: frequency, suffix s: index of the mode of vibration $s=1, 3, 5, \ldots$, c: velocity of sound. When we obtain the calculated values of frequencies in the above table, the value of c is taken as 340.67 m/s (this corresponds to 15°C), and

measured values also are given as their equivalence at 15°C.

From Table 2.3, we can conclude that the values of natural frequencies calculated on the basis of the acoustic theory hold sufficient accuracy even for a pipe-line of large scale.

Table 2.4 shows the measured values of fundamental frequencies ($s=1$) of the pipe-lines with different exit openings (or orifices).

TABLE 2.4. Effect of Small Opening on Frequency

Diameter of exit opening (mm)	$V=390.3\,l$			$V=0l$		
	$l=1.541$ m (c/s)	$l=3.091$ m (c/s)	$l=4.601$ m (c/s)	$l=3.060$ m (c/s)	$l=4.575$ m (c/s)	$l=7.938$ m (c/s)
0	7.58	5.44	4.43	27.3	18.25	10.55
14.8	7.56	5.51	4.41	27.9	18.86	10.64
20.0	7.56	5.52	4.48	28.9	18.74	10.76
25.0	7.68	5.55	4.48			
30.0	7.94	5.49	4.51			

This table shows that the small exit opening of the pipe-line increases slightly the frequency of the air column.

Hitherto we have shown the experimental results for the fundamental mode of vibration, but for the higher mode, experimental data show that the Eq. (2.2) holds good and small exit opening increases the value of frequency like the case of fundamental mode.

In the following we show the experimental results of the damping of free vibration. When we increase the area of opening (or orifice) attached at the tank-wall, the damping of vibration of the fundamental mode increases very fast, but

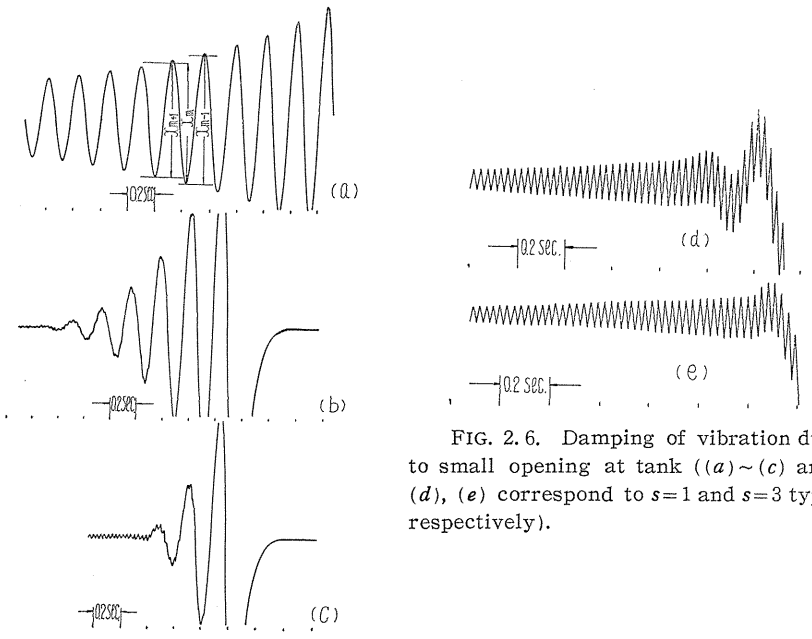

FIG. 2.6. Damping of vibration due to small opening at tank ((*a*)~(*c*) and (*d*), (*e*) correspond to $s=1$ and $s=3$ type respectively).

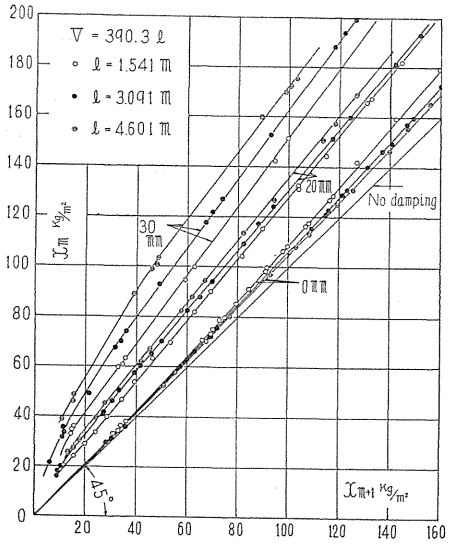

FIG. 2.7. Damping of vibration of fundamental mode ($V=390.3\,l$).

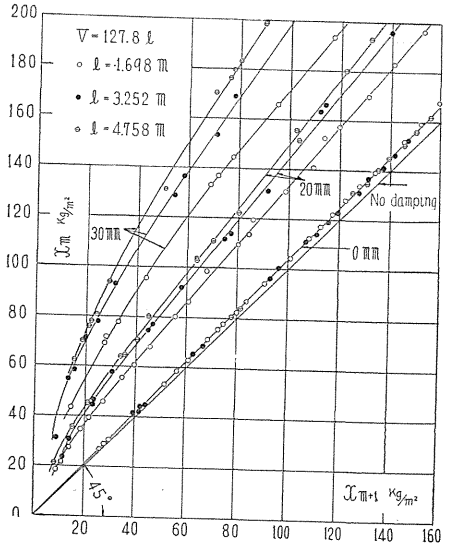

FIG. 2.8. Damping of vibration of fundamental mode ($V=127.8\,l$).

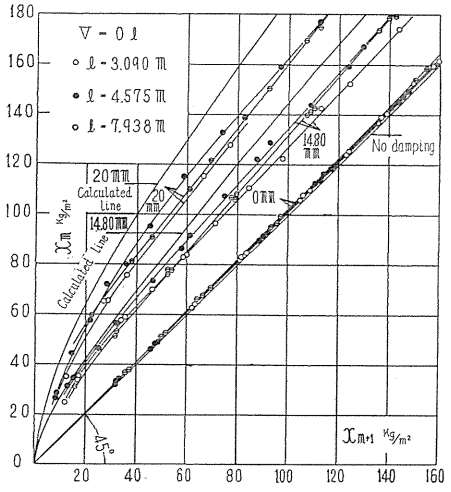

FIG. 2.9. Damping of vibration of fundamental mode ($V=0\,l$).

that of the higher mode increases only gradually.

Some examples of obtained photographs (used pipe-line is No. I-3) are given in Fig. 2.6, and in these, (*a*), (*b*) and (*c*) are fundamental modes and correspond to the diameter of orifice 0, 20 and 30 mm respectively. While (*d*) and (*e*) are second modes and corespond to 35 and 45 mm of orifice diameter.

Then in Fig. 2.7~2.9, the results of the measurement of damping for the fundamental mode are plotted, and the figures correspond to the pipe-lines I, II and III respectively. For the cases of Fig. 2.7 and Fig. 2.8, the used orifices are 0, 20 and 30 mm in diameter, and for Fig. 2.9, these are 0, 14.8 and 20 mm.

These figures are obtained by the following method. That is, the values of the successive double amplitudes x_{m-1}, x_m, x_{m+1}, ... (indicated in Fig. 2.6 (a)) are taken. And a point, which has x_m as the value of ordinate and x_{m+1} as abscissa, is located in the figure, and many points are obtained by the same procedure. When the damping of vibration is viscous (or linear) damping, a line joining these points is a straight line and passes the origin. Then using the following expression

$$p = p_0 e^{-\varepsilon t} \sin \omega t \qquad (2.3)$$
(p_0: inital value of p),

we can define the damping coefficient ε as follows;

$$\tan \theta = e^{\varepsilon \pi/\omega} \qquad (2.4)$$

where, θ is the inclination of the straight line.

By the expression mentioned above, we can easily see the nature of the damping which the vibrating air column exhibits. And from these figures (for example Fig. 2.7), we can see that the lines corresponding to the orifice of 0 mm (the pipe end or tank wall is closed entirely), curve upwards slightly, on the other hand those corresponding to the pipe-lines with the opening curve downwards.

From this fact, we can presume that the mechanisms of the damping are quite different between two cases and can conclude that the damping is not viscous.

Further, when the tank-wall has an opening, the value of damping increases with the area of the opening, and corresponding this, the line moves left in the figures. This tendency becomes remarkable as the tank volume V becomes smaller. And if the area of the opening and th length of the pipe-line are fixed (each figure contains the experimental result for the pipe-line of nearly equal length), the degree of the damping decreases with the tank volume. Moreover, the upward curvature of the line corresponding to the orifice of 0 mm, decreaces with increasing value of length l and decreasing value of tank volume V, and becomes straight.

For the pipe-lines without tank, the closed end is a node for all modes of vibration. And in these cases, when the area of the opening at the pipe end reaches a certain value, the record of the pressure shows only a very irregular vibration, and for the larger area of the opening, the vibration which corresponds to the pipe-line with two open ends arises. For an example, the experimental results are shown in Table 2.5, and dimensions of the pipe-line used are as follows: $l=1.86$ m, $A=0.006757$ m^2. From this table, we can see that the transition of the mode arises at rather small area of the opening. The meaning of the equivalent damping coefficient written in the table, shall be explined later.

TABLE 2.5. An Example of Transition of Mode of Vibration

(Area of opening) / (Cross sectional area of pipe)	Calculated value of frequency (c/s)	Measured value of frequency c/s	Equivalent damping coefficient (rad./s)
0 (one end is closed)	45.79	44.8	2.3
0.06		irregular variation of pressure	
0.27		85.5	5.1
0.65		88.3	4.7
1 (both ends are open)	91.57	88.5	3.8

(3-3) A consideration on damping of free vibration

First, we derive the theoretical formulae describing the damping effect of the opening on the vibrating air column, by a simple hydraulic consideration, the calculated values of damping by the formulae are compared with the measured values.

When the area of an opening is small, the values of the frequency of air column are nearly equal to those for the case of closed end. So we can write the equation of the mode of vibration as follows,

$$p_s = P_s \sin k_s x \tag{2.5}$$

where, P_s is the maximum amplitude of a pressure variation and p_s is the maximum value of the amplitude at a position x.

Here we assume that the air flows out from the opening during a half period of vibration, in which the air pressure inside the pipe end (or tank) is higher than that of outside, and the kinetic energy of air flow $\overline{W}$ is lost from the vibrating system. Similarly we assume that in another half period, the air flows into the pipe through the opening and the kinetic energy of this flow is compensated by the potential energy of the vibrating air column and this is lost entirely. Moreover, we adopt the formulae of stationary flow for the air flow through the opening, considering that the frequencies of phenomena are rather low.

Under the assumptions mentioned above, and using Eq. (2.5) we obtain the expression of the lost energy $\overline{W}$ in a half period of outflow,

$$\begin{aligned}\overline{W} &= \int_0^{T/2} \zeta S_0 \sqrt{\frac{2 p_s \sin \omega_s t}{\rho}} \cdot p_s \sin \omega_s t \, dt \\ &= \frac{\zeta S_0 \sqrt{2}}{\sqrt{\rho}} \sin^{3/2} k_s l \cdot P_s^{3/2} \int_0^{T/2} \sin^{3/2} \omega_s t \, dt \\ &= \frac{\zeta S_0 \sqrt{2}}{\sqrt{\rho}} \sin^{3/2} k_s l \cdot P_s^{3/2} \frac{1}{\omega_s} \frac{\Gamma\left(\frac{1}{2}\right) \cdot \Gamma\left(\frac{5}{4}\right)}{\Gamma\left(\frac{7}{4}\right)}\end{aligned} \tag{2.6}$$

where, ζ: coefficient of discharge, S_0: area of opening, T: period of vibration.

And the same equation holds for another half period of inflow. So we obtain the rate of dissipation energy W_1 as follows;

$$W_1 = \frac{\sqrt{2}\,\zeta S_0}{\sqrt{\rho}\,\pi} \sin^{3/2} k_s l \cdot P_s^{3/2} \frac{\Gamma\left(\frac{1}{2}\right) \cdot \Gamma\left(\frac{5}{4}\right)}{\Gamma\left(\frac{7}{4}\right)}. \tag{2.7}$$

The potential energy of the air column in the pipe-line V_0 can be evaluated as follows. That is, when the pressure rise at a position x in a pipe-line is Δp, the amount of compression of infinitesimal volume Adx is $Adx\Delta p/K$: where K is a bulk modulus. And the potential energy of compressed air of pressure p_s is

$$\int_0^{p_s} (Adx/K) p dp = \frac{1}{2} \frac{A}{K} p_s^2 dx.$$

Integrating this throughout the pipe-line, we obtain the value of V_0,

$$V_0 = \frac{1}{2}\frac{A}{K}\int_0^l p_s^2 dx + \frac{V}{K}(p_s)_{x=l}^2 = \frac{P_s^2 A}{4K\sigma_s} \tag{2.8}$$

where

$$1/\sigma_s = l\left\{1 + \frac{Al/V}{(Al/V)^2 + (k_s l)^2}\right\}. \tag{2.9}$$

Writing the pressure amplitude $P_s \sin k_s l$ at tank or pipe end as P_V and inserting it to the equation

$$\frac{dV_0}{dt} = -W_1, \tag{2.10}$$

we obtain the equation which describes the rule of damping,

$$\sqrt{P_V} = \sqrt{P_{V0}} - 0.2782\, KS_0\zeta(2/\rho)^{1/2}(2\sigma_s \sin^2 k_s l)(1/A)t \tag{2.11}$$

where P_{V0} is the initial value of P_V.

When the value Al/V is small and the mode of vibration is fundamental ($s=1$), above equation (2.11) is approximately written as

$$\sqrt{P_V} = \sqrt{P_{V0}} - 0.2782\, KS_0\zeta(2/\rho)^{1/2}(1/V)t. \tag{2.12}$$

The results from the above theory, are given in Fig. 2.10, together with the measured values. In the calculation we adopt $\zeta=0.6$, and the calculated lines from Eq. (2.11) are shifted to the left by the amounts equal to the difference of the values of abscissa between the measured lines of damping and the straight line which passes the origin and makes an angle of 45° with the holizontal axis (this line means no damping). Here by "measured lines" we mean the measured values

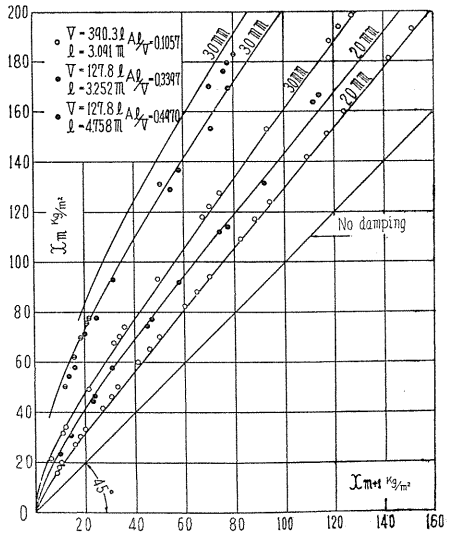

FIG. 2.10. Damping of vibation of fundamental mode (comparison between theoretical values and measured ones).

of the damping in the same pipe-line but without the opening, eventhough the mechanism of damping is quite different in this case.

As shown in the figure, the theory holds good. In this experiment, the range of values Al/V is 0.0527~0.497 and we can say that the damping effect of the opening can be estimated by Eq. (2.11) with sufficient accuracy for the pipe-lines in above range.

Further, for a pipe-line without a tank (that is $Al/V=\infty$), Eq. (2.11) reduces to the following form,

$$\sqrt{P_V} = \sqrt{P_{V0}} - 0.2782\, KS_0\zeta(2/\rho)^{1/2}(2/Al)t \tag{2.13}$$

and this equation gives rather larger values of damping than the measured ones: the caluculated lines of damping are shown in Fig. 2.9.

From above discussion, the damping effect of a small opening at the pipe end or tank wall on the vibration of air column is clarified.

And on the basis of this fact, we can infer as follows; a small opening whose position is near a node of a mode of vibration has a powerful damping effect on the vibration by the mechanism discussed above (needless to say, if the opening is large the mode of vibration itself changes), contrary the opening near a loop has less effect.

Above inference is confirmed by experiments. Some examples are given in Fig. 2.11. In the figure, the curves III, IV and V are experimental results for the pipe-line of $l=1.825$ m, $V=390.3\,l$, and III corresponds to the case of without opening, V to the case in which the opening is on the pipe wall near the open end (the distance is 7.9 cm and diameter of opening is 33 mm) and IV to the case in which the opening is at tank wall (diameter of opening is 30 mm). And only the curve IV, for which the opening is at a node of vibration, shows a large damping (frequency corresponding to this curve is nearly equal to those of III and V).

In addition, the curve II shows an example of damping of the vibration of second mode and is obtained under the following conditions; $l=13.00$ m, $V=390.3\,l$

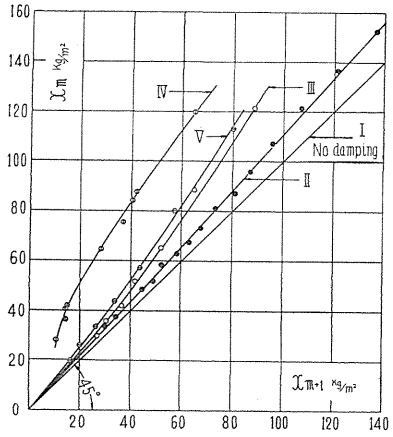

FIG. 2.11. Relation between position of small opening and damping of vibration.

and the opening is at tank wall. For this case, the position of the opening is near a loop of the second mode ($\sin k_s l=0.13$) and the form of the curve II is rather similar to that of a line of damping corresponding to the fundamental mode and without opening (cf. Fig. 2.6 (*d*), (*e*)).

In the next place, we consider the mechanism of damping of air column in the pipe-line without small opening.

By the usual method in the acaustics, the damping due to the acaustic radiation can be caluculated. In the method, the oscillating volume flow at open end of pipe is replaced by a simple source, the strength of which is equal to that volume flow. And by this method we obtain the formulae describing the nature of damping as below,

$$P_V = P_{V0} e^{-(\lambda_0/2\nu_0)t} \tag{2.14}$$

where,

$$\lambda_0 = (\omega_s A)^2/(8\pi Kc \sin^2 k_s l),$$
$$\nu_0 = A/(4 K\sigma_s \sin^2 k_s l)$$

and c: velocity of sound, K: bulk modulus.

Eq. (2.14) gives a viscous damping and can not explain the fact that the line describing the damping on the x_m, x_{m+1} plane has upward curvature, and moreover gives too small a value of damping compared with the measured one; for an example, $\tan\theta=1.0001$ (cf. Eq. (2.4)) for the pipe line of $l=2$ m, $V=390.3\ l$ and $A=0.01335$ m^2 and this value is too small.

In conclusion, it can be said that when the frequency of air column is low as in the case of surging, the damping effect due to the acaustic radiation is negligible and other factor plays an important role. Then we handle the problem by hydraulic consideration.

Under the assumptions that the energy loss due to the abrupt enlargement and contraction of air flow occurs at the junction of the pipe and the tank and at the open end of pipe, and that the vibration is in a normal mode, the rate of dissipation of vibrating energy W_1 is obtained in the form that $W_1 \propto P_V^3$. The energy loss due to the pipe friction can also be considered as $W_1 \propto P_V^3$. Puting these relations in Eq. (2.10), we obtain the formula describing the damping of air column as below,

$$\frac{1}{P_V} = \frac{1}{P_{V0}} + \nu_1 t \tag{2.15}$$

where, ν_1 is a constant depending on the dimensions of pipe-line.

The above equation shows that the damping is not viscous and the line of damping represented on the x_m, x_{m+1} plane has upward curvature; this means that the damping ratio increases with the amplitude of vibration.

As mentioned above, this equation explains the experimental result qualitatively, but quantitative agreement with the measurement is not so good, excluding the case of short pipe-line (about 3 m in length). This discrepancy is attributed to the fact that the energy loss due to the pipe friction for the vibrating air flow can not be estimated exacltly. However, from above discussion, we can see that

when a discontinuity of cross sectional area or accessories which act as resistance to the air flow (for examples a valve or a blower) exist, most of energy is lost in the form $W_1 \propto P_r^3$. And we can also presume that the discontinuous cross sectional area or the valve has the larger damping effect on the vibrating air column the nearer is their position to a loop of vibration.

(3-4) Effects of valve, opening and blower on vibrating air column

The effect of the valve, inserted at a point of pipe-line, on the vibrating air column is examined. The type of the pipe-line is the same as that shown in Fig. 2.3, and the exit opening (orifice) is closed. Three different ratios of the opening area to the cross sectional area of the pipe-line are used and they are 0.505, 0.249 and 0.1245 (about 1/2, 1/4 and 1/8) respectively. Here as a model of a valve, a thin iron plate with a opening is used, where this is set in the pipe-line in such a manner that the opening is concentric with the cross section of the pipe. The position of the iron plate in the pipe-line and the measured frequency of the air column are summarized in Table 2.6, where the position of plate is shown by the distance from the junction of the pipe to the tank for the pipe line with a tank, and from the closed end for the pipe-line without tank.

From this table, we can see that the opening of valve has no effect on the frequency and the mode of vibration, when the value of opening ratio is larger than 0.1.

TABLE 2.6. Opening Ratio and Frequency

No. of experiment	Distance from junction (m)	Frequency (c/s)
$l=4.610$ m $V=390.3\,l$ Opening ratio 0.505		
L_1	0.031	4.42
L_2	1.543	4.42
L_3	3.096	4.41
L_4	4.610	4.42
Same pipe-line Opening ratio 0.249		
L_1	0.031	4.43
L_2	1.543	4.46
L_3	3.096	4.44
Same pipe-line Opening ratio 0.1245		
L_1	0.031	4.41
L_2	1.543	4.41
L_3	3.096	4.39
L_0	without iron plate	4.44
$l=4.575$ m $V=0\,l$ Opening ratio 0.505		
L_1	1.511	18.5
L_2	3.061	18.3
L_3	4.575	18.1
L_0	without iron plate	18.3

Fig. 2.12 shows the results of mearsurement of damping. As seen in this figure, the damping of vibration occurs in such a manner that the damping ratio

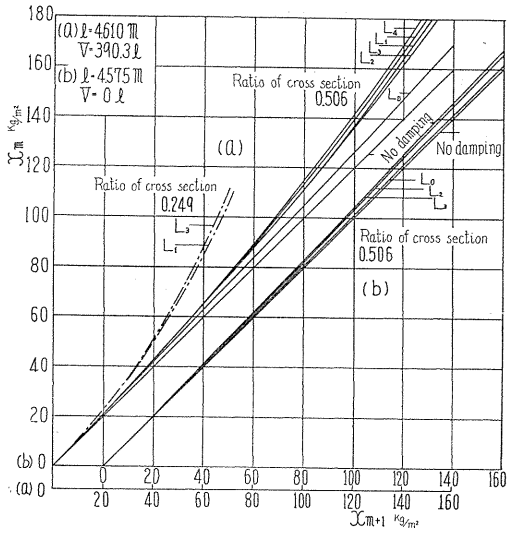

FIG. 2.12. Damping of vibration due to throttle valve inserted at a point of pipe-line.

increases with the increased amplitude (as mentioned in preceding section), and the magnitude of damping increases with the decreased value of opening ratio. When the opening ratio is fixed, the damping takes the larger value the nearer its position to a loop of vibration (for a fundamental mode, the open end of the pipe is the only loop).

Further, in the figure, the L_1 in (a) shows the larger damping than L_2 or L_3 and this fact contradict the above discussion. However, this is explained as follows; that is, for the case of L_1, the position of plate is very near to the junction of the pipe to the tank, and air flow diverges in the tank with the smaller areal ratio than the cases of L_2 or L_3.

From above consideration, we can presume that, when we controll the discharge by a valve, and if the system is in the surging state, the frequency is not affected by the opening ratio of the valve until the valve is nearly closed position; and when this state is attained, the type of surging will change into the type having a node at the closed valve.

Next, the effect of the blower (not driven) on the vibrating air column is examined. When a blower is connected to a pipe-line, the passage in the blower becomes a part of the vibrating air column, then the frequency of such system differs from the value calculated by Eq. (2.2) considerably.

The effect of the passage of the blower on the frequency of pipe-line can be represented by introducing the notion of equivalent pipe length (denote this as Δl). This Δl is defined as follows; with the measured frequency of the pipe-line with the blower, the value of l corresponding to that frequency is calculated by the Eq. (2.2), then the difference between the obtained value of l and the real length of the pipe is Δl.

The values of Δl obtained for many pipe-lines (l=1.5~31.5 m) are shown in Fig. 2.13. In this figure, the abscissa is the frequency and the ordinate is Δl. In

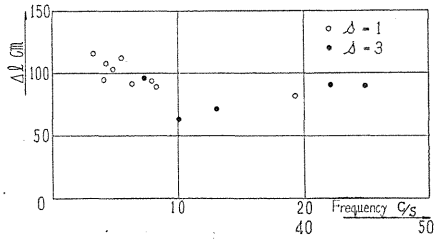

FIG. 2.13. Equivalent pipe length.

this experiment, the blower B_1 is used. It can be seen from above figure that the value of Δl varies depending on the pipe length and the mode of vibration, but the degree of variation is not so large. And for blower B_1, the value of Δl is in the range of 70~110 cm and this value is about 1.5~2.4 times as large as the mean diameter of the volute chamber of the blower.

Fig. 2.14 shows the damping effect of the blower on the vibrating air column in the pipe-line. And this figure is drawn with the experimental data for the pipe-line I in Table 2.2. The lines (1), (2) and (3) correspond to the case of pipe-line without blower. From this figure, we can see that the blower acts as a damping factor in the manner as the valve; that is the damping ratio increases with the increased amplitude, and this tendency becomes more remarkable in the case of a short pipe.

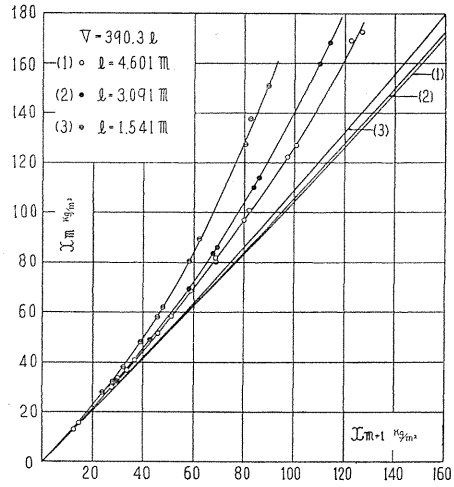

FIG. 2.14. Damping effect of blower on vibrating air column.

In Fig. 2.15, the values of equivalent damping coefficient (denote this as ε) corresponding to the mode of $s=1$, which are measured with many different pipe-lines without exit opening, are plotted against the amplitude of pressure variation (measured at tank or closed end). Regarding the damping of the vibrating air column as viscous one (cf. Eqs. (2.3) and (2.4)) we can estimate the equivalent

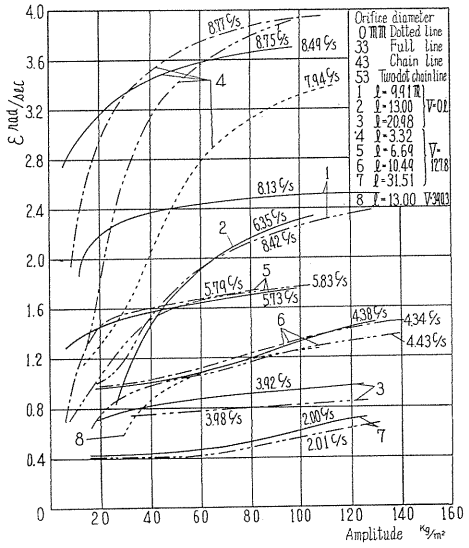

FIG. 2. 15. Equivalent damping coefficients for various pipe-lines.

damping coefficient ε from the inclination of the line on the x_m, x_{m+1} plane which passes through the point (x_m, x_{m+1}) and the origin of the coordinates. The values of ε obtained in this manner are plotted against the value of abscissa $(x_m+x_{m+1})/4$.

Further, the frequencies are also shown in the figure. From this figure, it can be seen that the value of ε decreases with decreased frequency (or in other words, increased pipe length) in most cases.

4. *Conclusions*

In this chapter, as a preparation for the study on the surging phenomenon, we have done the measurement of the characteristic curve of the blower, and the study on the free vibration of air column. The obtained results are summarized as follows:

1. The values of natural frequencies calculated on the basis of the acaustic theory hold sufficient accuracy even for a pipe-line of large scale.

2. An opening at the end of pipe-line has little effect on the frequency of vibrating air column, if its area is not so large that it must be regarded as an open end.

3. When the amplitude of pressure variation is not so large, a valve inserted into the pipe has little effect on the frequency even if the opening ratio is as low as 0.1.

4. The value of equivalent pipe length Δl of a blower is nearly constant in spite of the variation of the pipe length and the mode of vibration, and it is about 1.5~2.4 times as large as the mean diameter of the volute chamber of the blower.

5. When either the valve or the blower is in the pipe-line, the damping ratio of vibration of air column increases with the amplitude.

6. The damping effect of an opening on any mode of vibration of air column

is the greatest, when its position coincides with a node of the mode, and this fact can be utilized when we contrive the scheme for preventing the surging.

Chapter III. Experiments on Surging: Blower is Connected at Suction End of Pipe-Line[33)34)]

1. Preliminaries

In the preceding chapter we have shown the results of preparative experiments. And in this chapter we describe the results of experiments on the surging phenomenon.

On the surging, several researches have been conducted up to the present. However it is not yet clarified the relation between the actual state in which the surging occurs and the dimensions of pipe-line. So in the studies stated in the present chapter, we pay special attention to this question.

2. Experimental apparatus and methods of experiments

The blower B_1, shown in Table 2.1, is chiefly used in the experiments.

The pipe-lines (5 in. in diameter) are shown in Fig. 3.1. By varying pipe lengths l, tank volumes V, revolutions of vane-wheel n and relative positions of blower in the pipe-line ξl, the effects of these factors on the surging phenomenon have been examined. However, the detailed discussion on the effects of the last factor will be given in the next chapter.

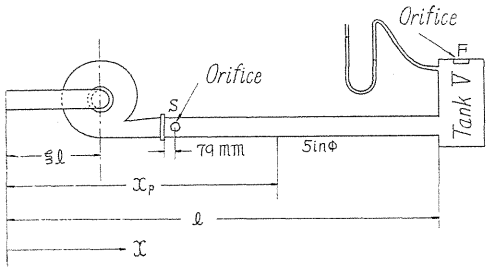

FIG. 3.1. Pipe-line.

Three series of pipe-lines are examined, and these correspond to the tank volume $V=0$ l (one end of the pipe is directly closed), $V=127.8$ l and $V=390.3$ l respectively and for each tank volume pipe length is varied in the range $l=9.91$ ~ 20.98 m, $l=3.32\sim 31.51$ m and $l=1.825\sim 24.45$ m.

Because the blower is driven by a D.C. motor, the number of revolutions n can be changed at any time from 900 to 5000 r.p.m.

Discharge is measured by wall-orifices, and is controlled by diameter of orifices. Since the position of exit opening (or orifice) has direct effect on the surging, which will be discussed later, two positions of an orifice are examined. One is position F and the other is S as shown in Fig. 3.1.

To investigate the surging phenomenon, the pressure variation and the velocity variation of air column in the pipe-line must be measured. The pressure indicator for pressure measurement has been made as shown in Fig. 3.2. This is

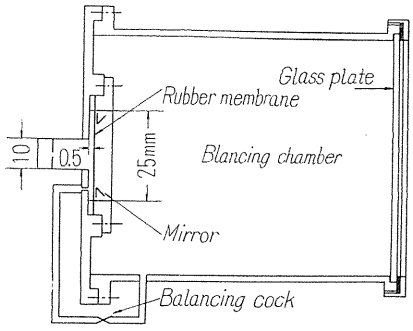

FIG. 3.2. Pressure indicator.

connected to a pressure tap on the wall of the pipe-line or to the tank through a short rubber tubing (about 40 mm in length and 10 mm in diameter). The record is obtained on bromide paper by the same optical system as mentioned in the preceding chapter.

The pressure in the balancing chamber of this indicator balances the static pressure of the blower through a balancing cock which is closed when the record is taken. This indicator can take sufficiently high frequency (above 500 c/s) as compared with the frequency of the surging. And the swing of the light beam on the bromide paper is exactly proportional to the pressure variation.

Velocity variation is measured by a hot wire anemometer. Output voltage of this anemometer amplified by a D.C. amplifier is recorded by an electro-magnetic oscillograph. The circuit is shown in Fig. 3.3. For the measuremsnt, the constant current method is adopted. A large resistance R_1 (about 120 Ω) is inserted in series in order to make the current variation of the circuit induced by the resistance variation of hot wire H (5 mm in length and 3/100 mm in diameter) negligiblly small. Consequently it is expected that the current in hot wire is held constant. The circuit constracted by R_2 and E_2 is to cancel the mean value of voltage drop of hot wire. Only the variation of valtage drop due to the resistance variation, which corresponds to the pulsation of air flow, is amplified by the D.C. amplifier.

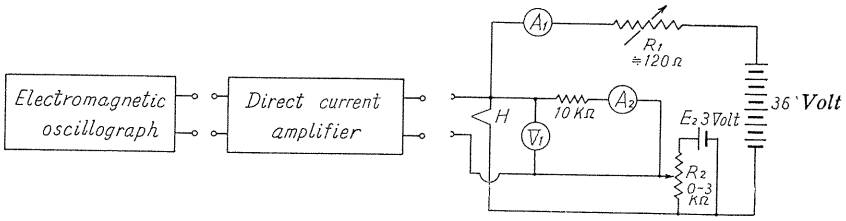

FIG. 3.3. Electric circuit for measurement of velocity variation.

3. *Results of experiments*

(3-1) Feature of surging

In order to know the feature of vibrating air column in the surging state, the amplitudes of pressure variation are measured at several points along the pipe-

line. The results are shown in Figs. 3.4, by dotted lines. Here the abscissa indicates the distance between the position where measurement is made and the junction of the pipe-line and the blower (in the case of (3) only, the origin of the abscissa is taken at the suction end of pipe-line), and the ordinate shows the non-dimensional amplitude expressed as the ratio to its maximum value. In this figure, the graphs (1) and (2) are results corresponding to two positions of exit opening or orifice (position S for (1) and position F for (2)) in the pipe-line of $l=24.45$ m, $V=390.3$ l, $A=0.01335$ m^2, $\xi=0$ ($n=3645$ r.p.m. for (1), $n=4640$ r.p.m. for (2) and non-dimensional discharge $\varphi\fallingdotseq 0.023$ for both).

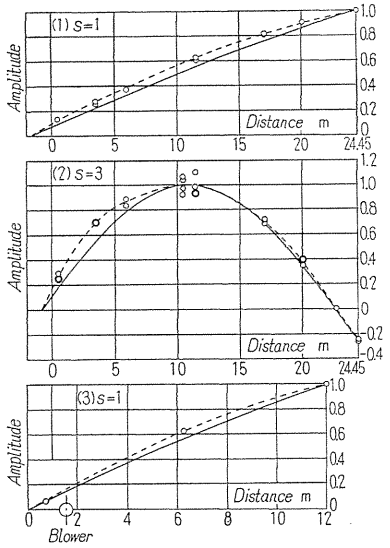

FIG. 3.4. Varation of pressure amplitude of surging along pipe-line.

The graph (3) corresponds to the case of $l=12.02$ m, $V=127.8$ l, $\xi=0.127$ and orifice position S. In this case the blower has a suction pipe and the phase of the pressure variation in the suction side is nearly equal to that in the delivery side.

For comparison, the curves representing the normal modes of free vibration are shown by full lines in each graph of Fig. 3.4. The value for these curves are calculated by Eqs. (2.2) and (2.5) shown in preceding chapter, that is:

$$p_s=P_s\sin k_s x, \qquad k_s l\cdot\tan k_s l=Al/V \tag{3.1}$$

where, suffix s, an odd integer, is the index of normal mode, p_s is the magnitude of pressure variation at position x, and P_s is the maximum value of p_s.

From these graphs, we can conclude that the variation of amplitude along the pipe-line resembles that of a normal mode of free vibration determined only by the boundary conditions and dimensions of pipe-line.

Some wave forms obtained for (1) in Fig. 3.4 are shown in Fig. 3.5. Here $x=5.946$ m for (a), $x=11.44$ m for (b), $x=17.00$ m for (c) and $x=24.54$ m for (d).

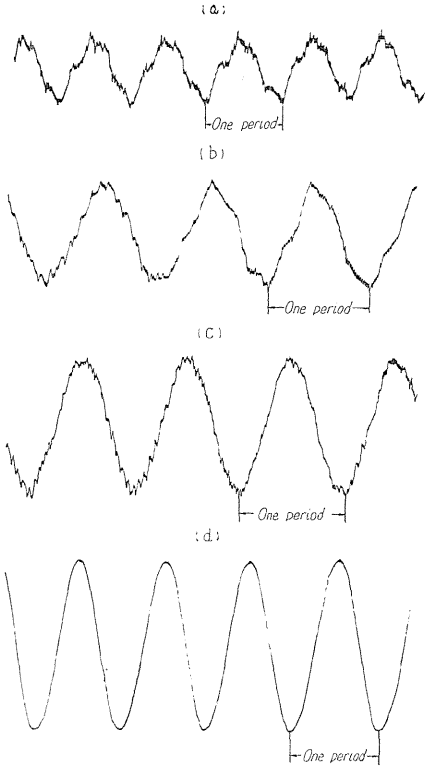

FIG. 3.5. Variation of wave form of surging along pipe-line.

From this figure we can see the fact that the wave form changes along the pipe-line (as discussed in Chapter I) but a component which corresponds to a normal mode (here $s=1$) is dominant as mentioned above.

Other examples of oscillograms are shown in Fig. 3.6. In this figure, (a) and (b), which correspond to the cases of (1) and (2) of Fig. 3.4 respectively, show the pressure variations in the tank and at the position of its maximum value respectively. The wave form is nearly sinusoidal, especially in the case where the type of surging is $s=1$. Fig. 3.6 (c) shows simultaneous indication of pressure and velocity in a pipe-line. The difference of phase angle between the velocity and the pressure is about 90°, resembling to the case of standing wave in free vibration, although in this photographic record, the wave form of velocity is distorted by a non-linear characteristic of the hot wire anemometer.

Using such a record as (c), we can describe a locus of the point representing the instantaneous state of air column at the measured position, on the φ, ψ coordinates plane; and this locus is a closed curve and changes its shape and dimension depending on the measured position.

(3-2) Frequency of surging

The frequency of surging changes with dimensions of the pipe-line. The values of frequencies for many different cases, are summarized in Table 3.1, and the corresponding natural frequencies are also shown in the same table for comparison.

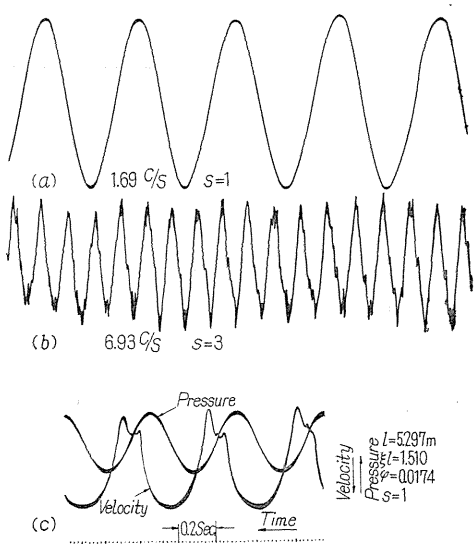

FIG. 3.6. Wave forms of surging.

TABLE 3.1. Frequency of Surging and Natural Frequency (15° C)

Conditions of experiment	Orifice diameter (mm)	Number of revolutions of blower (r.p.m.)	Frequency of surging (c/s)	Natural frequency (c/s)
	33	3150	5.13	5.73
	〃	3645	5.14	
	〃	4140	5.17	
	〃	4640	5.16	
$l=6.69$ m				
$V=127.8\,l$	43	3395	5.23	5.79
$\xi=0$	〃	3890	5.20	
Orifice position S	〃	4340	5.20	
Type of surging $s=1$	53	3645	5.30	
Vane-wheel No. 1	〃	4140	5.31	
	〃	4390	5.30	
	0			5.54
$l=10.94$ m	33	3890	4.11	4.43
Other conditions are the same as above	43	3395	4.13	4.38
Vane-wheel No. 1	53	3890	4.15	4.43
Vane-wheel No. 2	33	3395	4.08	4.38
$l=24.41$ m	33	3890	2.42	2.47
Other conditions are the same as above	53	〃	2.41	2.48
Vane-wheel No. 1				
$l=31.51$ m	33	3645	1.96	2.00
Other conditions are the same as above	53	〃	1.96	2.01
$l=20.98$ m				
$V=0\,l$	33	3890	3.72	3.92
Other conditions are the same as above				
$l=5.157$ m	23.51	4680	3.60	3.99
$V=390.3\,l$	29.51	〃	3.63	
$\xi=0$	35.95	〃	3.66	
Orifice position F	41.0	〃	3.60	
Vane-wheel No. 1	0			3.93
Type of surging $s=1$				
$l=24.45$ m	33	3235	6.80	7.24
$V=390.3\,l$	〃	4440	6.96	
$\xi=0$	〃	4680	6.92	
Orifice position F	29.51	〃	7.00	
Vane-wheel No. 1	0			7.13
Type of surging $s=3$				

These natural frequencies are measured under the condition that the blower is not driven. Working discharge of the blower corresponding to the orifice diameter of 0 and 53 mm (shown in Table 3.1) is $\varphi=0$ and $\varphi\fallingdotseq 0.066$ respectively in non-dimensional representation. When orifice diameter is zero, namely the discharge is zero, the surging does not occur, so for this case only the natural frequency is shown in the table.

As we can see in Table 3.1, the frequency of surging is almost independent of the number of revolutions and the type of vane-wheel, but determined only by dimensions and boundary conditions of the pipe-line. The frequency of surging is somewhat (2~10% in the present experiment) smaller than the natural frequency.

(3-3) Effects of working discharge and number of reveolutions of blower on surging

When the number of revolutions n is small, as the discharge of the blower is increased from cut-off condition, the state of air flow in the pipe-line becomes only slightely unstable in the range of $d\psi/d\varphi>0$. When n is larger than a certain value, however the surging clearly occurs in a part of the same range of φ, and the amplitude of surging varies with the discharge and takes a maximum value at a certain point in this range (but for the blower B_2, the feature of variation is different to a certain extent; in this case the amplitude of surging is muximum at cut-off and decreases with the value of φ).

An example is shown in Fig. 3.7. Conditions of this experiment are as follows: $l=13.00$ m, $V=127.8$ l, exit opening (orifice) S, and static pressure of the blower at cut-off are 269, 209 and 126 kg/m^2 corresponding to three blower speeds $n=3890$, 3395 and 3650 r.p.m. respectively.

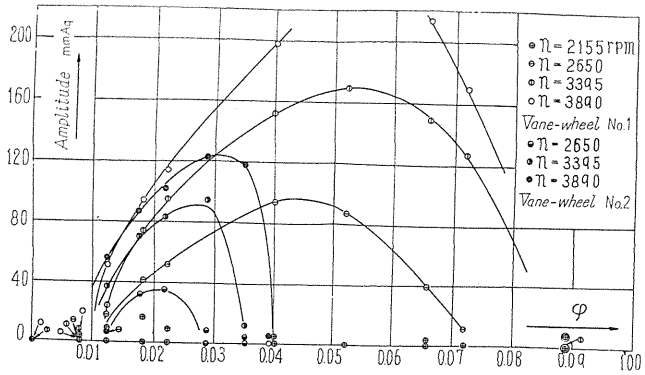

FIG. 3.7. Effects of rotating speed and working discharge of blower on surging.

In the figure, the amplitude of surging (the value at tank) is plotted against the non-dimensional discharge φ. Two groups of curves correspond to the cases for vane-wheel No. 1 and No. 2 respectively. Values of parameter n are also shown in the figure. The type of the surging corresponds to the normal mode $s=1$, for all cases.

From this figure, we can conclude that both the surging range of discharge and the amplitude increase with n.

The amplitudes of pressure variation at tank or closed end of pipe are plotted against n in Fig. 3.8. Here the results for six different pipe-lines are shown, where curves are drawn from the point at which the amplitude of surging becomes nearly constant. For all curves, the orifice position is S and the type of surging is $s=1$. Full line and chain line in this figure correspond to the cases $\varphi \fallingdotseq 0.0225$ and $\varphi \fallingdotseq 0.039$ respectively.

From this figure, we can say that in cases of orifice position S, when the volume of tank is constant, the surging is apt to be built up with the length of pipe-line, and the larger the value of $d\psi/d\varphi$, the more the surging is apt to occur; the value of $d\psi/d\varphi$ at $\varphi \fallingdotseq 0.025$ is larger than the value at $\varphi \fallingdotseq 0.039$ for this blower, as shown in Fig. 2.2.

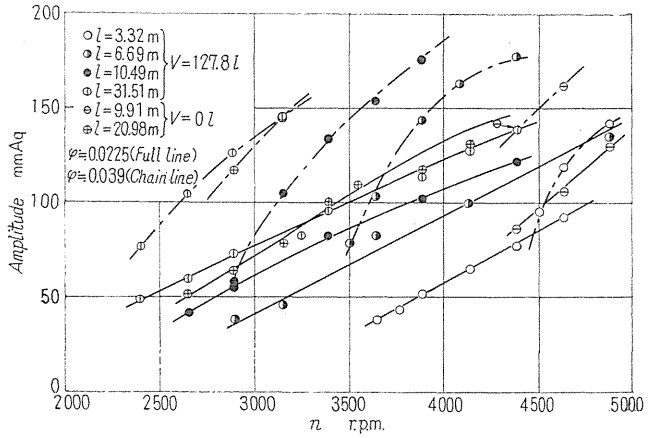

FIG. 3.8. Relation between rotating speed of blower and pressure amplitude of surging.

(3-4) Effects of length of pipe-line on surging

The relation between the amplitude of pressure variation and the length of the pipe-line is investigated with five pipe-lines of different length but with the same tank ($V=390.3$ l). In this experiment, the blower is connected to one end of the pipe-line ($\xi=0$) and the number of revolutions of blower n is kept constant.

The state of surging varies with the length of pipe-line, and the features of variation are entirely different for the two cases of orifice position S and F. These features will be discussed below separately.

Fig. 3.9 shows the result corresponding to the case of orifice position S, where $n=3475$ r.p.m. and the static pressure of the blower is about 217 kg/m^2 at cut-off. Here the abscissa is non-dimensional discharge φ and the ordinate is the amplitude of pressure variation at the tank. In this case, the component of pressure variation corresponding to the mode $s=1$ is dominant and that corresponding to $s=3$ is very small and unstable (the type of surging is $s=1$).

As seen in this figure, the amplitude of pressure variation increases with increase of pipe length, and the surging range of discharge also slightly increases with it.

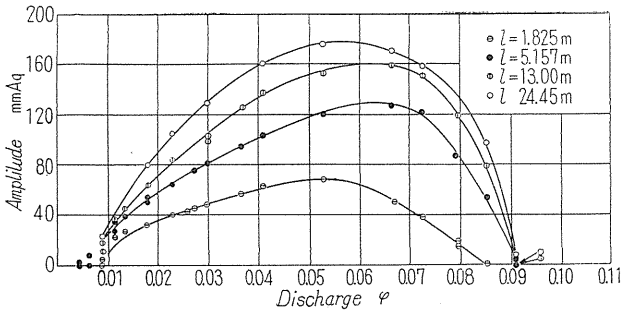

FIG. 3.9. Relation between pipe length and pressure amplitude of surging (orifice position S and type of surging $s=1$).

The results obtained for the cases of orifice position F are shown in Fig. 3.10 (a), (b) and Fig. 3.11, where the value of n is 4680 r.p.m. and the static pressure of the blower is about 385 kg/m² at out-off. In these figures, both components of pressure variation, which corresponding to $s=1$ and $s=3$, are shown separately. Values of amplitudes plotted in Fig. 3.10 are measured at the tank, and those in Fig. 3.11 are at the position corresponding to the node of $s=3$ type.

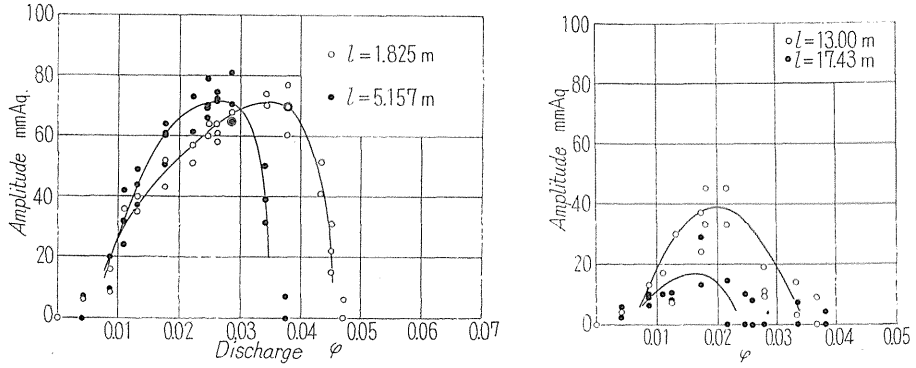

FIG. 3.10. Relation between pipe length and pressure amplitude of surging (orifice position F and type of surging $s=1$).

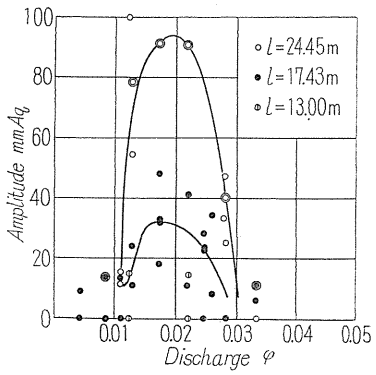

FIG. 3.11. Relation between pipe length and pressure amplitude of surging (orifice position F and type of surging $s=3$).

We can see from Fig. 3.10 and Fig. 3.11, the surging of the type $s=1$ is dominant when the length of pipe-line is short, but as the length of pipe-line increases, the type $s=1$ decreases and the type $s=3$ becomes dominant. But in the cases where the type $s=3$ is dominant, the type $s=1$ is dominant for very small discharge region of the blower.

As seen in these figures, the surging range of discharge and the amplitude of surging are remarkably smaller than those of $s=1$ in Fig. 3.9.

(3-5) Effects of volume of tank on surging

To investigate the effect of the volume of tank on the surging, two cases of valume ($V=127.8$ l and $V=0$ l) are examined in addition to the case of $V=390.3$ l which was discussed in the preceding section. For the case of $V=127.8$ l, the length of pipe-line l is changed from 3.32 to 31.51 m and n from 1500 to 5000 r.p.m., and for the case of $V=0$ l, l from 9.91 to 20.98 m and n from 1500 to 5000 r.p.m.

When the exit opening is at the end of pipe-line (orifice position F), sustained surging does not occur for all cases, and the air flow fluctuates only slightly in the range of discharge in which $d\psi/d\varphi>0$. From the above results and the result which was shown in the preceding section, it can be seen that the surging is apt to build up with increased volume of tank for the case of orifice position F.

For the case of orifice position S, the surging occurs for any pipe-line when n is larger than a certain value which depends on the tank volume and other conditions, and the type of this surging is always $s=1$.

An example of the results is shown in Fig. 3.12, where the amplitude of pressure variation (at tank) is plotted against n for various values of parameter φ.

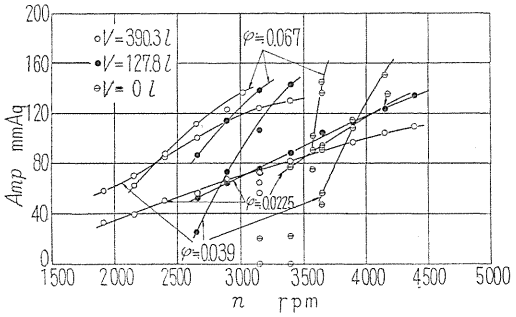

FIG. 3.12. Relation between tank volume and pressure amplitude of surging.

From these results, it can be seen that the surging occurs at low speed for larger tank volume, but its amplitude increases more rapidly with increased speed for smaller tank volume.

4. Considerations on results of experiments

(4-1) Variation of discharge in surging state

So far we have treated mainly the pressure variation of surging. Now, we consider the discharge variation at the position of the blower.

Several examples of curves, which indicate the relation between the amplitude

of discharge variation and the working discharge of the blower, are shown in Fig. 3.13, where both quantities are expressed in terms of non-dimensional quantity φ. These curves are drawn using the results of experiments with the vane-wheel No. 1 in Fig. 3.7, and the results for the pipe-line of $l=24.45$ m in Fig. 3.11, on the assumption that the relation between the pressure variation and the velocity variation in the surging state is same as that in the free vibration (cf. Fig. 3.4 (a) and Eq. (3.1)).

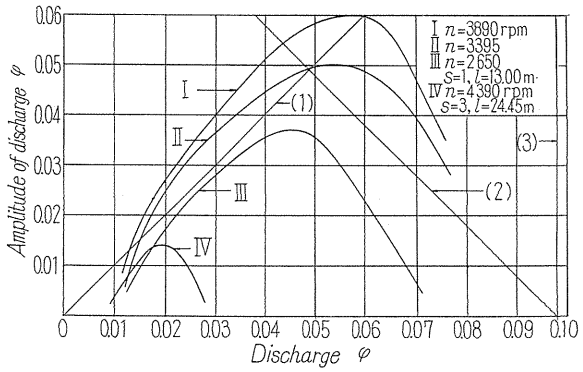

FIG. 3.13. Relation between working discharge of blower and amplitude of discharge variation.

Straight lines (1), (2) and (3) in Fig. 3.13 are drawn for easier appreciation of the graph: that is, the line (3) indicates the position of working discharge at which the blower shows a maximum head, the lines (1) and (2) make an angle of 45° with the horizontal axis, and when the curves exist in the domain above the line (1), it show that backward air flow occurs in a certain duration in one cycle of the surging and when they exist in the domain above the line (2), it shows that the discharge enters in the range of $d\psi/d\varphi<0$ beyond the point of maximum head.

From this figure, we can see that the state of surging changes with the number of revolutions n, from the state with no backward flow to the state with violent backward flow, and that the characteristic of the blower plays a more important role in determining the amplitude of the surging with an increased n (in the range of discharge of descending characteristic $d\psi/d\varphi<0$, the blower has a damping effect on the vibration as discussed in Chapter I).

(4-2) Effects of dimensions of pipe-line on surging

In Section (3-4), it has been shown that the state of the surging changes with l in quite different ways for the two cases of orifice position F and S.

In this section we explain this fact. Fig. 3.14 shows the relation between the values of the dissipation energy per unit time in the normal mode of free vibration (denote this as W_1) and the length of pipe-line. The values of W_1 are calculated from the results of experiments on the damping of the free vibration of air columns, which have been shown in Chapter II, and the ordinate in this figure is not the absolute value of the dissipation energy but its ratio to the value of the shortest one in a group of pipe-lines with the same tank.

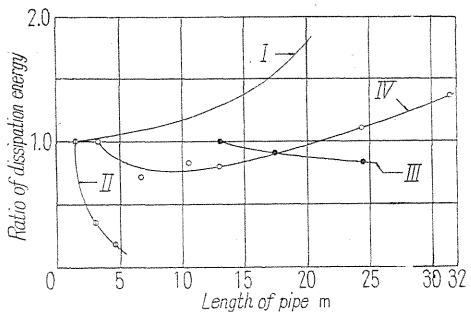

FIG. 3.14. Relation between energy dissipation and pipe length.

The curves I, II and III in Fig. 3.14 correspond to the cases of Section (3-4) (V=390.3 l), and the curve I is the case for orifice position F and the type of surging s=1 (orifice diameter is 30 mm, pressure amplitude at tank is 100 kg/m^2), the curve III, for orifice position F and s=3 (measured values for orifice diameter 20 mm are used for calculation), and the curve II, for orifice position S and s=1 (pressure amplitude at tank is 50 kg/m^2).

In the case of the curve I only, W_1 increases rapidly with l (it is worthy of notice that, in this case the position of the exit opening is at the node of vibration).

From this fact it can be considered that to elongate the pipe-line is more disadvantageous in case I for the occurence of the surging than in other cases.

As we have mentioned already, experimental results show that, for the case I, it becomes more difficult for the surging to occur with increased l but for the cases II and III, it is still apt to occur.

Therefore, we can conclude that the feature, in which the surging varies with l, is considerably influenced by the feature, in which W_1 varies with l.

In addition, the curve IV in Fig. 3.14 corresponds to the case of V=127.8 l and orifice position S. When the value of l is small, this curve declines as the curve II does, and the pressure amplitude of surging becomes large with l (cf. Fig. 3.8) again resembling to the case of curve II.

In conclusion, it can be said that the feature of the surging is determined by the mutual relation between the dimensions of the pipe-line and its accessories (exit opening or valve), because the dimensions of the pipe-line determine the normal modes of vibration and an accessory of the pipe-line has different damping effect on different mode of vibration (cf. Fig. 3.14) as mentioned in preceding chapter.

5. Conclusions

The results obtained from this experiment may be summarized as follows:

1. In the surging state, the air column in a pipe-line vibrates in a certain manner resembling to that of a normal mode of free vibration.

2. The more rapid the revolution of a blower becomes, the more violent the surging grows, and the more important role the characteristic of a blower plays in determining the amplitude of the surging.

3. When the length and area of a cross section of the pipe-line are fixed, the

surging is apt to build up according to the volume of tank.

4. The feature of the surging is considerably influenced by the conditions under which the energy is dissipated from vibrating air column through exit opening.

5. The surging usually occurs in the type corresponding to the fundamental mode of free vibration, but when the conditions of the pipe-line (*i.e.* dimensions of pipe-line and position of exit opening) are such that it has large damping effect on the vibration of this mode, the surging occurs in a type corresponding to higher mode.

Chapter IV. On Effects of Position of Blower in the Pipe-Line on Surgiug[35]

1. Preliminaries

In the preceding chapter, we have clarified the feature of surging, the frequency, the relation between the amplitude of surging and number of revolutions of the blower, and so on. And in this chapter, we examine the effect of the blower position in the pipe-line on the surging.

2. Experimental apparatus and methods of experiment

The blower B_1, shown in Table 2.1, is used in this experiment, with No. 1

TABLE 4.1. Dimensions of Pipe-line, Blower Position and Position at which Measurement is Made

Pipe-line	Blower position			Position at which measurement is made	
	ξ	Length of suction pipe (m)	Remarks	x_p (m)	Remarks
I $l=5.157$ m, $V=390.3\,l$, $n=4680$ r.p.m., Orifice F	0	0	loop of all modes	tank	node of $s=1$
	0	0		2.30	node of $s=3$
	0.293	1.51		tank	node of $s=1$
	0.654	3.37		tank	node of $s=1$
II $l=24.45$ m, $V=390.3\,l$, $n=4680$ r.p.m., Orifice F	0	0	loop of all modes	tank	node of $s=1$
	0	0		11.44	node of $s=3$
	0.1348	3.29		tank	node of $s=1$
	0.1348	3.29		11.44	nede of $s=3$
	0.2270	5.55	loop of $s=9$	tank	node of $s=1$
	0.2270	5.55		11.50	nobe of $s=3$
	0.2270	5.55		9.03	node of $s=9$
	0.3335	8.15	loop of $s=7$	tank	node of $s=1$
	0.3335	8.15		11.63	node of $s=3$, 7
	0.5015	12.26	loop of $s=5$	tank	node of $s=1$
	0.5015	12.26		5.95	node of $s=5$(suction side)
	0.5015	12.26		18.19	node of $s=5$(delivery side)
	0.9254	22.71	loop of $s=3$	tank	node of $s=1$
	0.9254	22.71		11.35	node of $s=3$
III $l=24.45$ m, $V=390.3\,l$, $n=4680$ r.p.m., Orifice S	0	0	loop of all modes	tank	node of $s=1$
	0.1348	3.29		tank	node of $s=1$
	0.2270	5.55	loop of $s=9$	tank	node of $s=1$
	0.3335	8.15	loop of $s=7$	tank	node of $s=1$
	0.9254	22.71	loop of $s=3$	tank	node of $s=1$

TABLE 4.1. (*Continued*)

Pipe-line	Blower position			Position at which measurement is made	
	ξ	Length of suction pipe (m)	Remarks	x_p (m)	Remarks
IV $l=20.04$ m $V=960.6\,l$ $n=4430$ r.p.m. Orifice F	0	0	loop of all modes	tank	node of $s=1$
	0	0		10.24	node of $s=3$
	0.1884	3.77		tank	node of $s=1$
	0.1884	3.77		9.76	node of $s=3$
	0.5170	10.35	loop of $s=5$	tank	node of $s=1$
	0.5170	10.35		9.54	node of $s=3$
	0.5170	10.35	loop of $s=3$		node of $s=5$
	0.9795	19.19		tank	node of $s=1$
	0.9795	19.19		10.03	node of $s=3$
	0.9795	19.19		5.39	node of $s=5$

vane-wheel. The pipe-line has the same form as that shown in Fig. 3.1. The volumes of tank at the end of pipe-line are $V=390.3\ l$ and $V=960.6\ l$.

In this experiment, the relation between the pressure amplitude and the discharge is measured for many positions of blower in a pipe-line, under the conditions of constant pipe-length and of constant number of revolutions of the blower.

And the pressure amplitude of air column and the discharge of the blower are measured by the same way mentioned in preceding chapter.

In Table 4.1, the dimensions of pipe-lines, the index of the blower position in the pipe-line, the position at which the measurement is made (denote this as x_p, this x_p is measured from a suction end ($x=0$) of the pipe-line) are summarized. The values of ξ and x_p are selected under following consideration. By the experiments of preceding chapter, it is confirmed that in the surging state, the amplitude of pressure and velocity variation varies along the pipe-line in a manner resembling that of a normal mode. So first we calculate the normal modes of free vibration by the following formulae (cf. Eq. (2.2) and Eq. (2.5)),

$$p_s = P_s \sin k_s x,$$
$$v_s = (P_s/\rho c)\cos k_s x = v_{\max}\cos k_s x$$

where,

$$k_s l \cdot \tan k_s l = Al/V, \qquad \omega_s = k_s c = 2\pi f_s, \tag{4.1}$$

P_s : maximum value of pressure amplitude,
p_s : pressure amplitude at x,
$v_{\max}$: maximum value of velocity amplitude,
v_s : velocity amplitude at x,
c : velocity of sound,
A : area of cross section of pipe-line (here, $A=0.01335$ m^2),
s : index of normal mode of vibration and an odd integer when we write $k_s = \alpha_s s\pi/(2\,l)$.

In Fig. 4.1, the variations of pressure amplitude along the pipe-line are shown taking the value of P_s as unit, for the pipe-lines II, III and IV shown in the Table 4.1; here (a) and (b) correspond to the pipe-line II, III and IV respectively, and for the former $s=1\sim9$, and for the latter $s=1\sim5$.

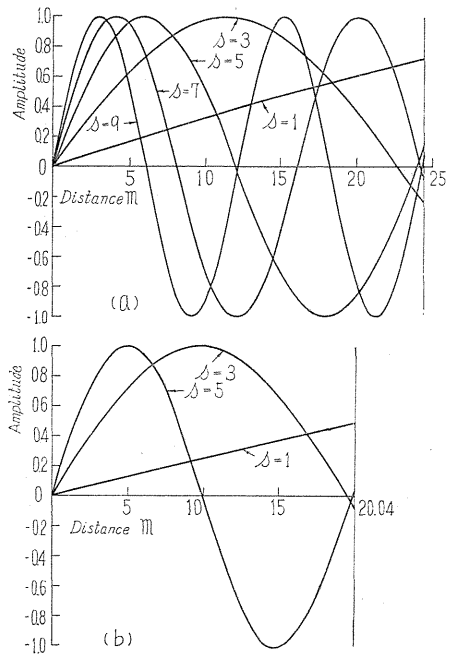

FIG. 4.1. Variation of pressure amplitude along pipe-line for various normal modes.

The discussion in Chapter I shows that, when the position of the blower in a pipe-line coincides with a node of a mode of vibration, the blower does not affect the vibration of that mode. Then from the contrast between a loop and a node as physical phenomena, we can presume that the blower have a drastic effect on the vibrating air column, when it is situated near a loop. So the value of ξ is selected, as far as possible, so that it coincides with a loop of a mode of vibration, and x_p corresponds a node.

The damping effect of the blower on the vibrating air columm is also measured for each blower position, to clarify the causes which affect the variation of the surging due to the blower position.

3. *Results of experiments*

Experimental result for the pipe-line I in Table 4.1, is shown in Fig. 4.2. In this figure the abscissa is the working discharge of the blower and the ordinate is the pressure amplitude of surging, and the parameter is ξ.

In this experiment the type of surging occured is $s=1$. This is known from the following observation. The pressure amplitude shows its maximum value at tank, which corresponds to a fundamental mode ($s=1$), and not only the wave form is nearly sinusoidal but also the frequency of the wave is nearly equal to the free vibration of $s=1$ type. Moreover the amplitude of component of vibration, which corresponds to $s=3$ type is nealy zero, even at the measuring point corresponding to a node of that mode; the position of the node is near the middle of the pipe-line.

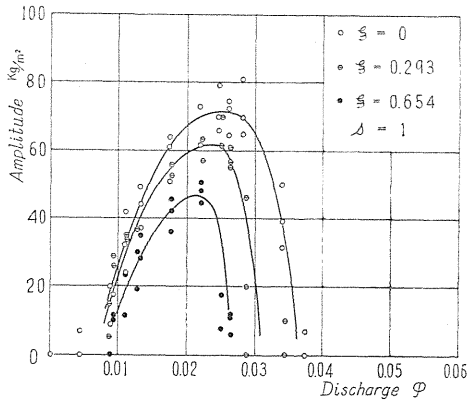

FIG. 4.2. Relation between pressure amplitude of surging and blower position in pipe-line (pipe-line I).

From this figure, it can be seen that the surging of $s=1$ type is most violent when the blower is connected to the end of the pipe-line ($\xi=0$), and less violent it becomes the nearer the blower position is to the tank. And the static pressure of the blower in the cut-off state, is about 381 kg/m².

Fig. 4.3 shows the experimental result for the pipe-line II in Table 4.1. Here the type of surging is $s=3$. As seen in the figure, the feature of surging remarkably changes depending on the value of ξ. That is, the surging occurs most violently when $\xi=0$, but in $\xi=0.277$, the vibration of air column almost disappers and this state of rather stable flow continues to the value of $\xi=0.5$, and beyond this value the fluctuation of flow occurs again and increases with the value of ξ, and the flow falls into the surging state and at $\xi=0.925$ the most violent surging takes place again (where the most part of the pipe-line is a suction pipe). In this figure, all plotted values of the pressure amplitude are those measured at a point of pipe-line corresponding to a node of $s=3$ type. And in the range of very small discharge ($\varphi \fallingdotseq 0.01$), the surging of $s=1$ type is dominant, and for that range, the values of pressure amplitude of $s=1$ type measured at tank are plotted. And the static pressure of the blower is about 381 kg/m² at cut-off state.

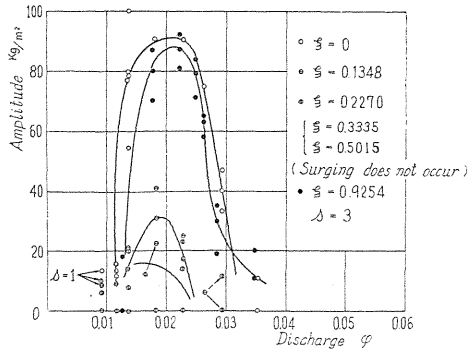

FIG. 4.3. Relation between pressure amplitude of surging and blower position in pipe-line (pipe-line II).

The frequency of the surging of $s=3$ type is almost independent of the value of ξ. This fact is shown in Table 4.2, and for comparison, the measured value and the calculated value by the formula (4.1) are given in the same table. In this table, the number of revolutions of the blower for each value of ξ is not kept constant, but it has little effect on the frequency of the surging as shown in Table 4.3. These experimental facts mentioned above support the conclusions in chapter I.

TABLE 4.2. Relation Between Blower Position and Frequency of Surging (Pipe-line is II, $s=3$ type, diameter of exit opening is 33 mm and values correspond to 15° C)

Blower position (ξ)	Frequency of surging (c/s)	Number of revolutions of blower (r.p.m.)	Natural frequency (c/s)
0	6.93	4390	
0.1348	6.92	4680	measured value=7.24
0.2270	7.09	4440	calculated value=7.50
0.3335	surging does not occur	4680	
0.5015	surging does not occur	4680	

TABLE 4.3. Relation Between Number of Revolutions of Blower and Frequency of Surging ($s=3$ type, diameter of exit opening is 33 mm, $\xi=0.1348$ and values correspond to 15° C)

Number of revolutions of blower (r.p.m.)	Frequency of surging (c/s)
3235	6.80
4440	6.96
4680	6.92

Moreover, in this experiment the surging does not occur in the type of $s=1$ (excluding in the range of very small discharge) and $s=5$, but in the case of $\xi=0.5015$, where the blower position almost coincides with a loop of the $s=5$ mode, the observation of pressure fluctuation at a point in the pipe-line corresponding to a node of that mode shows that the surging of $s=5$ type continues for a certain dulation, but it is unstable. From the results of this experiment, we can say in general that the surging corresponding to much higher mode is difficult to occur.

We examined also the relation between the pressure amplitude of surging and the number of revolutions of the blower. In this experiment, the value of non-dimensional discharge φ is kept constant ($\varphi \fallingdotseq 0.025$). The results are shown in Fig. 4.4. In this figure the abscissa is the number of revolutions of the blower, and the ordinate is the pressure amplitude of surging and the parameter is ξ. From this figure, it can be seen that the feature of the variation of the surging amplitude depending on the value of ξ is not affected by the number of revolutions of the blower n.

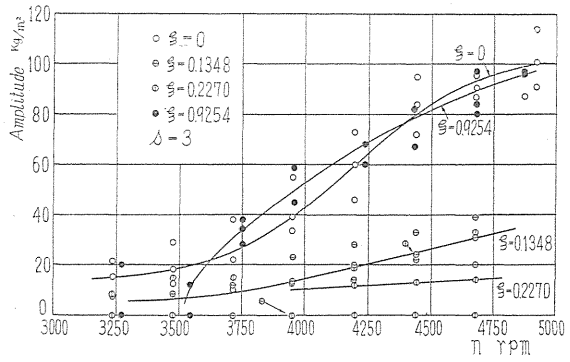

FIG. 4.4. Effect of rotating speed of blower on relation between pressure amplitude and blower position in pipe-line (pipe-line II).

Fig. 4.5 shows the result of experiment for the pipe-line III in Table 4.1. In this experiment, the exit opening is attached at the pipe-wall near the outlet of the blower (at S in Fig. 3.1), so its position moves towards the tank, with the change of the blower position. The type of surging occured is $s=1$.

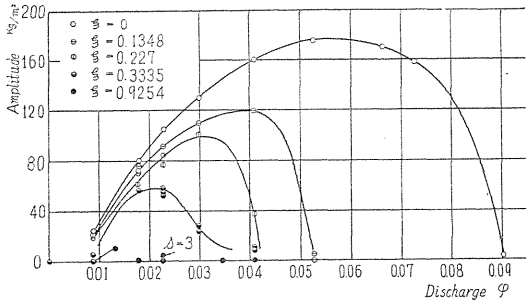

FIG. 4.5. Relation between pressure amplitude of surging and blower position in pipe-line (pipe-line III).

In Chapter II, we have shown that the damping effect of exit opening on the vibrating air column of any mode is greatest when its position is at a node of the mode, whereas it is least at a loop. In this pipe-line, $\xi=0$ is the case in which the exit opening position is near a loop of the mode $s=1$, and, in spite of the low speed of the blower, the surging zone and pressure amplitude is larger than those in the cases of pipe-lines I and II. And both the surging zone and pressure amplitude decrease with the increasing value of ξ, as is shown in Fig. 4.5. This tendency is similar to that for the pipe-line I, but the tendency is much more remarkable in this case. This experimental result may be attributed to the fact that the decrease of the amplitude is also induced by the increase of damping effect due to the approach of the exit opening to a node of vibration, in addition to the factors considered in the case of pipe-line I.

Moreover in this experiment, the static pressure of the blower is about 217 kg/m² at cut-off state. And this experimental result supports the conclusion con-

cerning the problem of the prevention of surging, mentioned in Chapter II, Section 4.

In Table 4.4 the relation between the blower position ξ and the frequency is shown. The table also containes the measured and calculated values of frequency of free vibration. From the record of the free vibration, it is clarified that, when $\xi=0$, the period of vibration is nearly independent of the amplitude, but when $\xi \neq 0$, it decreases with the decreasing amplitude. From this fact, we can presume that, in the pipe-line with the exit opening at the midway of the pipe-line, the mode of vibrating air column approaches gradually that of the pipe-line which has an open end at the position of the exit, with the decreasing amplitude. This tendency becomes more remarkable with shorter distance of exit position to the tank. The measured frequency listed in Table 4.4 is obtained by averaging the period of the photographic record during the time interval in which the amplitude of the damped pressure wave stay within the range from 200 to 150 kg/m^2. Then in the table, the frequency increases with the value of ξ. On the other hand, in spite of the change of the pressure amplitude with the increase of ξ, the frequency of surging is nearly constant. That is to say, when the surging once occurs the air column vibrates in the same mode independent of the position of exit opening. Moreover, the all values given in the table are those for the exit diameter 33 mm.

TABLE 4.4. Relation Belween Blower Position and Frequency of Surging
(Pipe-line is III, diameter of exit opening is 33 mm
and values correspond to 15° C)

Blower position	Frequency of surging (c/s)	Natural frequency (c/s)
0	1.69	1.73
0.1348	1.67	1.80
0.2270	1.69	1.88
0.3335	1.68	2.11
0.9254	surging does not occur	
		calculated vaiue=1.784

Fig. 4.6 shows the relation between the amplitude of surging and the number of revolutions of blower n, where $\varphi \fallingdotseq 0.025$. As seen in the figure, for $\xi=0.9254$, the surging of $s=3$ type occurs (when the value of n is large) in spite of the fact that the surging of any type does not occurs for $n=3\,475$ r.p.m. (cf. Fig. 4.5). This result may be explained as follows; for $\xi=0.9254$, the position of exit opening is near to a loop of the mode of $s=3$, and damping effect for that mode is very small, then the condition of self-excitation for that mode becomes to be satisfied first with the increased n. Further in the above figure, the plotted values of amplitude are measured in the tank, and the maximum value of the amplitude of $s=3$ type is about four times as large as the plotted value (as seen in Fig. 4.1 (a)). In the following, the experimental results for the pipe- line IV in Table 4.1 are shown in Fig. 4.7 (a)$\sim$(d). For this case, when ξ is fixed, a type of surging changes into another type at a certain value of discharge. And for each value of ξ, the pressure amplitudes

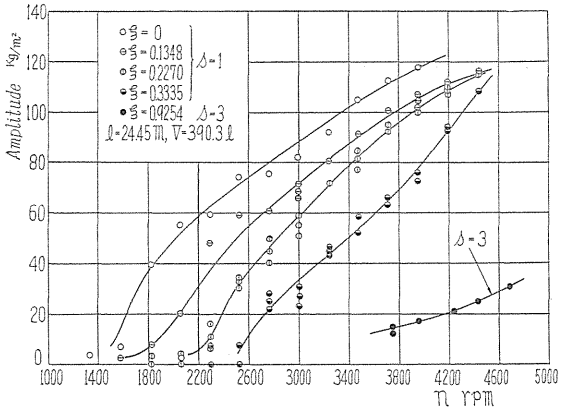

FIG. 4.6. Effect of rotating speed of blower on relation between pressure amplitude and blower position (pipe-line III).

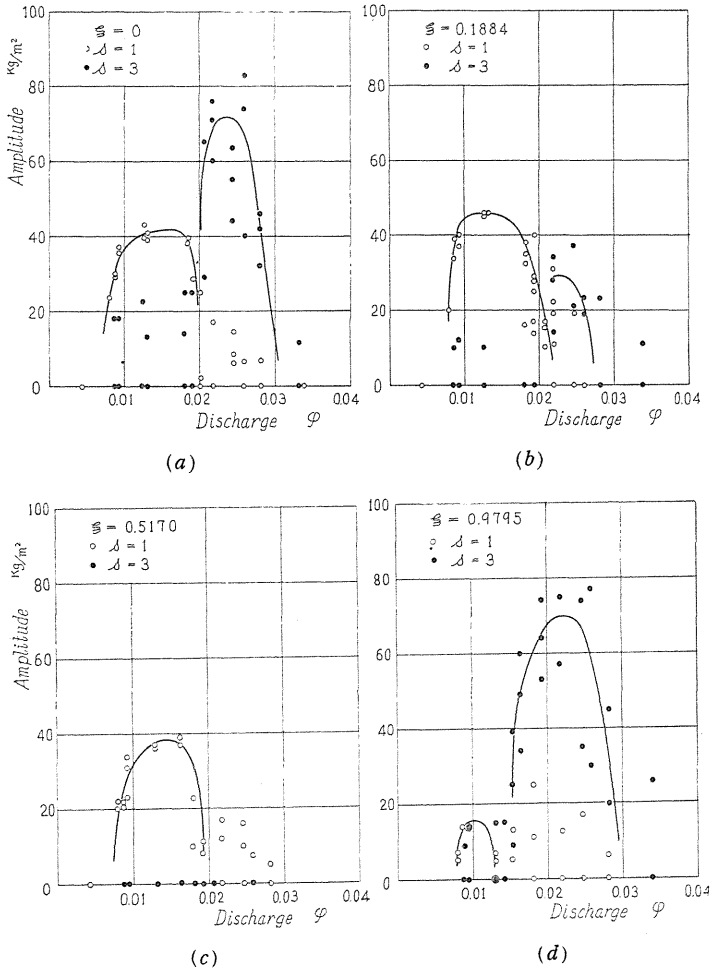

FIG. 4.7. Relation between pressure amplitude of surging and blower position in pipe-line; and change of type of surging.

of $s=1$ and $s=3$ type are plotted in the same figure, where the former is measured at the tank and latter, at a node of $s=3$ type respectively. Comparing $(a)\sim(d)$, we can see that the magnitude of surging amplitude of each type varies with the value of ξ in the same manner as the preceding examples. The feature of the change of the type of surging with the discharge is also observed and the result is as follows. Around the transition discharge, there is a period during which only one of the two types is dominant followed by another period in which two types coexist temporarily before either of them overcomes the other and this sort of transition repeats irregularly.

Further, in this experiment for the pipe-line IV, the static pressure of blower is about 337 kg/m² in the cut-off state $\varphi=0$.

4. Considerations on results of experiments

(4-1) Relation between blower position and amplitude of surging

As mentioned in Section 2, we may presume that the position of the blower in the pipe-line affects the state of surging through two mechanisms. One is related to the fact, as discussed in Chapter I, that the contribution of the blower characteristic to the vibrating air column has a close connection with the blower position, and the other is that, as shown in Chapter II, the effect of the blower as a resistance for the vibration depends on the blower position.

In the first place, we examine the latter.

In Fig. 4.8 and Fig. 4.9, the damping effect of the blower on the free vibration of air column is shown in the same manner as that used in Chapter II. Fig. 4.8 is obtained from the results of experiment carried out with the pipe-line I in Table

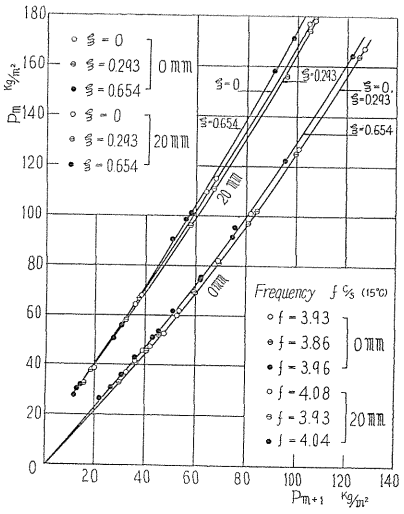

FIG. 4.8.

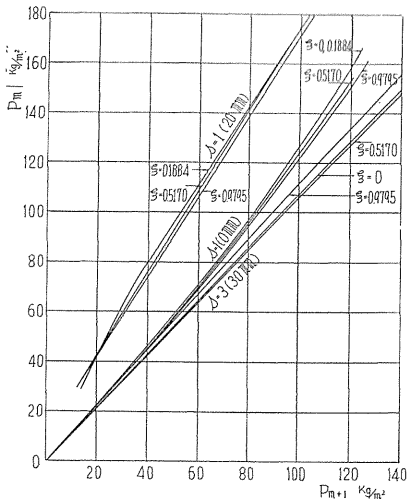

FIG. 4.9.

FIG. 4.8. Relation between damping of free vibration and blower position (pipe-line I).

FIG. 4.9. Relation between damping of free vibration and blower position (pipe-line IV).

4.1. Here the features of damping are shown for various values of ξ, and two groups of curves in the figure correspond to the exit opening diameter 0 mm and 20 mm (these openings are attached at the tank-wall) respectively. And Fig. 4.9 corresponds to the pipe-line IV in Table 4.1, and the experimental results for the types of vibration of $s=1$ and $s=3$ are shown in the same graph. Further, as shown in these figures, since the frequency is almost independent of the value of ξ, the damping of vibration is larger when the curve describing the damping comes towards left.

From above figures and the experimental results shown in Fig. 4.2 and Fig. 4.7, we can conclude that the change of the amplitude of surging due to the value of ξ can not be attributed to the change of damping. As an example, in Fig. 4.8, when the exit opening is 20 mm, the damping for $\xi=0$ is larger than that for $\xi=0.293$, however, as seen in Fig. 4.2, the amplitude of surging is larger in the former. The similar inference can be done for Fig. 4.7 and Fig. 4.9.

In the following, we consider the other mechanism which affect the change of the amplitude of surging with the value of ξ.

Table 4.5 shows the relation between the value of the blower position ξ and the velocity amplitude $v_{\max}\cdot|\cos k_s\xi l|$ (cf. Eq. (4.1)) at the blower position of a normal mode corresponding to the type of surging occured, where the value of $v_{\max}$ is taken as unit. Comparing this table to the figures given above, it can be seen clearly that the surging corresponding to a normal mode becomes violent when the blower approaches the position of a loop of that mode. And as seen in the table, for the case of $s=1$ type, the value of $|\cos k_1\xi l|$ varies only slightly with ξ, and corresponding to this fact, the amplitude of surging does not vary

TABLE 4.5. Velocity Variation at Blower Position

Pipe-line	ξ	$\lvert\cos k_s\xi l\rvert$
Pipe-line I $s=1$ $k_1=0.07910$	0 0.393 0.654	1 0.993 0.965
Pipe-line II $s=3$ $k_3=0.1384$	0 0.1348 0.2270 0.3335 0.5015 0.9254	1 0.898 0.719 0.428 0.126 1
Pipe-line III $s=1$ $k_1=0.03291$	0 0.1348 0.2270 0.3335 0.9254	1 0.994 0.983 0.964 0.734
Pipe-line IV $s=1$ $k_1=0.02451$	0 0.1884 0.5170 0.9795	1 0.995 0.968 0.891
Pipe-line IV $s=3$ $k_3=0.15360$	0 0.1884 0.5170 0.9795	1 0.837 0.014 0.981

too much either (cf. Fig. 4.2). On the other hand, for the case of $s=3$ type, the value of $|\cos k_3\xi l|$ varies remarkably with ξ, that is it diminishes from 1 to 0 and increases again to 1, and corresponding to this, the surging is the greatest in two blower positions where the value of $|\cos k_3\xi l|$ is nearly equal to 1.

In conclusion, we can say that the change of the amplitude of surging with ξ is solely due to this mechanism mentioned above. In other words, the magnitude of velocity (or discharge) variation in the blower is determined by the relation between the mode of vibration and the blower position, and this mutual relation governs the amount of energy given by the blower to the air column, and this energy plays the key role in determining the magnitude of surging.

From above discussion, we can expect to diminish or prevent the surging by adequate selection of the blower position in the pipe-line. And when the type of surging occured in the pipe-line is that which corresponds to a higher mode ($s=3$, $5, \ldots$), we may expect to prevent the surging entirely, selecting the blower position at a node of that mode. However, when the type of surging is $s=1$, the above method of preventing the surging may be less effective than the other cases.

(4-2) Change of type of surging

As shown in Fig. 2.6, in the pipe-line which has an exit opening at the tank-wall, the damping effect of opening on the vibrating air column increases rapidly with increased diameter when the type of vibration is $s=1$, however when the type of vibration corresponds to a higher mode, the increase is not so rapid.

From above fact, the phenomenon of the change of the type of surging, shown in Fig. 4.7, may be explained as follows. In the range of small discharge, the damping effect on the vibration of $s=1$ type is small because the exit opening is small, so the surging of this type occurs, but it becomes difficult to occur due to the rapid increase of damping with the increase of area of the opening (namely increase of discharge). On the other hand, the increase of the damping effect of the opening with the discharge is not so rapid for the vibration of $s=3$ type so the surging becomes to occur in this type rather than in $s=1$ type. However, the detailed analysis is left to Chapter VI.

5. Conclusions

The results are as follows:

1. The index $|\cos k_3\xi l|$ of the amplitude of velocity variation at the blower position in the pipe-line is an important factor in determining the state of the surging.

2. When a blower is placed at a position of the loop of a mode of free vibration of air column in the pipe-line, the surging corresponding to that mode is most violent.

3. By placing a blower at a node, the surging can be lessened or checked entirely.

4. The position of the blower has almost no effect on the frequency of surging.

5. The type of surging may change with the position of the blower and the working discharge of the blower.

Chapter V. On an Approximate Solution of Surging[36]

1. Preliminaries

As was shown in Chapter III and Chapter IV, the air column in a pipe-line vi-

brates in the surging state, in a manner similar to that of a normal mode of vibration.

This fact suggests the possibility that, in dealing with the surging phenomenon, we may regard the blower as an energy source that supplies the air column with energy for vibration of the type which corresponds to a normal mode determined by the dimensions and boundary conditions of pipe-line.

Even though we can not deduce the exact solution of the surging phenomenon from this standpoint, it enables us not only to recognize the phenomenon as the self-exciting vibration of continuous body, but also to deduce various aspects of the phenomenon by relatively simple calculation. This approximation method may be powerful for solving the surging problem in a pipe-line of complex construction, for which the exact solution is difficult to obtain.

The approximation method in which the self-exciting factor (the blower, in this case) is regarded as an energy source, is usually used in many other fields of vibration problem. Here we examine the effectiveness of this method for solving the surging problem, refering to the experimental results obtained in Chapter III and Capter IV.

2. Discussion on qualitative standpoint

First, based on the assumption that the characteristic of the blower is expressed approximately by a cubic curve, a formula for determining the amplitude of the surging is derived. Then the validity of the formula is examined qualitatively by comparing its predictions with the experimental results.

We consider the pipe-line of the shape shown in Fig. 3.1. As was mentioned in Chapter IV, when the opening at tank is nearly cut-off (cf. Eq. (4.1) in Chapter IV, here we use q instead of p_x in Eq. (4.1) and v instead of v_x), the vibration of normal mode is as follows;

$$q = a \sin k_s x \cdot \sin \omega_s t, \tag{5.1}$$

$$v = \frac{a\omega}{k_s K} \cdot \cos k_s x \cdot \cos \omega_s t = \frac{a}{\rho c} \cdot \cos k_s x \cdot \cos \omega_s t \tag{5.2}$$

where k_s is a root of following equation

$$k_s l \cdot \tan k_s l = Al/V \tag{5.3}$$

and

$$k_s c = \omega_s = 2\pi f_s \tag{5.4}$$

(hereafter we omit suffix s for simplicity).

We assume here that, in the surging state, the air in the suction and delivery pipe vibrates in such a manner that its velocity and pressure are represented by the sum of the mean value and variable component represented by (5.1) and (5.2). That is; denoting the pressure and the velocity of the air in the pipe-line by p and u, and the mean values by p_0 and u_0 respectively, we can write

$$p = p_0 + q, \qquad u = u_0 + v. \tag{5.1'}$$

If u_0 is small, we can put $p_0 = 0$ for suction pipe, taking the atmospheric pressure as the datum.

Under above assumption, and the assumption that the blower can be regarded as an energy source, we can derive the formula which represents the amplitude of surging by equating the value of vibration energy supplied by the blower to the air column, to the value of vibration energy which dissipates from the air column. The process is as follows. The characteristic curve of the blower is represented in the p, u plane (pressure versus velocity plane) as $p=f(u)$. Shifting the origin of coordinates along the characteristic curve to the point corresponding to the working discharge (velocity u_0), the characteristic curve is written as $g(v)$, where the variable velocity v is taken as the independent variable. Using Eq. (5.2), the vibration energy T_0 suppulied by the blower to the air column during one period of vibration, is evaluated as follows;

$$\begin{aligned} T_0 &= \oint A g(v_{x=\xi l})\, v_{x=\xi l} \cdot dt \\ &= \frac{Aa}{\rho c} \cos k\xi l \int_0^{2\pi/\omega} g\Big(\frac{a}{\rho c} \cos k\xi l \cdot \cos \omega t\Big) \cos \omega t \cdot dt. \end{aligned} \tag{5.5}$$

Next, we consider the dissipation energy from the air column during one period of vibration. Even though the value of dissipation may be affected by many factors, such as the condition of exit opening, the dimensions of pipe-line, discontinuity of cross sectional area of pipe-line etc, it is expected that, if the energy supply from the blower is absent, the pressure variation of the air column around the static pressure level would die down in a manner represented by Eq. (5.6)

$$q = a \sin kx \cdot e^{-\varepsilon t} \sin \omega t. \tag{5.6}$$

Here, ε is the equivalent damping coefficient.

Then the value of dissipation energy E_0 is evaluated as the decrement of potential energy of air column during one surging period. That is, bearing in mind that the amount of work needed for compression of the air at the point x in the pipe-line to the pressure of p_x is

$$\int_0^{p_x} p_x (A dx/K)\, dp_x = (1/2)(A/K)\, p_x^2\, dx,$$

and reffering to the Eq. (5.6), we obtain

$$\begin{aligned} E_0 &= (1/2)(A/K) \int_0^l \{(ae^{-\varepsilon(-2\pi/2\omega)} \sin kx)^2 - (ae^{-\varepsilon(+2\pi/2\omega)} \sin kx)^2\}\, dx \\ &\quad + (1/2)(V/K)\{(ae^{-\varepsilon(-2\pi/2\omega)} \sin kl)^2 - (ae^{-\varepsilon(+2\pi/2\omega)} \sin kl)^2\} \end{aligned} \tag{5.7}$$

where, the first and second term represent the values of decrease of potential energy of air in the pipe and the tank respectively (here the bulk modulus K is regarded as constant). Now, assuming ε is small, and neglecting the higher terms (above the second) of series expantion of exponenrial functions, and using Eq. (5.3), Eq. (5.7) reduces to the following form;

$$E_0 = 2Aa^2\varepsilon/(4\sigma K f) = Aa^2\varepsilon/(2\sigma\rho c^2 f) \tag{5.8}$$

where

$$f = \omega/2\pi, \qquad 1/\sigma = l\Big\{1 + \frac{Al/V}{(Al/V)^2 + (kl)^2}\Big\}.$$

The amplitude of surging is obtained as the value of a which satisfies the equation $T_0 = E_0$.

For the qualitative comparison of this theory with the experimental results, we assume that the shape of characteristic curve can be represented by a symmetrical cubic (shown in Fig. 5.1),

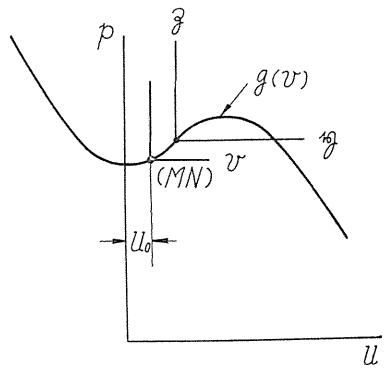

FIG. 5. 1. Approximate representation of characteristic curve of blower by a cubic.

$$\vartheta = \alpha\eta - \beta\eta^3 \qquad (\alpha,\ \beta > 0).$$

And taking the origin of coordinate at an arbitrary point (M, N) on the curve, this can be written as

$$g(v) = (\alpha - 3\beta M^2)\, v - 3\beta M v^2 - \beta v^3. \tag{5.9}$$

And the amplitude a is obtained as

$$a = \sqrt{\{(\alpha - 3\beta M^2)\, c\rho \cos^2 k\hat{\xi} l (c/K) - \varepsilon\} / \{(3/4)\, \beta c\sigma \cos^4 k\hat{\xi} l (c/K)^3\}}. \tag{5.10}$$

Alternatively, representing the characteristic curve by the non-dimensional form by following formulae

$$\varphi = Q/\pi D b u_p = 6.079\ Q/nD^3\Omega,$$

$(\Omega = b/D,\ n$: the number of revolutions r.p.m.)

$$\psi' = P'/(1/2)\,\rho u_p^2 = 729.5\ P'/\rho n^2 D^2,$$

(P': effective static pressure)

Eq. (5.10) reduces to the following form

$$a = \frac{nD^3\Omega\rho c}{6.079\, A \cos^2 k\hat{\xi} l} \sqrt{\frac{0.008333\,(An/D\Omega)\,(p_1 - 3p_3\varphi_0^2)\,\sigma \cos^2 k\hat{\xi} l - \varepsilon}{(3/4) \times 0.008333\,(An/D\Omega)\, p_3 \sigma}} \tag{5.11}$$

where p_1, p_3 and φ_0 correspond to α, β and M respectively when $g(v)$ is represented in φ, ψ' plane, and

$$\alpha = (\rho u_p^2/2) \cdot (A/\pi D b u_p) p_1,\quad \beta = (\rho u_p^2/2) \cdot (A/\pi D b u_p)^2 p_3,\quad M = (\pi D b u_p/A)\, \varphi_0.$$

Especially if the damping factor does not exist in the pipe-line ($\varepsilon = 0$), then Eq. (5.11) takes the following form

$$a = (nD^3\Omega\rho c/6.079A\cos k\xi l)\sqrt{(p_1 - 3p_3\varphi_0^2)/(3/4\,p_3)}. \tag{5.12}$$

In the following, we shall compare these formulae with the experimental results shown in Chapter III and IV.

Fig. 5.2 shows the relation between the pressure amplitude of surging and non-dimensional working discharge φ. In this figure, the curves (1), (2), (3) indicate the measured values of pressure amplitude (at tank). They are shown as the examples for comparison and correspond to the cases in which $l = 13.00$ m, $V = 127.8$ l, $A = 0.01335$ m^2, $\xi = 0$, the blower being B_1 (vane-wheel No. 1) and $n =$ 3,890, 3,395 and 2,650 r.p.m. respectiveiy. The curves denoted by the numbers 1~6 (without parenthesis) are obtained by calculating Eq. (5.11), where the type of surging is taken as $s=1$, because the curves (1), (2) and (3) also correspond to the case where $s = 1$. In the calculation of these curves, the coefficients of odd powers of approximate cubic for the measured characteristic curve are adopted as the values for p_1 and p_3, and the curves are plotted by adequately selecting the zero point of abscissa. For other parameters in Eq. (5.11), the actual dimensions of experimental apparatus are used, and the value of ε is selected adequately.

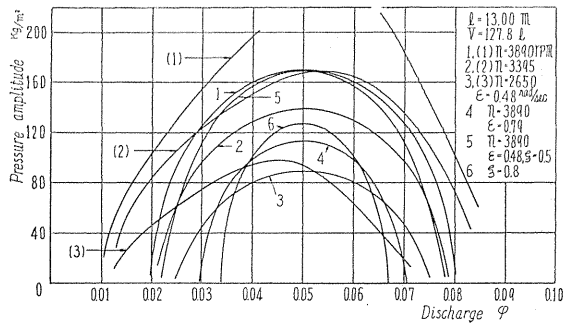

FIG. 5.2. Qualitative comparison between evaluated values of pressure amplitude of surging by approximation theory and experimental values.

In Fig. 5.2, the curves 1, 2 and 3 correspond to the different values of n (number of revolutions), and as we can see in the figure, both the correlation between the amplitude and working discharge, and the decreasing tendency of the amplitude and the surging zone with decreasing n agree qualitatively with those of experimental results (cf. curves (1), (2) and (3)).

The curves 1, 5 and 6 correspond to the different values of ξ, and the decreasing tendency of the amplitude and the surging zone with increasing ξ agrees with the experimental results shown in Fig. 4.2.

The curves 1 and 4 correspond to the different values of ε, and these curves show that the amplitude and the surging zone decrease with the increasing ε in accordance with the physical consideration.

Further, Eq. (5.12) indicates that, when $\varepsilon=0$ and the working discharge φ_0 is held constant, the amplitude of surging is proportional to the value of number of revolutions n, and as is seen in Fig. 3.8, the experimental results also show the similar facts: in Fig. 3.8, for the small value of working discharge, which corresponds to the small value of ε, the amplitude is proportional to the value of n (other examples are seen in the report of H. Kusama and S. Tsuji[6]).

3. Discussion on quantitative standpoint

In this section, we examine the approximate theory by the quantitative comparison with the experimental results.

Two aspects of comparison being made here are the condition of self-excitation (or condition of unstability) and the pressure amplitude of surging. First, the condition of unstability is deduced from Eq. (5.5) and (5.8) as $(T_0-E_0)_{a\to 0}>0$, or

$$(\alpha-3\beta M^2)\,\sigma\cos^2 k\xi l-\rho\varepsilon>0.$$

Here the value $(\alpha-3\beta M^2)$ is, as is seen from Eq. (5.9), the inclination of the characteristic curve of the blower at the point corresponding to the working velocity M, and denoting this as ρm, we obtain the following formula

$$m\sigma\cos^2 k\xi l-\varepsilon>0. \tag{5.13}$$

Incidentally this representation coincides with that shown by Y. Shimoyama[3]; who deduced the same formula from the ordinary differential equation of second order which describes the surging phenomenon approximately.

The calculated values $(m\sigma-\varepsilon)$ from Eq. (5.13) are shown in Table 5.1 in comparison with the experimental results. In the calculation, as the value of ε, we adopt the measured value obtained from the experimental data of free vibration of air column. And as the condition of stability, the formula $m\sigma-\varepsilon<0$ was used, because for all cases in this experiment, the value of ξ was zero (or the blower is connected to the suction end of the pipe-line).

Further in the last column of the table, the measured values of maximum amplitude of pressure in the pipe-line are shown, for the cases in which the surging occurred. As is seen in the table, Eq. (5.13) gives a fairly good criterion for stability.

In the following, we compare the calculated values of the pressure amplitude by the approximate theory with the measured values.

Fig. 5.3 shows the relation between the pressure amplitude of surging and the non-dimensional discharge φ, where the number of revolutions n is fixed. In the figure, the abscissa is the non-dimensional discharge φ of the blower, and the ordinate is the maximum pressure amplitude of surging in the pipe-line. In the calculation of the amplitude, the value of T_0 (cf. Eq. (5.5)) is obtained for each value of a by the graphical integlation, using the measured characteristic curve (graphical integlation is carried out by the method given by Y. Shimoyama[3]). On the other hand, E_0 (cf. Eq. (5.8)) is evaluated for each value of a using the actual dimensions of pipe-line. The value of amplitude a of surging is determined as the value which satisfies $T_0=E_0$.

In the figure, the curve 3 represents the experimental results, and the curves 1, 2 and 4 are the calculated ones; where, in the case of the curve 1, the measured

value of damping coefficient of the free vibration is used for the value of ε, and for the curve 2, the dissipation energy E_0 is estimated to be approximately 30%

TABLE 5.1. Comparison of Condition of Self-excitation with Experimental Results

Pipe-line	Diameter of opening (orifice) (mm)	n (r.p.m.)	φ	$m\sigma$	ε	$m\sigma-\varepsilon$	Measured value of pressure amplitude (kg/m²)
$l=6.69$ m $V=127.8\,l$ $\xi=0$ Orifice position S	cut-off	4640	0	−0.34	0.7	−1.04	surging does not occur
	20	4640	0.0081	0	0.7	−0.7	surging does not occur
	33	2400	0.0227	1.40	1.1	0.30	6
	33	2895	0.0227	1.69	1.1	0.58	39
	33	3645	0.0230	2.11	1.1	1.01	84
	33	4140	0.0230	2.40	1.1	1.30	101
	33	4890	0.0229	2.84	1.1	1.74	136
	43	3150	0.0415	1.50	0.7	0.80	8.5
	43	3395	0.0420	1.60	0.7	0.90	80
	43	4390	0.0419	2.06	0.7	1.36	178
	53	3150	0.0671	0.92	0.7	0.22	0~20
	53	3890	0.0670	1.14	0.7	1.14	100
	66	4390	0.114	−0.45	0.7	−1.15	surging does not occur
$l=10.49$ m $V=127.8\,l$ $\xi=0$ Orifice position S	33	1800	0.0229	0.765	0.80	−0.035	surging does not occur
	33	2150	0.0229	0.917	0.80	0.117	surging does not occur
	33	2400	0.0229	1.02	0.80	0.22	11
	33	3890	0.0229	1.65	0.80	0.85	103
	43	2150	0.411	0.743	0.980	−0.24	surging does not occur
	43	2400	0.411	0.828	0.980	−0.15	surging does not occur
	43	2895	0.411	1.00	0.980	0.02	20~80
	43	3395	0.411	1.18	0.980	0.20	135
$l=9.91$ m $V=0\,l$ $\xi=0$ Orifice position S	33	2400	0.0229	1.60	1.83	−0.23	surging does not occur
	33	2895	0.0229	1.94	1.83	0.11	surging does not occur
	33	3395	0.0229	2.27	1.83	0.44	surging does not occur
	33	3890	0.0229	2.59	1.83	0.76	0~26
	33	4390	0.0229	2.93	1.83	1.10	87
	33	4640	0.0229	3.10	1.83	1.27	86~102

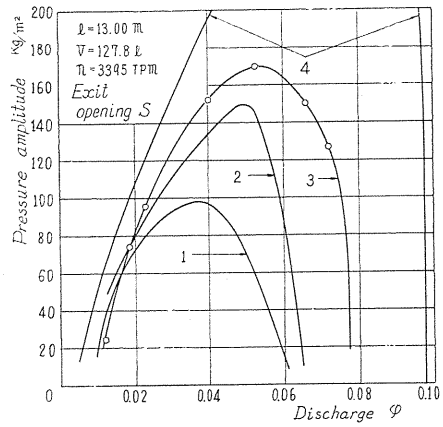

FIG. 5.3. Quantitative comparison between evaluated values of pressure amplitude and experimental values.

less than that of curve I, and the curve 4 corresponds to the case where $\varepsilon=0$ (in this case, the amplitude of surging is determined by the characteristic of the blower only).

As is seen in Fig. 5.3, the agreement of the curve 1 and 3 is not satisfactory, but if we note the difficulty of estimating the dissipation energy in the surging state, this result is considered to be unavoidable. However, if we make allowance for the estimation of the dissipation energy E_0, as is seen in the case of the curve 2, we may obtain a sufficiently accurate result.

In Table 5.2, the culculated values of pressure amplitude for various values of n are compared with the measured values, where the value of non-dimensional discharge φ is fixed for respective group of n. As is seen in the table, the agreement is fairly good when the value of φ is small; the small value of φ corresponds to the small area of exit opening or to the small value of energy dissipation from the opening, and in this case the characteristic of blower plays an important role in determining the amplitude.

From the results shown in Section 2 and 3, we can conclude that the approximation method is fairly effective in dealing with the surging problem.

TABLE 5.2. Comparison of Calculated Values of Pressure Amplitude with Measured Values

Conditions of experiment	Number of revolutions of blower n (r.p.m.)	Calculated values of pressure amplitude (kg/m^2)	Measured values of pressure amplitude (kg/m^2)
$l=20.98$ m $V=0\,l$ $\varphi=0.0225$ $\xi=0$ Orifice position S	2400	surging does not occur	surging does not occur
	2650	40	20～53
	2895	69	70
	3395	90	102
	3890	112	119
	4140	124	132
Pipe-line is same as above $\varphi=0.0592$	2895	50	57
	3150	60	102
	3395	70	140
$l=10.49$ m $V=127.8\,l$ $\varphi=0.0225$ $\xi=0$ Orifice position S	2400	surging does not occur	surging does not occur
	2650	45	24～50
	2895	54	55
	3395	71	84
	3890	86	103
	4390	100	123
	4640	108	131
$l=12.00$ m $V=127.8\,l$ $\varphi=0.025$ $\xi=0.1273$ Orifice position S	2650	surging does not occur	surging does not occur
	2895	50	22～44
	3395	63	76
	3890	78	103
	4390	93	129

Chapter VI. A Consideration on the Type of Surging[38]

1. Preliminaries

As we have seen from the discussion in Chapter III and IV, the surging occurs in such a manner that only a component of vibration corresponding to a

normal mode is dominant. And as mentioned in Section (4-2) of Chapter IV, the dominant component may change with the value of discharge.

We have given there the qualitative discussion as to the causes of these experimental results, but in this chapter, we treat the problem of the type of surging raher more theoretically but with some experimental emphasis.

2. Approximate differential equation of surging

To treat this problem by the method used in Chapter I, is practically imposible, with the exception of the case of a very simple pipe-line. Even for such a simple pipe-line, if we take into account of the damping factor in the pipe-line, which always exists in actuality, the handling becomes very difficult.

So we treat the problem by another method.

In the first place, we deduce the differential equation which describes the surging phenomenon (in the process of deduction of equations, we refer to the method given by Y. Shimoyama[3]). It is however difficult to treat the problem from the viewpoint that the system has infinite degrees of freedom, so an approximate treatment is used.

We consider the pipe-line of the shape shown in Fig. 3.1 in Chapter III. And we use the following nomenclature,

p : pressure of air in the pipe-line,
u : velocity of air in the pipe-line,
c : velocity of sound,
K: bulk modulus of air,
p_0: static pressure of blower,
t : time,
A: area of cross section of the pipe-line,
l : length of pipe-line,
V: volume of tank connected to the pipe end.

In advance of the deduction of the differential equation of surging, we express the nature of the vibration of air column in the pipe-line. When the amount of variation of u, p and ρ are small, the differential equations which describe the vibration of air column are as follows,

$$\frac{\partial^2 u}{\partial t^2} = c^2 \frac{\partial^2 u}{\partial x^2}, \tag{6.1}$$

$$\frac{\partial^2 p}{\partial t^2} = c^2 \frac{\partial^2 p}{\partial x^2} \tag{6.2}$$

where $c^2 = K/\rho$.

Leaving the blower out of consideration, and assuming that the exit openning at the tank acts on the reflection of the wave in the same manner as that in the cutt-off state, and bearing in mind that, at the suction end or $x=0$, the condition of open end is fulfilled, we can write the solution of Eqs. (6.1) and (6.2) in the following form

$$p = \sum_s q_s \sin k_s x, \qquad u = \sum_s q_s' \cos k_s x \tag{6.3}$$

where q_s and q_s' are the functions of time determined by Eqs. (6.1) and (6.2). Moreover in the equation of continuity

$$\frac{\partial \rho}{\partial t} + u\frac{\partial \rho}{\partial x} + \rho\frac{\partial u}{\partial x} = 0, \tag{6.4}$$

we neglect the small term $u\partial\rho/\partial x$ and using the expression $dp/d\rho = c^2 = K/\rho$, we can write Eq. (6.4) in the next form

$$\frac{\partial p}{\partial t} = -K\frac{\partial u}{\partial x}. \tag{6.5}$$

From Eqs. (6.3) and (6.5) we obtain the formula which shows the relation between q_s and q_s' as following

$$q_s' = \dot{q}_s/k_s K. \tag{6.6}$$

As to the value of k_s, putting the Eq. (6.3) into the following formula, which expresses the condition at the junction of the pipe and the tank

$$\left(\frac{\partial p}{\partial t}\right)_{x=l} = \frac{KAu_{x=l}}{V},$$

we can see that k_s is a root of following equation

$$k_s l \cdot \tan k_s l = Al/V, \tag{6.7}$$

where in the expression $k_s = \bar{\alpha}_s \cdot s\pi/(2l)$, s is an odd interger.

In the following, using the equations obtained in the preceding discussion, we deduce the differential equation of the surging. Now, we indicate the position of blower in the pipe-line as $x = \xi l$. Then refering to the Eqs. (6.3) and (6.6), we can represent p and u in the following forms, in which we use q_s as a generalized coordinate,

$$p = p_0 + \sum_s q_s \sin k_s x, \qquad u = u_0 + \sum_s (\dot{q}_s/k_s K) \cdot \cos k_s x, \tag{6.8}$$

where for the suction pipe ($x < \xi l$), we may put $p_0 = 0$. Now we take account of the effect of the blower on the system, as a generalized force which acts at a point $x = \xi l$.

Then the differential equations which describe the surging phenomenon may be deduced by use of Lagrange's equation of motion

$$\frac{\partial(\partial T_m/\partial \dot{q}_s)}{\partial t} - \frac{\partial T_m}{\partial q_s} + \frac{\partial F}{\partial \dot{q}_s} + \frac{\partial E_0}{\partial q_s} = Q_s, \tag{6.9}$$

where the kinetic energy T_m, the potential energy E_0, the dissipation function F and the generalized force Q_s are calculated in the manner which will be mentioned later. Since we try to solve the surging problem approximately, we regard the system as that of two degrees of freedom, or in other words, take account of only two values of s ($s=1$ and $s=3$). Even if we handled the problem from the standpoint of infinite degrees of freedom, the differential equations would be deduecd without difficulty, but it would be impossible to solve them. This is why we assume that the system has two degrees of freedom, from the beginning.

The kinetic energy T_m is obtained as follows; with Eqs. (6.8) and (6.7)

$$T_m(1/2)\rho A\int_0^l u^2dx=(1/2)\rho Alu_0^2+(\rho Au_0/K)\sum_{s=1,3}(\dot{q}_s/k_s^2)\sin k_sl$$
$$+(\rho A/4K^2)\sum_{s=1,3}(\dot{q}_s^2/k_s^2\sigma_s), \tag{6.10}$$

where

$$1/\sigma_s=l[1+(Al/V)/\{(Al/V)^2+(k_sl)^2\}].$$

In above evaluation, the energy of air in the tank are neglected.

Next, the potential energy V_0 may be evaluated as follows, assuming that the working pressure of blower is low or bulk modulus K is constant. When the pressure rise at the position x is $\Delta\bar{p}$, the amount of compression of a thin layer of air of thickness dx is $(Adx/K)\Delta\bar{p}$. And the work done required to raise the pressure to the value $\bar{p}$ is

$$\int_0^{\bar{p}}\bar{p}(Adx/K)d\bar{p}=(A/2K)\bar{p}^2dx$$

and using Eq. (6.8) we have

$$E_0=(A/2K)\int_0^l(\sum_{1,3}q_s\sin k_sx)^2dx+(V/2K)(\sum_{1,3}q_s\sin k_sl)^2),$$

where the first and second terms indicate the energy in the pipe-line and in the tank respectively. Then, by use of Eq. (6.7), we have

$$E_0=(A/4K)\sum_{1,3}(q_s^2/\sigma_s). \tag{6.11}$$

We leave the discussion of the dissipation function F for later paragraph and, for a while, assume that there is no damping in the system.

Next, the generalized force Q_s is evaluated as follows. The pressure variation δ_{p_s} corresponding to an infinitesimal variation of the generalized coordinate q_s is $\delta_{p_s}=\delta_{q_s}\sin k_sx$ (cf. Eq. (6.8)). And the volume change of air column in the pipe-line, the range of which is $\xi l\leqq x\leqq l$, and of air in the tank corresponding to δ_{p_s} is

$$\delta\mathfrak{V}=\int_{\xi l}^l(\delta_{p_s}Adx)/K+(\delta_{p_s})_{x=l}\cdot(V/K)=(A/Kk_s)\cos k_s\xi l\delta_{q_s}.$$

Denoting the delivery pressure of blower by P, the work provided by the blower to the system is $(P-p_0)\delta\mathfrak{V}$, corresponding to δ_{q_s}. Equating this value to $Q_s\delta_{q_s}$, we have

$$Q_s=(P-p_0)A\cos k_s\xi l/k_sK,$$

where P is determined by the characteristic of the blower, and using the working velocity of the blower u_0 and working delivery pressure p_0, we can write as follows;

$$P=p_0+g(u_{x=\xi l}-u_0)=p_0+g(v)=p_0+g\{\sum_{1,3}\dot{q}_s\cos k_s\xi l/(k_sK)\}.$$

Here $g(v)$ represents the form of characteristic curve of the blower, where the

origin of coordinates is taken so as to coincide with the working point of the blower on the characteristic curve. Then we have

$$Q_s = A\cos k_s\xi l \cdot g\{\sum_{1,3}\dot{q}_s \cos k_s\xi l/(k_s K)\} \cdot (1/k_s K). \tag{6.12}$$

Inserting the values of T_m, E_0 and Q_s given in Eqs. (6.10)~(6.12) into the Lagrange's equation of motion, we have

$$\ddot{q}_1 + c^2k_1^2 q_1 - 2c^2k_1\sigma_1 \cos k_1\xi l \cdot g\{\dot{q}_1 \cos k_1\xi l/(k_1 K) + \dot{q}_3 \cos k_3\xi l/(k_3 K)\} = 0, \tag{6.13-a}$$

$$\ddot{q}_3 + c^2k_3^2 q_3 - 2c^2k_3\sigma_3 \cos k_3\xi l \cdot g\{\dot{q}_1 \cos k_1\xi l/(k_1 K) + \dot{q}_3 \cos k_3\xi l/(k_3 K)\} = 0, \tag{6.13-b}$$

where ck_1 and ck_3 are the angular frequencies of normal mode of vibration of the air column, as easily seen by putting the value of p of Eq. (6.3) in Eq. (6.2); so we write as $ck_1 = \omega_1$ and $ck_3 = \omega_3$.

In the process of deduction of above equations, we left the dissipation function F out of consideration. As the energy dissipation from the vibrating system depends on various factors as discussed in Chapter II and III, so it is a vexed question to introduce a damping term into the differential equations of surging, in an adequate form. Here we introduce the damping term by the following consideration. Neglecting the third therms of above equations, they reduce to the equations which describe the vibration of normal mode of $s=1$ and $s=3$ respectively. Now, in the actual free vibration of air column in the pipe-line, it may be considered that the state of damping is expressed approximately as below,

$$p = p_0 e^{-\varepsilon t} \sin \omega_s' t \qquad (\omega_s' \fallingdotseq \omega_s) \tag{6.14}$$

where suffix 0 indicates the initial value.

By the experiment in Chapter II, we know that the value of ε varies depending on the mode of vibration even in the same pipe-line. From preceding consideration, introducing the damping terms $2\varepsilon_1\dot{q}_1$ and $2\varepsilon_3\dot{q}_3$ into two equations of (6.13) respectively, we express the damping characteristic of the system, and have

$$\ddot{q}_1 + \omega_1^2 q_1 + 2\varepsilon_1\dot{q}_1 - 2c\sigma_1\omega_1 \cos k_1\xi l \cdot g\{\dot{q}_1 \cos k_1\xi l/(k_1 K) + \dot{q}_3 \cos k_3\xi l/(k_3 K)\} = 0, \tag{6.15-a}$$

$$\ddot{q}_3 + \omega_3^2 q_3 + 2\varepsilon_3\dot{q}_3 - 2c\sigma_3\omega_3 \cos k_3\xi l \cdot g\{\dot{q}_1 \cos k_1\xi l/(k_1 K) + \dot{q}_3 \cos k_3\xi l/(k_3 K)\} = 0. \tag{6.15-b}$$

Above equations are the foundamental ones for the approximate treatment of the surging problem.

3. Representation of characteristic curve of blower by polinominal

To solve the Eq. (6.15), we must give the definite form to the function $g(v)$. The measured characteristic curve of the blower B_1 (indicate this as I) and an approximated curve by a sextic (indicate this as II) are shown in Fig. 6. 1, where the curve I is measured under the conditions that the diameter of pipe-line is 5 inchs, the number of revolutions of the blower is 4,390 r.p.m. In the figure the abscissa is the velocity of air flow (m/s) and the ordinate is the pressure (kg/m^2), and the origin is selected adequately.

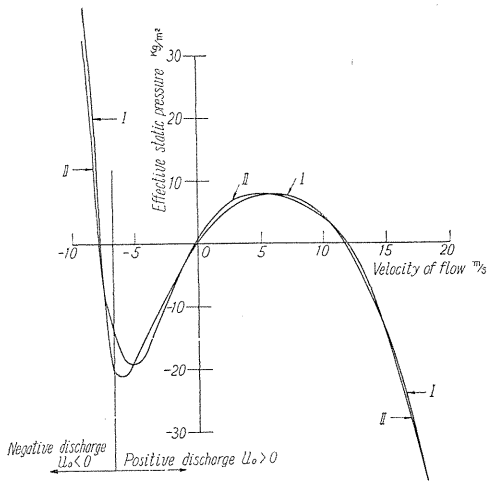

FIG. 6. 1. Approximate representation of characteristic curve of blower by a sextic.

It may be said that the agreement is satisfactory, but when we use this representation of a sextic, the discussion of Eq. (6.15) becomes very complex. So we adopt a cubic having the form $\mathfrak{y}=\alpha\mathfrak{v}-\beta\mathfrak{v}^3$ (α, $\beta>0$) as the approximation for the characteristic curve of the blower. Choosing the origin of the coordinates at the point corresponding to the working velocity on the characteristic curve (cf. Fig. 5.1 and Eq. (5.9), we can express the approximate cubic as

$$g(v)=(\alpha-3\beta M^2)\,v-3\beta M v^2-\beta v^3. \tag{6.16}$$

Further, in Eq. (6.15), the fourth terms may be assumed to be small in general and we write $\alpha=\mu\alpha'$ and $\beta=\mu\beta'$ ($\mu\ll 1$), then Eq. (6.16) reduces to

$$g(v)=\mu\{(\alpha'-3\beta' M^2)\,v-3\beta' M v^2-\beta' v^3\}. \tag{6.17}$$

Here we examine whether it is adequate or not to base our discussion of surging problems on Eq. (6.17), by taking an example from the system of one degree of freedom. If the adoption of Eq. (6.17) is justifiable in the case of one degree of freedom, the same equation is equally or more adequate for the case of two degrees of freedom.

Now in Eq. (6.15-a), taking only the dependent variable q_1 into account, we have

$$\ddot{q}_1+\omega_1^2 q_1+2\varepsilon_1\dot{q}_1-2c\sigma_1\omega_1\cos k_1\xi l\cdot g\{\dot{q}_1\cos k_1\xi l/(k_1K)\}=0$$

where

$$g\{\dot{q}_1\cos k_1\xi l/(k_1K)\}=\mu[(\alpha'-3\beta' M^2)\{\dot{q}_1\cos k_1\xi l/(k_1K)\}$$
$$-3\beta' M\{\dot{q}_1\cos k_1\xi l/(k_1K)\}^2-\beta'\{\dot{q}_1\cos k_1\xi l/(k_1K)\}^3].$$

Assuming that the damping term is also small, we put $2\varepsilon_1=\mu\gamma$. Furthermore if it is assumed that the third and fourth terms are both small, we may handle the problem as quasi-linear, and the solution of the above equation may be writen as

$q_1 = a\cos\omega_1' t(\omega_1' \fallingdotseq \omega)$. Then using the method of the first approximation given by N. Kryloff and N. Bogoliuboff,[39] we obtain the equation which represents the variation of a as follows

$$\dot{a} = \mu a\{(\alpha' - 3\beta' M^2)(c^2/K) \cdot 2\sigma_1 \cos^2 k_1\xi l - (3\beta'/4) \cdot 2c\sigma_1 \cos^4 k_1\xi l \cdot (c/K)^3 a^2 - \gamma_1\}. \tag{6.18}$$

Thus the condition of self-excitation is obtained from the condition $\left(\frac{da}{dt} > 0\right)_{a=0}$ as follows,

$$\mu\{(\alpha' - 3\beta' M^2)(c^2/K) \cdot 2\sigma_1 \cos^2 k_1\xi l - \gamma_1\} = 2\{(\alpha - 3\beta M^2)(c^2/K)\sigma \cos^2 k_1\xi l - \varepsilon_1\} > 0. \tag{6.18'}$$

The stationary value of a, or the amplitude of sustained vibration, is obtained as the value of a which fulfills $\dot{a} = 0$, namely

$$a = \sqrt{\{(\alpha - 3\beta M^2) c\sigma_1 \cos^2 k_1\xi l(c/K) - \varepsilon_1\}/\{(3/4)\beta c\sigma_1 \cos^4 k_1\xi l(c/K)^3\}}. \tag{6.19}$$

This formula coincides with the formula (5.10) which is deduced by simple energy consideration. It was already shown in Chapter V that this formula (5.10) gives the qualitative representation of the nature of surging phenomenon fairly well. From foregoing consideration, we can say that the adoption of Eq. (6.17) in the discussion of Eq. (6.15) for the case of two degrees of freedom, is also justifiable.

4. Solution of differential equation

Using the formulae $ck_1 = \omega_1$, $ck_3 = \omega_3$ given in Section 2, and considering that $1/(k_1 K) = c\omega_3/(\omega_1\omega_3 K)$ and $1/(k_3 K) = c\omega_1/(\omega_1\omega_3 K)$ and putting $c/(\omega_1\omega_3 K) = h$, $h\cos k_1\xi l = h_1$, $h\cos k_3\xi l = h_3$, $2c\sigma_1 \cos k_1\xi l = A_1$, $2c\sigma_3 \cos k_3\xi l = A_3$, $2\varepsilon_1 = \mu\gamma_1$ and $2\varepsilon_3 = \mu\gamma_3$, Eq. (6.13) reduces to

$$\ddot{q}_1 + \omega_1^2 q_1 - \mu A_1\omega_1\{(\alpha' - 3\beta' M^2) v - 3\beta' M v^2 - \beta' v^3\} + \mu\gamma_1\dot{q}_1 = 0, \tag{6.13'-a}$$

$$\ddot{q}_3 + \omega_3^2 q_3 - \mu A_3\omega_3\{(\alpha' - 3\beta' M^2) v - 3\beta' M v^2 - \beta' v^3\} + \mu\gamma_3\dot{q}_3 = 0 \tag{6.13'-b}$$

where

$$v = h_1\omega_3\dot{q}_1 + h_3\omega_1\dot{q}_3. \tag{6.20}$$

In above equations (6.13'-a) and (6.13'-b), if $\mu = 0$, we have

$$\ddot{q}_1 + \omega_1^2 q_1 = 0, \qquad \ddot{q}_3 + \omega_3^2 q_3 = 0.$$

And the solutions are

$$q_1 = a\cos(\omega_1 t + \phi_1), \qquad q_3 = b\cos(\omega_3 t + \phi_3).$$

For the case of $\mu \neq 0$, if we can assume that μ is small, the equations may be considered to be quasi-linear, and the solutions may be written as

$$q_1 = a\cos(\omega_1 t + \phi_1) + \mu c_1 b\cos(\omega_3 t + \phi_3') + q_1', \tag{6.21-a}$$

$$q_3 = b\cos(\omega_3 t + \phi_3) + \mu c_3 a\cos(\omega_1 t + \phi_1') + q_3' \tag{6.21-b}$$

where c_1 and c_3 are functions of a and b in general, and q_1' and q_3' are the terms which contain higher harmonics and combination harmonics. Hereafter we indicate the small term of order μ as $0(\mu)$.

In solving the Eq. (6.13), we linearize the nonlinear terms by the method of N. Kryloff and N. Bogoliuboff. Namely, reffering to Eq. (6.17), we put

$$N_t = (\alpha' - 3\beta' M^3)\, v - 3\beta' M v^2 - \beta v^3.$$

Using Eq. (6.20), and we replace the q_1 and q_3 in this formula by Eqs. (6.21-a) and (6.21-b), and the N_t reduces to

$$N_t = -L_1 a\omega_1 \sin(\omega_1 t + \phi_1) - L_3 b\omega_3 \sin(\omega_3 t + \phi_3) + K_1 + K_2, \tag{6.22}$$

where K_1 is the harmonic term of $0(\mu)$, and K_2 is the term containing higher harmonics and combination harmonics and is also of $0(\mu)$. K_2 contains terms with angular frequencies $2\omega_1 \pm \omega_3$, $2\omega_3 \pm \omega_1$ and so on and we assume that none of these angular frequencies are equal to ω_1 or ω_3. For the pipe-line having a tank, the angular frequencies corresponding to the normal modes are incommensurable in general (cf. Eq. (6.7)), and the above assumption is reasonable. And for the pipe-line without tank also, the above assumption may be considered adequate in many cases, by reason of the existence of the volume (for an example, a volute chamber of blower) in the pipe-line. So we confine our discussion to the cases where the above assumption is correct.

Further, L_1 and L_3 in Eq. (6.22) are expressed as follows

$$L_1 = \bar{\alpha} h_1 \omega_3 - \bar{\beta}\omega_1^2\omega_3^3(h_1^3 a^2 + 2h_1 h_3^2 b^2), \tag{6.23-a}$$

$$L_3 = \bar{\alpha} h_3 \omega_1 - \bar{\beta}\omega_1^3\omega_3^3(2h_1^2 h_3 a^2 + h_3^3 b^2) \tag{6.23-b}$$

where $\bar{\alpha}_1 = \alpha' - 4\bar{\beta}M^2$, $\bar{\beta} = (3/4)\beta'$.

Here taking into account only the harmonic terms of ω_1 and ω_3 which are quantities of first order (indicate this as 0(1)), Eq. (6.22) is written as

$$N_t \fallingdotseq \bar{L}_1\dot{q}_1 + \bar{L}_3\dot{q}_3. \tag{6.24}$$

We consider the linearized equation shown below in place of the original Eq. (6.13′),

$$\ddot{q}_1 + \omega_1^2 q_1 - \mu A_1\omega_1(\bar{L}_1\dot{q}_1 + \bar{L}_3\dot{q}_3) + \mu\gamma_1\dot{q}_1 = 0, \tag{6.25-a}$$

$$\ddot{q}_3 + \omega_3^2 q_3 - \mu A_3\omega_3(\bar{L}_1\dot{q}_1 + \bar{L}_3\dot{q}_3) + \mu\gamma_3\dot{q}_3 = 0. \tag{6.25-b}$$

In above equations, putting $q_1 = I_1 e^{st}$ and $q_3 = I_3 e^{st}$, we have

$$s = (\mu/2)(A_1\omega_1\bar{L}_1 - \gamma_1) \pm j\omega_1, \tag{6.26-a}$$

$$s = (\mu/2)(A_3\omega_3\bar{L}_3 - \gamma_3) \pm j\omega_3. \tag{6.26-b}$$

And putting,

$$m_1 = (1/2)(A_1\omega_1\bar{L}_1 - \gamma_1), \quad l_1 = j\omega_1 \quad (j^2 = -1), \tag{6.27-a}$$

$$m_3 = (1/2)(A_3\omega_3\bar{L}_3 - \gamma_3), \quad l_3 = j\omega_3, \tag{2.27-b}$$

the solutions of Eq. (6.25) may be written as

$$q_1 = E_{11}e^{(\mu m_1 + l_1)t} + E_{12}e^{(\mu m_1 - l_1)t} + F_{11}e^{(\mu m_3 + l_3)t} + F_{12}e^{(\mu m_3 - l_3)t}, \tag{6.28-a}$$

$$q_3 = E_{31}e^{(\mu m_1 + l_1)t} + E_{32}e^{(\mu m_1 - l_1)t} + F_{31}e^{(\mu m_3 + l_3)t} + F_{32}e^{(\mu m_3 - l_3)t} \tag{6.28-b}$$

or alternatively

$$q_1 = e^{\mu m_1 t}\bar{a}_1 \cos(\omega_1 t + \bar{\phi}_1) + e^{\mu m_3 t}\bar{b}_1 \cos(\omega_3 t + \bar{\phi}_3'), \tag{6.29-a}$$

$$q_3 = e^{\mu m_1 t}\bar{a}_3 \cos(\omega_1 t + \bar{\phi}_1') + e^{\mu m_3 t}\bar{b}_3 \cos(\omega_3 t + \bar{\phi}_3). \tag{6.29-b}$$

The ratio of amplitude $\bar{a}_3/\bar{a}_1$ and $\bar{b}_1/\bar{b}_3$, and the difference of phase angles $\bar{\phi}_1 - \bar{\phi}_1'$ and $\bar{\phi}_3 - \bar{\phi}_3'$ may be determined as follows:

$$F_{11}/F_{31} = (I_1/I_3)_{s=\mu m_3 + l_3} = U + jW$$

where

$$U = \frac{\mu^2 A_1 \omega_1 L_3 m_3 \{\mu^2 m_3^2 - 2\mu^2 m_1 m_3 + (\omega_1^2 - \omega_3^2)\} + 2\mu^2 A_1 \omega_1 L_3 \omega_3^2 (m_3 - m_1)}{(\mu^2 m_3^2 - 2\mu m_1 m_3 + \omega_1^2 - \omega_3^2)^2 + 4\mu^2 \omega_3^2 (m_3 - m_1)^2},$$

$$W = \frac{\mu A_1 \omega_1 L_3 \omega_3 \{\mu^2 m_3^2 - 2\mu^2 m_1 m_3 + (\omega_1^2 - \omega_3^2)\}}{(\mu^2 m_3^2 - 2\mu m_1 m_3 + \omega_1^2 - \omega_3^2)^2 + 4\mu^2 \omega_3^2 (m_3 - m)^2} \tag{6.30}$$

and

$$F_{12}/F_{32} = (I_1/I_3)_{s=\mu m_3 - l_3} = U - jW$$

and other two ratios are obtained similarly and using these four ratios we have

$$\begin{aligned}\bar{b}_1/\bar{b}_3 &= \{(F_{11} + F_{12})^2 + j^2(F_{11} - F_{12})^2\}^{1/2} / \{(F_{31} + F_{32})^2 + j^2(F_{31} - F_{32})^2\}^{1/2} \\ &= (F_{11} \cdot F_{12}/F_{31} \cdot F_{32})^{1/2} = (U^2 + W^2)^{1/2}.\end{aligned}$$

As seen in Eq. (6.30), $U = 0(\mu^2)$, $W = 0(\mu)$ and using these, we have

$$\bar{b}_1/\bar{b}_3 \fallingdotseq |W| \fallingdotseq |(\mu A_1 \omega_1 \omega_3 L_3/(\omega_1^2 - \omega_3^2))| = 0(\mu), \tag{6.31-a}$$

similarly

$$\bar{a}_3/\bar{a}_1 \fallingdotseq |(\mu A_3 \omega_1 \omega_3 L_1/(\omega_3^2 - \omega_1^2))| = 0(\mu). \tag{6.31-b}$$

The difference of phase angles $\bar{\phi}_3' - \bar{\phi}_3$ is obtained by Eqs. (6.26)~(6.28),

$$\begin{aligned}\bar{\phi}_3' - \bar{\phi}_3 &= \tan^{-1}\{j(F_{31} - F_{32})/(F_{31} + F_{32})\} - \tan^{-1}\{j(F_{11} - F_{12})/(F_{11} + F_{12})\} \\ &= \tan^{-1}(-W/U) = \tan^{-1}(0(\mu)/0(\mu^2)) \fallingdotseq \tan^{-1} \pm \infty,\end{aligned}$$

where the sign must be selected considering the sign of W/U. Namely, we have

$$\bar{\phi}_3' - \bar{\phi}_3 = \pm(\pi/2) \tag{6.32-a}$$

similarly

$$\bar{\phi}_1' - \bar{\phi}_1 = \pm(\pi/2). \tag{6.32-b}$$

Equation (6.29) represents the solution of the linearized differential equation (6.25), and we may consider that the nature of the solution of the original differential equation (6.13′) resembles to that of Eq. (6.25) so far as the harmonic terms are concerned, because the magnifude of non-linear terms of (6.13′) is $0(\mu)$. Accordingly comparing Eq. (6.29) with Eq. (6.21), and reffering Eqs. (6.26) and (6.31), we can write

$$a = e^{\mu m_1 t}\,\bar{a}_1, \qquad b = e^{\mu m_3 t}\,\bar{b}_3, \tag{6.33}$$

$$\mu c_3 = \bar{a}_3/\bar{a}_1, \qquad \mu c_1 = \bar{b}_1/\bar{b}_3, \tag{6.34}$$

and

$$da/dt = \bar{a}_1 \cdot \mu_{m_1} e^{\mu m_1 t} = \mu_{m_1} a = (\mu/2)(A_1\omega_1 L_1 - \gamma_1)\,a, \tag{6.35-a}$$

$$db/dt = \bar{b}_3 \cdot \mu_{m_3} e^{\mu m_3 t} = \mu_{m_3} b = (\mu/2)(A_3\omega_3 L_3 - \gamma_3)\,b. \tag{6.35-b}$$

And using the relation of Eq. (6.34) and reffering to Eq. (6.31) we can put

$$c_3 = A_3\omega_1\omega_3 L_1/(\omega_3^2 - \omega_1^2), \qquad c_1 = A_1\omega_1\omega_3 L_3/(\omega_3^2 - \omega_1^2). \tag{6.36}$$

As discussed above, we have deduced the solution of the original differental equation (6.13′) from the solution of linearized differential equation (6.25). On the other hand we can prove that the solution of (6.13′) may be written in the form of (6.21) and this form of solution satisfies the (6.13′) within the accuracy of $0(\mu^2)$, if a and b fulfill Eq. (6.35), and c_1, c_3 and $\phi_3' - \phi_3$, $\phi_1' - \phi_1$ take the values of Eqs. (6.36) and (6.32) respectively. Here, we omit the proof.

5. Existence and stability of stationary solutions

As the feature of pressure variation of the surging may be represented by Eq. (6.8), and q_1 and q_3 are written in the form of Eq. (6.21), so we can realize the feature of pressure variation in the surging state, if we can solve the Eq. (6.35). We examine this equation presently.

Replacing L_1 and L_3 of Eq. (6.35) by Eq. (6.23), we have

$$da/dt = (\mu/2)\{\bar{\alpha}A_1 h_1\phi_0 - \bar{\beta}A_1\phi_0^3(h_1^3 a^2 + 2h_1 h_3^2 b^2) - \gamma_1\}\,a, \tag{6.35′-a}$$

$$db/dt = (\mu/2)\{\bar{\alpha}A_3 h_3\phi_0 - \bar{\beta}A_3\phi_0^3(2h_1^2 h_3 a^2 + h_3^3 b^2) - \gamma_3\}\,b \tag{6.35′-b}$$

where $\phi_0 = \omega_1\omega_3$. Andfrom above equations we have

$$da/db = \frac{a\{\bar{\alpha}A_1 h_1\phi_0 - \bar{\beta}A_1\phi_0^3(h_1^3 a^2 + 2h_1 h_3^2 b^2) - \gamma_1\}}{b\{\bar{\alpha}A_3 h_3\phi_0 - \bar{\beta}A_3\phi_0^3(2h_1^2 h_3 a^2 + h_3^3 b^2) - \gamma_3\}}. \tag{6.37}$$

The manner in which a and b vary with time, is obtained from Eq. (6.35′) and the mutual relation of a and b is deduced from Eq. (6.37).

Now we are concerned most about the stationary solutions of Eq. (6.35′), and the condition of stationary solution is $da/dt = db/dt = 0$. It is easily seen that four stationary solutions are posible, namely

$$\begin{aligned}
&\text{(i)} && \begin{cases} a = 0, \\ b = 0, \end{cases} \\
&\text{(ii)} && \begin{cases} \bar{\alpha}A_1 h_1\phi_0 - \bar{\beta}A_1\phi_0^3(h_1^3 a^2 + 2h_1 h_3^2 b^2) - \gamma_1 = 0, \\ \bar{\alpha}A_3 h_3\phi_0 - \bar{\beta}A_3\phi_0^3(2h_1^2 h_3 a^2 + h_3^3 b^2) - \gamma_3 = 0, \end{cases} \\
&\text{(iii)} && \begin{cases} a = 0, \\ \bar{\alpha}A_3 h_3\phi_0 - \bar{\beta}A_3\phi_0^3(2h_1^2 h_3 a^2 + h_3^3 b^2) - \gamma_3 = 0, \end{cases} \\
&\text{(iv)} && \begin{cases} \bar{\alpha}A_1 h_1\phi_0 - \bar{\beta}A_1\phi_0^3(h_1^3 a^2 + 2h_1 h_3^2 b^2) - \gamma_1 = 0, \\ b = 0, \end{cases}
\end{aligned} \tag{6.38}$$

Indicating a set of a and b which satisfies the respective group of equations as $(a_0,\ b_0)$, we have

$$\text{(i)}\quad \begin{cases} a_0 = 0, \\ b_0 = 0. \end{cases}$$

$$\text{(ii)}\quad \begin{cases} a_0 = h_3\{(2D_3A_1h_1 - D_1A_3h_3)/(3\bar{\beta}\phi_0^3A_1A_3h_1^3h_3^3)\}^{1/2} \\ \quad = \{(D_1\sigma_3\cos^2 k_3\xi l - 2D_3\sigma_1\cos^2 k_1\xi l)/3\bar{\beta}\cos^4 k_1\xi l\cdot\cos^2 k_3\xi l\cdot(2c^4\sigma_1\sigma_3/K^3)\}^{1/2}, \\ b_0 = h_1\{(2D_1A_3h_3 - D_3A_1h_1)/(3\bar{\beta}\phi_0^3A_1A_3h_1^3h_3^3)\}^{1/2} \\ \quad = \{(D_3\sigma_1\cos^2 k_1\xi l - 2D_1\sigma_3\cos^2 k_3\xi l)/3\bar{\beta}\cos^4 k_3\xi l\cdot\cos^2 k_1\xi l\cdot(2c^4\sigma_1\sigma_3/K^3)\}^{1/2}, \end{cases}$$

$$\text{(iii)}\quad \begin{cases} a_0 = 0, \\ b_0 = (D_3/\bar{\beta}A_3\phi_0^3h_3^3)^{1/2} = [\{2\bar{\alpha}\sigma_3\cos^2 k_3\xi l(c^2/K) - \gamma_3\}/\bar{\beta}\cdot 2c\sigma_3(c/K)^3\cos^4 k_3\xi l]^{1/2}, \end{cases}$$

$$\text{(iv)}\quad \begin{cases} a_0 = (D_1/\bar{\beta}A_1\phi_0^3h_1^3)^{1/2} = [\{2\bar{\alpha}\sigma_1\cos^2 k_1\xi l(c^2/K) - \gamma_1\}/\bar{\beta}\cdot 2c\sigma_1(c/K)^3\cos^4 k_1\xi l]^{1/2}, \\ b_0 = 0, \end{cases}$$

where
$$D_1 = \bar{\alpha}A_1h_1\phi_0 - \gamma_1,\quad D_3 = \bar{\alpha}A_3h_3\phi_0 - \gamma_3,$$

or changing the notations we have

$$\begin{aligned} D_1 &= (\alpha' - 3\beta'M^2)\ (c^2/K)\cdot 2\sigma_1\cos^2 k_1\xi l - \gamma_1, \\ D_3 &= (\alpha' - 3\beta'M^2)\ (c^2/K)\cdot 2\sigma_3\cos^2 k_3\xi l - \gamma_3. \end{aligned} \tag{6.39'}$$

$D_1>0$, $D_3>0$ represent the condition under which the vibration corresponding to the normal mode $s=1$ and $s=3$ exist respectively, when we treat the surging phenomenon from the viewpoint of one degree of freedom. And in that treatment, the stationary amplitude of surging coincide with a_0 of (iv) or b_0 of (iii). These facts may be verified by comparing Eq. (6.39') and (iv), (iii) with Eq. (6.18') and Eq. (6.19) respectively. Accordingly we may say that D_1 and D_3 are the indices which measure the degree of easiness of the occurence of self-excitation.

As an example, when $D_3<0$, as seen from Eq. (6.39), the stationary value of b (excepting $b=0$) does not exist, and at the same time if $D_1>0$ is satisfied, a_0 of (iv) alone has meaning as a stationary value of a and this value of a_0 coincides with the value of a of Eq. (6.19). Similarly when $D_3>0$, $D_1<0$ are satisfied, b_0 of (iii) alone has meaning and this value coincides with the value of stationary anplitude which is obtained from the treatment in which q_3 is the only dependent variable. When $D_1<0$, $D_3<0$, the stationary values of a and b excepting zero does not exist.

Accordingly, we confine our discussion to the case where the conditions $D_1>0$ and $D_3>0$ are both fulfied. In this case, it is seen that the set of solution $(a_0,\ b_0)$ of (ii) can exist only under the following condition, by reason that the numerators in the radical signs must be positive,

$$D_1A_3h_3/2 < D_3A_1h_1 < 2D_1A_3h_3. \tag{6.40}$$

In the next paragraph, we examine the stability of the four sets of solutions shown above. A solution $(a_0,\ b_0)$ is nothing but a singularity of Eq. (6.37), and

we examine its stability by the Poincáre's theory.[40] Namely, in the coordinate plane a, b, taking the origin on a singularity, and putting $a=a_0+\bar{\eta}$ and $b=b_0+\bar{\xi}$, we have

$$\frac{d\bar{\eta}}{d\bar{\xi}}=\frac{-2\,\bar{\beta}A_1\phi_0^3a_0(a_0h_1^3\bar{\eta}+2\,h_1h_3^2b_0\bar{\xi})+\bar{\eta}\{D_1-\bar{\beta}A_1\phi_0^3(h_1^3a_0^2+2\,h_1h_3^2b_0^2)+0(\bar{\xi}^2,\ \bar{\eta}^2)}{\bar{\xi}\{D_3-\bar{\beta}A_3\phi_0^3(2\,h_1^2h_3a_0^2+h_3^3b_0^2)\}-2\,\bar{\beta}A_3\phi_0^3b_0(b_0h_3^3\bar{\xi}+2\,h_1^2h_3a_0\bar{\eta})+0(\bar{\xi}^2,\ \bar{\eta}^2)}, \tag{6.41}$$

where $0(\bar{\xi}^2,\ \bar{\eta}^2)$ indicates the terms of higher degrees of $\bar{\xi}$ and $\bar{\eta}$.

Poincáre's theory shows that the characters of singularities of above equation are similar to those of the equation which has not the terms $0(\bar{\xi}^2,\ \bar{\eta}^2)$, and that the singularities of the differential equation

$$d\bar{\eta}/d\bar{\xi}=(\mathfrak{A}\bar{\xi}+\mathfrak{L}\bar{\eta})/(\mathfrak{C}\bar{\xi}+\mathfrak{b}\bar{\eta})$$

are classified as follows, under tne condition $\mathfrak{A}\mathfrak{b}-\mathfrak{L}\mathfrak{B}\neq 0$;

(I) $(\mathfrak{L}-\mathfrak{C})^2+4\,\mathfrak{A}\mathfrak{b}>0$ { nodal point if $\mathfrak{A}\mathfrak{b}-\mathfrak{L}\mathfrak{C}<0$ { stable if $\mathfrak{L}+\mathfrak{C}<0$ / unstable if $\mathfrak{L}+\mathfrak{C}>0$ / saddle point if $\mathfrak{A}\mathfrak{b}-\mathfrak{L}\mathfrak{C}>0$

(II) $(\mathfrak{L}-\mathfrak{C})^2+4\,\mathfrak{A}\mathfrak{b}<0$ { center if $\mathfrak{L}+\mathfrak{C}=0$ / focal point if $\mathfrak{L}+\mathfrak{C}\neq 0$ { stable if $\mathfrak{L}+\mathfrak{C}<0$ / unstable if $\mathfrak{L}+\mathfrak{C}>0$

(III) $(\mathfrak{L}+\mathfrak{C})^2+4\,\mathfrak{A}\mathfrak{b}=0$ nodal point { stable if $\mathfrak{L}+\mathfrak{C}<0$ / unstable if $\mathfrak{L}+\mathfrak{C}>0$.

Eq. (6.41) reduces to the following forms corresponding to four cases of Eq. (6.39),

(i) $d\bar{\eta}/d\bar{\xi}=D_1\bar{\eta}/(D_3\bar{\xi})$,

(ii) $d\bar{\eta}/d\bar{\xi}=\{a_0A_1(2\,h_1^2h_3b_0\bar{\xi}+a_0h_1^3\bar{\eta})\}/\{b_0A_3(b_0h_3^3\bar{\xi}+2\,h_1^2h_3a_0\bar{\eta})\}$,

(iii) $d\bar{\eta}/d\bar{\xi}=\bar{\eta}\{D_1-\bar{\beta}A_1\phi_0^3(2\,h_1h_3^2b_0^2)\}/(-2\,\bar{\beta}A_3\phi_0^3b_0^2h_3^3\bar{\xi})$,

(iv) $d\bar{\eta}/d\bar{\xi}=(-2\,\bar{\beta}A_1\phi_0^3a_0^2h_1^3\bar{\eta})/\bar{\xi}\{D_3-\bar{\beta}A_3\phi_0^3(2\,h_1^2h_3a_0^2)\}$.

And the characters of singularity are as follows respectively.

(i)
$$(\mathfrak{L}-\mathfrak{C})^2+4\,\mathfrak{A}\mathfrak{b}=(D_1-D_3)^2\geqq 0,$$
$$\mathfrak{A}\mathfrak{b}-\mathfrak{L}\mathfrak{C}=-D_1D_3<0,$$
$$\mathfrak{L}+\mathfrak{C}=D_1+D_3>0.$$

Taking account of $D_1>0$ and $D_3>0$, we see that (0, 0) is an unstable nodal point, namely the vibrations of amplitudes a and b build up.

(ii) The singularity $(a_0,\ b_0)$ is a saddle point (except the case of $\mathfrak{A}\mathfrak{b}-\mathfrak{L}\mathfrak{C}=0$), namely this stationary value, which is limited within the existence range by Eq. (6.40), is theoretically possible alike the case (i), but is unstable and can not exist actually.

(iii) The singularity $(0,\ b_0)$ is a saddle point if $D_1A_3h_3>2\,D_3A_1h_1$, and a stable nodal point if the inequality sign is reverse.

(iv) Resembling the above, $(a_0, 0)$ is a saddle point if $D_3A_1h_1 > 2D_1A_3h_3$, and a stable nodal point if the inequality sign is reverse.

From above discussion, we can see that the character of singularity changes depending on the relation between the value of $D_1A_3h_3$ and $D_3A_1h_1$. The results of above discussion is described in Fig. 6.2. In the figure, the features of change of the character of singularity which corresponds to each stationary value, which is indicated in the left side of the figure, are described against $\kappa_0 = D_1A_3h_3/(D_3A_1h_1)$. Hereafter we examine this figure.

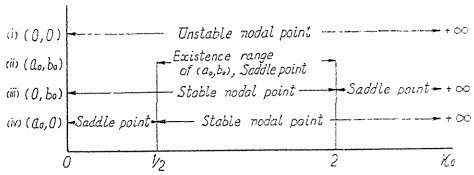

FIG. 6.2. Relation between nature of singularity and κ_0 ($\kappa_0 = D_1A_3h_3/D_3A_1h_1 = D_1\sigma_3 \cos^2 k_3\xi l/D_3\sigma_1 \cos^2 k_1\xi l$).

As mentioned already with regard to Eq. (6.39'), in the treatment of one degree of freedom, if $D_1 > 0$ the vibration of angular frequency ω_1 builds up and a stationary value of amplitude exist (in the treatment of two degrees of freedom, the situation is same if $D_3 < 0$ is also satisfied). But in this case, where $D_1 > 0$ and $D_3 > 0$ are both satisfied, as seen in (iv) of this figure, the stationary value $(a_0, 0)$ is unstable (saddle point) under the condition $D_1 > 0$, and can not exist until the value of D_1 becomes large compared with D_3 and the condition $\kappa_0 > 1/2$ bocomes to be fulfilled.

Similarly, in the case (iii), the condition under which the stationary value $(0, b_0)$ which corresponds to the vibration of angular frequency ω_3 is stable, is not $D_3 > 0$ only but both $D_3 > 0$ and $\kappa_0 < 2$; where D_3 has a certain magnitude relative to D_1. And in the case (ii), the stationary value (a_0, b_0) is unstable (saddle point) in all range where it can exist, accordingly the state, in which the two vibrations of finite applitudes corresponding to the angular frequencies ω_1 and ω_3 exist simultaneously, is actually impossible.

Further, in the range of $1/2 < \kappa_0 < 2$, both (iii) and (iv) are stable, but it is impossible to know which state appears actually, from above consideration. In the next section, we treat this problem.

6. Solution curve of differential equation (6.37)

The relation between the amplitudes a and b, which correspond to the vibration of angular frequencies ω_1 and ω_3 respectively, is obtained by solving Eq. (6.37). But as it is difficult to solve this analytically so we adopt a graphical method.

First we rewrite the Eq. (6.37) in non-dimensional form, namely denoting the stationary value a_0 of the case (iv) as $\bar{a}_0$, and putting

$$\bar{y} = a/\bar{a}_0,\ \bar{x} = b/\bar{a}_0,\ A_3h_3/A_1h_1 = (\sigma_3 \cos^2 k_3\xi l)/(\sigma_1 \cos^2 k_1\xi l) = \Theta,$$

we have

$$d\bar{y}/d\bar{x} = \bar{y}[1-\{\bar{y}^2+2\bar{x}^2(\cos^2 k_3\xi l/\cos^2 k_1\xi l)\}]/\bar{x}\Theta[(1/\kappa_0)-\{2\bar{y}^2+\bar{x}^2(\cos^2 k_3\xi l/\cos^2 k_1\xi l)\}]. \tag{6.42}$$

Especially for $\xi=0$, where the blower position is at the suction end of pipeline, Eq. (6.42) reduces to the next form, because $\cos k_1\xi l=\cos k_3\xi l=1$,

$$d\bar{y}/d\bar{x} = \bar{y}\{1-(\bar{y}^2+2\bar{x}^2)\}/\bar{x}\Theta\{(1/\kappa_0)-(2\bar{y}^2+\bar{x}^2)\}. \tag{6.42'}$$

Two examples of solution curves of Eq. (6.42') are shown in Fig. 6.3 and Fig. 6.4. The value of Θ is 1.5 for both curves (this value is calculated with the real dimentions of experimental apparatus), and κ_0 is 0.2 for the former and 1.0 for the latter. In Fig. 6.3, the singularities corresponding to (i), (iii), and (iv) exist, as known from Fig. 6.2, however the (iii) alone is stable and because of this fact, the solution curves converge into this singularity. And in Fig. 6.4, all singulsrities (i)~(iv) exist, and two of them, namely (iii) and (iv) are stable,

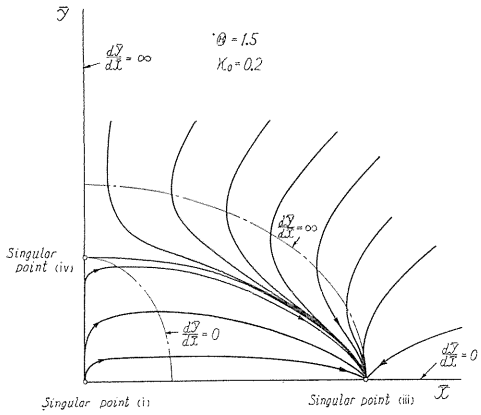

FIG. 6.3. An example of solution curve of Eq. (6.42') ($\kappa_0=0.2$).

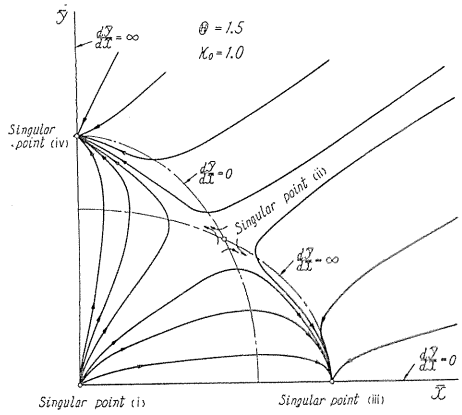

FIG. 6.4. An example of solution curve of Eq. (6.42') ($\kappa_0=1.0$).

and the solution curves converge into either of the two, depending on their initial values. The coodinate plane is devided into two domains in which the solution curves conveges into respective singularities, and the ratio of domains is decided by the value of κ_0; namely the domain corresponding to the singularity (iv) increases with the value of κ_0 and when $\kappa_0=2$ the singularity (ii) coincides with (iii) and all solution curves in the coordinate plane converge into the singularity (iv). That is, we can recognize as follows, under the condition $1/2<\kappa_0<2$, both singularity (iii) and (iv) are stable, however there is, so to speak, a degree of stability, and the singularity (iv) becomes more stable comparing with (iii) nearer the value of κ_0 to 2. Further under the condition $\kappa_0>2$, we obtain the figure in which all solution curves converge into the singularity (iv), in contrast with Fig. 6.3. We can summarize the results of analytical discussion carried out in preceding sections as follows.

(1) Both vibrations corresponding to the angular frequencies ω_1 and ω_3 can not have the finite amplitudes simultaneously (the singularity (ii) is a saddle

point), accordingly the surging does not occur in such a feature.

(2) When we consider the suring problem from the standpoint that the system has one degree of freedom, the condition under which the vibration corresponding to ω_1 or ω_3 occurs, are $D_1>0$ or $D_3>0$ for respective cases and if either of the two is fulfilled, the surging of corresponding type sustains stably.

(3) When $D_1>0$ and $D_3>0$ are fulfilled at the same time, the condition, under which the vibration of angular frequency ω_1 sustaines with stable amplitude a_0, is not $D_1>0$ but $\kappa_0>1/2$, where D_1/D_3 has a certain magnitude. Similarily, the condition for stable amplitude of vibration of ω_3 is not $D_1>0$ but $\kappa_0<2$. That is, the selection of the type of vibration, so to speak, arises. In other words, the surging occurs in the type in which the occurence is easier. In addition, it must be emphasized that above statement does not mean that the wave form of surging is always a sinusoidal corresponding to a normal mode, but means that, because the components of higher frequencies which are contained in the wave form of surging are apt to be influenced drastically by the damping factors in the pipe-line, and the surging is observed in a certain type in which one of components corresponding to the normal modes of low degree is dominant.

(4) Under the condition $1/2<\kappa_0<2$, both vibrations of angular frequencies of ω_1 and ω_3 are stable, however, only one vibration arises actually depending on the initial condition, and the value of κ_0 indicates the degree of stability.

The conclusions mentioned above are deduced with the aid of a cubic as an approximate curve for the real characteristic curve of the blower. And because the real characteristic curve is of asymmetrical in form, an algebraic equation of higher degrees is required for the more accurate approximation, and we have shown that a sextic is sufficient. Making use of a sextic as an approximation curve for the real characteristic curve, we proved that above conclusions hold grood, however the discussion is omitted here.

In addition, we may say that the representation of characteristic curve by a cubic of the form given in Eq. (6.16) is adequate for many blowers, but it may be possible that above conclusions do not hold for a blower with the characteristic curve of special form.

7. Experiments

To examine the conclusions mentioned above, we compare these with the experimental results shown in Fig. 4.7 of Chapter IV, and in addition we show the results of experiment carried out newly.

In Fig. 4.7 (*a*) or (*b*), the type of surging changes from that corresponding to $s=1$, into that corresponding to $s=3$ at a certain discharge, and both types of vibration of constant amplitude can not exist simultaneously, and this fact supports the conclusion (1).

And in the range of small discharge, the vibration of $s=1$ type is dominant and $s=3$ type arrises at a discharge, the value of which is almost equal to the value in which the $s=1$ type becomes unstable. This phenomenon may be explained as follows. As we have already mentioned about this phenomenon in Section (4-2) of Chapter IV, the increase of discharge is accompanied by the increase of the exist opening area, and this increase of opening area has the powerful damping effect on the vibration of $s=1$ type but rather small effect on the $s=3$ type, because the position of opening is near a node of $s=1$ type and a

loop of $s=3$ type. Accordingly, when we give attention to the values D_1 and D_3, which are indices expressing the degree of easiness of the self-excitation, we may say as follows: D_1 decreases rapidly from a certain velue of $D_1>0$ with the increasing discharge, and on the other hand D_3 decreases rather more slowly. And considering that the experimental results shows $\varepsilon_3>\varepsilon_1$ when the exit opening is entirely closed, and also that the surging is apt to occur in the type of $s=1$ in general, we may consider that $D_1 \gg D_3$ is fulfilled in the range of small discharge. Accordingly the discharge range in which the $s=1$ type is dominant corresponds to the confines of $\kappa_0>2$ in Fig. 6.2 (here, we pay attention to the line (iii) and (iv)), and with the increase of dicharge, the value of κ_0 moves to the left and finary comes into the confines of $\kappa_0<1/2$, and this state corresponds to the discharge range in which the $s=3$ type is dominant, but in a certain part of large discharge $D_1<0$ possibly holds.

Further by the observation of transition, it is clarified that, for a discharge near the transition, the one of both types is dominant in a certain duration and soon the other becomes dominant and these state repeat irregularly. We may consider that above range corresponds to the confines $1/2<\kappa_0<2$, however the theory shows that, in this confines, two types are stable and one of two is realized depending on the initial condition. Because in the actual phenomenon, various disturbances exist in the flow, for example, the separation of flow in the vane-wheel, and it may be considered that these disturbances induce the change of dominant type. That is, experimental results do not contradict the conclusions (3) and (4).

In the next place, we add another experiment carred out for the confirmation of the theory.

In this experiment, we use the pipe-line of the form shown in Fig. 3.1 of Chapter III, where $l=24.45$ m, $V=390.3\ l$ and $A\fallingdotseq 0.01335$ m^2. And the blower B_1 is connected to the suction end of the pipe-line and driven in the speed $n=4390$ r.p.m. The outlet openings F and S (cf. Fig. 3.1) are used simultaneously, and these diameters are selected so that the sum of discharge through the openings is held constant. By this method, we can controll the damping effect of the openings on both types of vibration, say $s=1$ and $s=3$, while fixing the value of discharge, because the opening S has only slight damping effect on both types as its position is near the loop for both vibrations and the damping effect is decided mostly by the magnitude of opening F only. That is, in both equations of (6.39′), fixing the first terms and varing the second terms γ_1 and γ_3, we can vary the values of D_1 and D_3 and accordingly the value of κ_0.

The results of experiment is summarized in Table 6.1, where ε_1 and ε_3 indicate the measured values of damping coefficients of free vibrations corresponding to the type $s=1$ and $s=3$ respectively. As seen in the table, the value of ε_1 increases rapidly with the diameter of opening but ε_3 increases slowly with it. In cases where ε_1 is rather small, the surging of $s=1$ type is dominant and the component of $s=3$ are unstable, and when the $s=1$ type bocomes unstable, the $s=3$ type arrises stably, in spite of the increase of ε_3, and in no case the surging with both components stable can occur. In above experimints, the change of condition from I to VI is equivalent to the change of the value of κ_0 from a large value to a small (see Fig. 6.2), and the experimental results show good agreement with the theory.

TABEL 6.1. Change of Type of Surging

No.	Opening diameter (mm)		Damping coefficient (rad./s)		Pressure amplitude (kg/m²)		Remarks
	S	F	ε_1	ε_3	a_0 ($s=1$)	b_0 ($s=3$)	
I	33	0	0.46~0.56	1.3	123	unstable 0~18	
II	29.51	14.80	1.54	1.6	99	unstable ≒0	frequencies (for case I) (c/s)
III	25.54	20.85	↓	2.0	66~82	unstable 0~26	surging $f_1=1.69$, $f_3=6.93$
IV	20.85	25.54	↓	2.0	rather unstable 0~17.3	28~54	free vibration $f_1=1.73$, $f_3=7.24$
V	14.80	29.51	increases rapidly	2.0	unstable 0~15	50~79	
VI	0	33		1.9	unstable 0~4	68~73	

8. Concusion

In this chapter, the vibration of air column is treated theoretically as a system of two degrees of freedom, and the condition which decides the type of surging is deduced. The theory is confirmed by experiments. As a conclusion we may say that the surging is observed in a certain form in which only one of the components corresponding to normal mode of lower degree is selected and builds up.

Acknowledgement

In concluding this paper, the author ackowledges his debt to the late Dr. Y. Shimoyama for guidance and valuable advice, and especially for his instruction over a long period of time. The author expresses his appreciation to Prof. Dr. Y. Furuya and Prof. Dr. T. Yamamoto for their guidance and valuable suggestion, to Prof. Dr. S. Uchida, Prof. Dr. S. Ōtsuka and Prof. Dr. M. Murakami for their encouragements and valuable advices. He also thanks Mr. Y. Yamada, Mr. K. Watabe and Mr. A. Tsujii for their assistance in some of these experiments. This reseach is indebted to the Laboratory of Hydraulics, Department of Mechanical Engineering, Nagoya University for laboratory use.

Notes and References

1) R. O. Bullock, W. W. Wilcox and J. J. Moses, Nat. adv. Comm. Aero. tech. Note, (March 1947).
2) S. Fujii, Trans. of Soc. of Mech. Engrs. (Japan), Vol. **14**, No. 48 (1948), 17.
3) Y. Shimoyama, Trans. of Soc. of Mech. Engrs. (Japan), Vol. **15**, No. 50 (1949), 50.
4) M. C. Huppert and W. A. Benser, J. aero. Sci., Vol. **20**, No. 12 (1953), 835.
5) H. W. Emmons, C. E. Pearson and H. P. Grant, Trans. A.S.M.E., Vol. **77**, No. 4 (1955), 455.
6) H. Kusama, S. Tsuji and Y. Oshida, Trans. of Soc. of Mech. Engrs (Japan), Vol. **22**, No. 117 (1956), 360.

7) Y. Katto, Trans. of Soc. of Mech. Engrs. (Japan), Vol. **26**, No. 162 (1960), 256.
8) Y. Katto, Trans. of Soc. of Mech. Engrs. (Japan), Vol. **26**, No. 162 (1960), 265.
9) Y. Katto, Bull. of J.S.M.E., Vol. **3**, No. 12 (1960), 484.
10) Y. Katto, Bull. of J.S.M.E., Vol. **3**, No. 12 (1960), 490.
11) C. E. Pearson, J. aero. Sci., Vol. **22**, No. 1 (1955), 10.
12) C. E. Pearson, J. aero. Sci., Vol. **22**, No. 11 (1955), 799.
13) H. Pearson and T. Bower, Aero. Quart. (Nov. 1949), 195.
14) J. M. Stephenson, J. aero. Sci., Vol. **19**, No. 1 (1952), 67.
15) R. O. Bullock and H. B. Finger, SAE Journal, Vol. **59** (Sept. 1952), 42.
16) R. O. Bullock and H. B. Finger, SAE Quart. Trans., Vol. **6**, No. 2 (1952), 220.
17) J. R. Foley, SAE Journal, Vol. **59** (Sept. 1951), 46.
18) M. Harada, Rep. of the Government Mechanical Laboratory, No. 38 (1960).
19) A. N. Sherstyuk, Acad. Nauk., SSSR 21 (1955), 195.
20) T. Itō, Rep. in 37th Regular Lecture Meeting of Soc. of Mech. Engrs (Japan)., No. 23 (1960), 65.
21) S. Uchida, Lecture in 54th Lecture Meeting of Soc. of Mech. Engrs (Japan)., (1954), 45.
22) For example, cf. T. Takagi, Lecture of Algebra (Daisūgaku Kōgi), (1946), 462.
23) For example, cf. T. Takagi, Lecture of Algebra (Daisūgaku Kōgi), (1946), 73.
24) T. Itō, Trans. of Soc. of Mech. Engrs. (Japan), Vol. **19**, No. 88 (1953), 43.
25) Y. Shimoyama and T. Itō, Trans. of Soc. of Mech. Engrs. (Japan), Vol. **23**, No. 125(1957), 25.
26) M. Maekawa, Trans. of Soc. of Mech. Engrs. (Japan), Vol. 2, No. 6 (1936), 106.
27) A. A. Putnam and W. R. Dennis, Trans. A.S.M.E., Vol. **75** (1953), 15. In reports 26) and 27), experimental results for the pipe-line of small scale are given.
28) H. Lamb, Dynamical Theory of Sound, 2nd. ed. (1931), 270.
29) P. Hadlatsch, V.D.I.Z. (Juni 1953), Nr. 17/18, 503.
30) P. Hadlatsch, V.D.I.Z. Nr. 20, 706.
31) S. Fujii and K. Takeishi, Trans. of Soc. of Mech. Engrs. (Japan), Vol. **51**, No. 359 (1948), 321.
32) R. Dziallas, Untersuchungen an einer Kreiselpumpe mit labiler Kennlinie, VDI-Verlag (1940).
33) Y. Shimoyama and T. Itō, Trans. of Soc. of Mech. Engrs. (Japan), Vol. **23**, No. 125 (1957), 32.
34) Y. Shimoyama and T. Itō, Bull. of J.S.M.E., Vol. **1**, No. 1 (1958), 57.
35) Y. Shimoyama and T. Itō, Trans. of Soc. of Mech. Engrs. (Japan), Vol. **23**, No. 125 (1957), 38.
36) T. Itō, Trans. of Mech. Engrs. (Japan), Vol. **26**, No. 162 (1960), 274.
37) T. Itō, Trans. of Mech. Engrs. (Japan), Vol. **26**, No. 162 (1960), 283.
38) T. Itō, Trans. of Soc. of Mech. Engrs. (Japan), Vol. **26**, No. 162 (1960), 289.
39) N. Kriloff and N. Bogoliuboff, Introduction to Non-Linear Mechanics (English Transration), (1947), 8.
40) For example, cf. J. J. Stoker, Nonlinear Vibrations (1950), 36.
41) H. Kusama and S. Tsuji, Trans. of Soc. of Mech. Engrs. (Japan), Vol. **22**, No. 121 (1956), 642.
42) S. Tsuji, Trans. of Soc. of Mech. Engrs. (Japan), Vol. **23**, No. 133 (1957), 628.
43) S. Tsuji, Bull. of J.S.M.E., Vol. **1**, No. 2 (1958), 156.
44) L. S. Dzung, Brown Boveri Rev., Vol. **39**, No. 8/9 (1952), 295.